

File 600/3-83-011

December 1982

STUDIES IN AIR QUALITY  
OF METEOROLOGY AT  
NORTH CAROLINA STATE UNIVERSITY

ENVIRONMENTAL SCIENCES RESEARCH LABORATORY  
OFFICE OF RESEARCH AND DEVELOPMENT  
U.S. ENVIRONMENTAL PROTECTION AGENCY  
RESEARCH TRIANGLE PARK, NORTH CAROLINA 27711

EPA-600/3-83-011

March 1983.

(NTIS) PB 83-181743

STUDIES IN AIR QUALITY  
METEOROLOGY AT  
NORTH CAROLINA STATE UNIVERSITY

by

Gerald F. Watson  
Allen J. Riordan  
Walter J. Saucier  
and  
Ted L. Tsui

Department of Marine, Earth and Atmospheric Sciences  
North Carolina State University  
Raleigh, North Carolina 27650

805554

Project Officer  
Lawrence E. Niemeyer  
Meteorology and Assessment Division  
Environmental Sciences Research Laboratory  
Research Triangle Park, North Carolina 27711

ENVIRONMENTAL SCIENCES RESEARCH LABORATORY  
OFFICE OF RESEARCH AND DEVELOPMENT  
U.S. ENVIRONMENTAL PROTECTION AGENCY  
RESEARCH TRIANGLE PARK, NORTH CAROLINA 27711

## DISCLAIMER

This report has been reviewed by the Environmental Sciences Research Laboratory, U.S. Environmental Protection Agency, and approved for publication. Approval does not signify that the contents necessarily reflect the views and policies of the U.S. Environmental Protection Agency, nor does mention of trade names or commercial products constitute endorsement or recommendation for use.

## ABSTRACT

This report summarizes eight studies in diverse areas of air quality meteorology resulting from a cooperative research program involving the graduate students and faculty of the atmospheric sciences program of North Carolina State University and the staff and facilities of the EPA Meteorology and Assessment Division.

Meteorological analysis of the St. Louis RAPS data has shown that: (1) The urban heat island strength during the day amounts to about  $0.5^{\circ}\text{C}$  and varies little with wind speed, cloud cover, or season. The nocturnal heat island, however, is highly responsive to all three factors as well as to anthropogenic heat sources. (2) Profiles of ozone above the urban nocturnal surface inversion are highly variable and apparently related to details of the wind structure. (3) Evaluation of the energy budget over concrete, blacktop, and soil surfaces suggests improvements in the parameterization of the surface heat flux in air quality models.

Studies of atmospheric visibility and suspended particulates reveal that: (1) Air transparency nation-wide has declined significantly between 1955 and 1972. The annual cycle in visibility is inversely related to that in relative humidity. (2) The relative contributions of haze, smoke, and dust to lowering visibilities in eastern Texas between 1949 and 1968 are determined. (3) Most sulfate concentration variability at fixed sites is due to the vagaries in long-range transport rather than to local conditions of temperature, humidity, or insolation.

Studies of the boundary layer mesoscale wind structure over the Appalachian Mountains indicate that: (1) A pronounced low-level jet with significant diurnal variability can form even during a period of air stagnation. (2) The standard 850 mb-level winds can be used to estimate surface winds in complex terrain given the valley-ridge orientation and time of day.

This report was submitted in fulfillment of Contract No. R805554-01 by North Carolina State University under the sponsorship of the U.S. Environmental Protection Agency. This report covers the period from October 19, 1977 to October 19, 1981 and work was completed as of October 31, 1981.

## CONTENTS

ABSTRACT. . . . .	iii
FIGURES . . . . .	vi
TABLES. . . . .	ix
ACKNOWLEDGMENTS . . . . .	xi
1. Introduction . . . . .	1
2. Conclusions. . . . .	2
3. Recommendations. . . . .	4
4. Climatological Aspects of the St. Louis Urban Heat Island . . . . .	5
5. A Study of the Vertical Distribution of Ozone and the Variability of the Wind Field Above a Nocturnal Radiation Inversion . . . .	18
6. Temporal Variation in the Surface Energy Budget Components for Three Land Use Patterns. . . . .	31
7. Trends in Atmospheric Visibility Across the United States from 1955 to 1972 . . . . .	42
8. A Visibility Study in the Eastern Half of Texas from 1949 to 1968 . . . . .	50
9. Synoptic-Scale Variability in Atmospheric Suspended Sulfate Concentrations. . . . .	62
10. Diurnal Variation of Wind Profiles Across Mountainous Terrain During an Air Stagnation Period . . . . .	73
11. A Mesoscale Analysis of Air Flow in Complex Terrain . . . . .	86
REFERENCES. . . . .	100

## FIGURES

<u>Number</u>		<u>Page</u>
4.1	Heat island strength by cloud cover category. . .	11
4.2	Heat island strength by wind speed category . . .	11
4.3	Heat island strength by cloud cover category and season. . . . .	12
4.4	Heat island strength by wind speed category and season. . . . .	13
4.5	Rate of change of temperature..seasonal averages. . . . .	14
4.6	Anthropogenic heat output..annual average . . . .	15
5.1	Map depicting RAPS facilities in St. Louis, Missouri. . . . .	25
5.2	Height-time section of wind speed for day 216 . .	26
5.3	Height-time section of wind direction for day 216 . . . . .	27
5.4	Layer-average trajectory for day 216. . . . .	28
5.5	200 m layer-average trajectory for day 216. . . .	29
5.6	Ozone and temperature versus altitude, day 216. .	30
6.1	Diurnal variation of net radiation over blacktop, concrete, and soil. . . . .	37
6.2	Same as Fig. 6.1 but for ground heat storage. Water content=0.35. . . . .	38
6.3	Same as Fig. 6.1 but for the sum of the sensible and latent heat fluxes. Water content=0.35 . . .	39
6.4	Diurnal variation of the ratio $G/F_n$ for blacktop and concrete. . . . .	40

<u>Number</u>		<u>Page</u>
6.5	Same as Fig. 6.4 but for soil . . . . .	41
7.1	Trend determined from deviations in visibility from the respective monthly mean (1955-1972) at Birmingham, AL. . . . .	46
7.2	Fast Fourier transform of visibility time series at Raleigh-Durham, NC . . . . .	47
7.3	Bimodal annual oscillation of visibility and relative humidity at National Airport (D.C.). . .	48
7.4	Bimodal annual oscillation of visibility and relative humidity at Cleveland, OH. . . . .	48
8.1	Percent frequency of the number of smoke days from a particular resultant wind direction at Houston, 1949-1968. . . . .	54
8.2	Same as Fig. 8.1 except for haze days . . . . .	55
8.3	Annual visibility frequencies (%) and linear trend lines in the four visibility ranges for Houston, 1949-1968. . . . .	56
9.1	National Air Surveillance Network stations whose data are employed in the present research . . . .	67
9.2	Time series of one year's sulfate data (1972) for Nashville, TN . . . . .	68
9.3	Regionally representative seasonal means (1969-1974) . . . . .	69
9.4	Patterns of synoptic weather (12 GMT) and sulfate concentration . . . . .	70
9.5	Sulfate concentration versus wind direction at St. Louis, MO, January-December 1969. . . . .	71
9.6	Patterns of synoptic weather (12 GMT) and sulfate concentrations. A reconsideration of Fig. 9.4. .	72
10.1	Geographic variation in annual SO <sub>2</sub> emission density . . . . .	77
10.2	Area and stations analyzed. . . . .	78

<u>Number</u>		<u>Page</u>
10.3	Representative sea level pressure analyses during the air stagnation period 16-22 July 1957 . . . .	79
10.4	Average wind speed profile for westerly flow at Washington, D.C. . . . .	80
10.5	Average wind speed profile for westerly flow at Akron, Ohio . . . . .	80
10.6	Time variation of the deviation in westerly wind from its daily mean at Washington, D.C. . . . .	81
10.7	Time variation of the deviation in westerly wind from its daily mean at Akron, Ohio . . . . .	82
10.8	Cross section of 06 GMT easterly flow (U component) across terrain. . . . .	83
10.9	Cross section of 12 GMT westerly flow (U component) across terrain. . . . .	84
10.10	Hodographs of the wind variation at DCA in the easterly and westerly flow. . . . .	85
11.1	Variations in the wind field within a symmetrical valley due to uneven heating of the variably sloped terrain (Defant, 1951). . . . .	93
11.2	Night and day wind roses at a valley (Nash) site. . . . .	94
11.3	Terrain surrounding the Nash site . . . . .	94
11.4	Night and day wind roses at a mountain (Hockey) site. . . . .	95
11.5	Terrain surrounding at the Hockey site. . . . .	95



## TABLES

<u>Number</u>		<u>Page</u>
4.1	Heat island strength---annual and seasonal averages. . . . .	16
4.2	Maximum contribution from anthropogenic heat emissions. Predictions from Summers' (1965) model . . . . .	16
4.3	Duurnal temperature amplitudes (July 8-11, 1976) . . . . .	17
4.4	Wind speed--annual average. . . . .	17
5.1	Comparison of the character of the morning profile and the estimated time of trajectory passage over southern Lake Michigan . . . . .	30
7.1	Stations used in this study and grouped according to geographical region. . . . .	49
8.1	Station information and data years used . . . . .	57
8.2	Number of days with obstructions to vision and mean daily visibility . . . . .	57
8.3	Results of the correlation between annual mean visibilities and the number of days with obstructions, 1949-1968 . . . . .	58
8.4	The total number of days with smoke and the mean population for all locations. . . . .	58
8.5	Number of days with haze and average relative humidity for each station . . . . .	59
8.6	Correlation coefficients between population growth and (a) the frequency with mean visibility less than 7 miles and (b) visibilities in the 13 to 15 mile range . . . . .	59

<u>Number</u>		<u>Page</u>
8.7	Distance and direction from the Gulf of Mexico and mean visibility for all locations . . . . .	60
8.8	Visibility trend analysis for season and locations with a downward trend (1949-1968). . . . .	61
10.1	Station identifiers and elevations . . . . .	78
11.1	Data collected at each of the eight fixed stations . . . . .	96
11.2	The frequency of surface winds coincident with the upper level winds . . . . .	97
11.3	Day to night variations in poor (<25%) and good (>60%) agreement of surface and upper level directions during the SW parallel and NW perpendicular analysis periods . . . . .	98
11.4	Percentage of time Tower and Hockey wind directions were within the indicated degrees of the 850 mb wind during the 00 and 12 GMT radiosonde releases. . . . .	99

## ACKNOWLEDGMENTS

The bulk of the work contained in this report is primarily the achievement of graduate students in the atmospheric sciences program of North Carolina State University, through the completion of their Master's theses. These students, whose names appear as principal authors of their respective contributions to this report, have adequately vindicated the original concept of "Graduate Research in Air Quality Meteorology."

The support of personnel of the EPA Meteorology and Assessment Division, through guidance of several of the graduate students in their research efforts, has been invaluable. Mr. George C. Holzworth and Dr. Jason K.S. Ching are deserving of special recognition in this regard.

Appreciation is also expressed to Dr. Walter D. Bach of the Research Triangle Institute for his contribution.



## SECTION 1

### INTRODUCTION

The proximity of the atmospheric sciences program at North Carolina State University (NCSU) to the Meteorology and Assessment Division and other EPA facilities has engendered over the past several years professional and scientific cooperation among personnel of the two organizations. NCSU graduate students have benefitted through work at the EPA laboratory and helpful guidance in thesis research by EPA staff. It was proposed that this on-going cooperative research effort be enhanced through a formal program which focused the joint effort of NCSU students and faculty, and EPA staff, toward solving specific problems of the EPA in air quality meteorology.

This report contains results of this cooperative effort in the form of summaries of eight research theses on diverse topics. The first three contributions (SECTION's 4-6) are concerned broadly with the meteorological analysis of the St. Louis Regional Air Pollution Study (RAPS) data. The topics include the climatology of the St. Louis heat island, the problem of ozone variability in the urban boundary layer, and the analysis of the urban surface-energy budget in an effort to improve parameterization of the surface heat fluxes in air quality models.

SECTION's 7-9 examine the impact of suspended particulates as manifest in the generally deteriorating transparency of the air, both regionally and nationally. The last paper in this series is concerned with the relationship of suspended sulfates to the large-scale air circulation and to other meteorological variables.

The final two reports (SECTION's 10 and 11) tackle the difficult problem of wind structure over the Appalachian Mountains. The implications of this wind structure to pollutant transport and dispersal in complex terrain is also considered.

The format of each of the following eight research contributions consists of an 'Abstract', an 'Introduction' which presents the scope of the problem and relevant literature, and a summary of major 'Results and Conclusions'. Tables and figures follow the text of each paper, and 'References' for all papers are given in a separate section. The abbreviated nature of these papers has necessitated the omission of detail regarding data sources, analysis methods, and explanation of results. The full research theses are, however, available to the EPA.

## SECTION 2

### CONCLUSIONS

Conclusions based on the eight research theses summarized in this report and worthy of special note are here listed by major topic.

Meteorological analysis of the St. Louis RAPS data:

- (1) The urban heat island strength during the day amounts to about  $0.5^{\circ}\text{C}$  and varies little with wind speed, cloud cover, or season. The nocturnal heat island, however, is highly responsive to all three factors, as well as to anthropogenic heat sources.
- (2) Variability in ozone profiles above the urban nocturnal surface inversion is significant and appears to be related to a similar variability in wind profiles. The relevant wind variability occurs on space and time scales unresolvable by the conventional radiosonde network.
- (3) Evaluation of the ratio of subsurface heat flux to net radiation over concrete, blacktop, and soil surfaces has shown that this ratio can be better parameterized in air quality models by incorporating its dependence on surface type and on day versus night conditions.

Atmospheric visibility and suspended particulates:

- (4) Visibility at 14 sites throughout the United States has declined significantly between 1955 and 1972. The annual cycle in atmospheric transparency is inversely related to that in relative humidity.
- (5) The relative contribution of haze, smoke, and dust to decreasing visibilities at several sites in eastern Texas during the period 1949 to 1968 are identified. The haze contribution is part of a regional-scale problem, while the smoke contribution is associated with local sources and the wind direction.

- (6) Most sulfate concentration variability at particular sites appears explained by long-range transport as dependent on the wind pattern, rather than by local conditions of temperature, humidity, or insolation.

Boundary layer wind structure in complex terrain:

- (7) The unexpected occurrence of a nocturnal low-level jet over the north-central Appalachian Mountains during a period of air stagnation has significant implications for regional pollutant transport.
- (8) Winds at the 850 mb level can be useful in describing near-surface winds in mountainous terrain depending on valley-ridge orientation and time of day. This relationship provides a simple parameterization of winds in complex terrain for anticipating pollutant dispersal.

### SECTION 3

#### RECOMMENDATIONS

Results of the work described in this report should, in many cases, be considered preliminary. Specific recommendations for further research work by the EPA include:

- (1) Use of the full St. Louis RAPS data-set (1974-77) to strengthen the conclusions of the study of the urban heat island based on 1976 data (SECTION 4). In particular, the role of rural soil moisture and of urban anthropogenic heat sources to the diurnal and seasonal heat island strength need further investigation.
- (2) Use of the full RAPS data-set to extend the two-month study period of energy budget evaluations for various types of surfaces (SECTION 6). The ultimate goal of formulating an improved parameterization of the surface heat flux in air quality models which properly accounts for seasonal variability and the urban environment seems achievable with an extension of this study.
- (3) Further regional assessments of trends in atmospheric visibility, like that in eastern Texas (SECTION 8), is one means of detecting the environmental impact of mass migrations of the U.S. populous as, for example, the apparent shift in population from the northeast to the "Sun Belt" states.
- (4) Further study of suspended sulfates and their relationship to source areas and meteorological variables (SECTION 9). However, major revelations would only seem possible with increased sampling resolution over that provided by the present National Air Surveillance Network, as well as improved means of particulate collection and chemical analysis.
- (5) Additional studies of the mesoscale boundary layer wind structure in complex terrain (SECTION's 10 and 11) with emphasis on consequent pollutant transport and dispersal over such regions.



## SECTION 4

### CLIMATOLOGICAL ASPECTS OF THE ST. LOUIS URBAN HEAT ISLAND

Joseph E. Steigerwald, G.F. Watson, and J.K.S. Ching

#### Abstract

The St. Louis urban heat island is studied using one year of temperature data (1976). Fluctuation in the strength of the urban heat island due to changes in cloud cover, wind speed, and season are explored.

The heat island strength varies diurnally and seasonally, and is largest on fall evenings and weakest on summer mornings. It is also very strong under low wind speed and clear sky conditions, with the wind speed exerting more control on the nocturnal heat island strength than cloud cover. The daytime heat island, the nocturnal heat island, and the transition periods are examined in detail. The nocturnal heat island and the transition periods vary greatly with changes in cloud cover, wind speed, and season; the daytime heat island varies little with changes in these factors.

Summers' (1965) heat island model was used to evaluate the contribution of the anthropogenic heat output to the urban heat island. The results were compared with results derived from an analysis of the St. Louis Heat Emission Inventory. The emission data comparison was inconclusive.

## INTRODUCTION

The term 'heat island' is used to describe the ground level air temperature difference between urban and rural areas. The urban area is normally warmer than the surrounding rural area. A heat island forms because cities are composed of materials whose thermal characteristics differ from the natural materials that they replace. This factor combined with anthropogenic heat emissions and the effect on wind speed and albedo caused by the city's physical presence produce a change in the microclimate encompassing the city. This microclimate is warmer and drier than that in the country-side, except in winter when it is warmer but more moist (Hage, 1977).

Many studies of the urban heat island have been made over the years. Howard (1883) conducted one of the first of many studies of the London, England heat island. Subsequently the heat islands of Paris, France (Renou, 1862); Dallas/Fort Worth, Texas (Ludwig, 1968); Cincinnati, Ohio (Clarke, 1969); Akron, Ohio (Martin and Powell, 1977); and Montreal, Canada (Oke, 1977), just to mention a few, have been described.

The first heat island studies were usually comparisons of two temperatures, one urban and one rural. Spacial features were pointed out by Schmidt who used an automobile to traverse the urban area to measure temperatures (Duckworth and Sandburg, 1954). Since then automobiles have been a major platform used in many heat island studies to get temperature readings at a number of points along a set route.

The use of a network of instruments at fixed sites is fairly common in recent field investigations of heat islands. The heat island studies of Austin, Texas (Wood, 1971) and St. Louis, Missouri (Shreffler, 1979) both used such a network.

The altered climate found in the cities needs to be studied because it affects the air flow in and around the city. Cities emit undesirable pollutants that affect those who live in and downwind of their source, and it is necessary to understand the transport capacity of the urban induced circulation. This circulation is, to a large degree, controlled by the magnitude of the urban heat island.

The present study utilizes data from the St. Louis Regional Air Pollution Study (RAPS) as a basis for better documenting and

understanding the urban heat island and how it varies with season and various meteorological parameters. As the urban heat island is better understood, the urban centers may be planned to enhance or dilute the heat island effect depending on what is most beneficial to the area. Once a reliable climatology for the urban area has been established, it can be incorporated into pollution distribution models to ensure that they model the pollutants as realistically as possible. The present study hopes to make a contribution to the climatology of the urban heat island.

## RESULTS AND CONCLUSIONS

The daytime urban-rural temperature difference, or heat island strength (H.I.S.), varies little from day to day; different winds speeds and cloud cover conditions have little effect on it. The annual average daytime H.I.S. is  $0.6^{\circ}\text{C}$ , varying only from  $0.5^{\circ}\text{C}$  in fall to  $0.7^{\circ}\text{C}$  in winter.

The daytime heat island is seasonally consistent because a very deep mixed layer is present through the day. Any changes or inputs that might affect the daytime H.I.S. are mixed throughout this layer diluting their effect. Thermal mixing accounts for this very deep mixed layer, often called the 'planetary boundary layer', which extends up to a kilometer or more in depth.

The nocturnal heat island is more complex and not as steady as the daytime heat island. The H.I.S. varies significantly with wind speed, cloud cover, and season. It is strongest in the fall ( $2.9^{\circ}\text{C}$ ) and weakest in the winter ( $1.6^{\circ}\text{C}$ ).

Wind speed exerts more influence on the urban heat island than does the amount of cloud cover. Figures 4.1 and 4.2 show the H.I.S. versus cloud cover and the wind speed, respectively. In general, the clearer the skies or the lower the winds, the more pronounced is the nocturnal heat island. These meteorological conditions favor a greater and more rapid cooling of the rural surface layer thus producing a larger urban-rural temperature difference than under other conditions. Table 4.1 lists the average nocturnal H.I.S. for all three cloud cover and wind speed groups. If cloud cover is constant, the H.I.S. drops steadily as wind speed increases. If wind speed is constant, the H.I.S. usually drops as cloud cover increases, but not in all cases, and certainly not at a steady rate.

The nocturnal heat island strength exhibits seasonal trends and these trends are modified by weather conditions. The winter, spring, and summer nocturnal heat islands attain their maximum values just after sunset, then the nocturnal H.I.S.

declines until morning. Fall is different, though, in that the maximum strength occurs just before sunrise. These trends are most obvious under partly-cloudy skies and/or moderate winds as suggested by Figures 4.3 and 4.4. High winds and overcast conditions muddle these trends, and low winds and clear skies yield a constant nocturnal H.I.S.

Graphs of the diurnal heating and/or cooling rates for the urban and rural area are a useful tool. When compared, the differences in these two curves show how the heat island grows, matures, and decays. The seasonal curves of the rate of temperature change (Figure 4.5) for the urban area are remarkably consistent throughout the year. All of the urban curves, except fall, have the same maximum and minimum rate of temperature change (about  $1.5^{\circ}\text{C}/\text{hour}$  and  $1.0^{\circ}\text{C}/\text{hour}$ , respectively). The rural rate of temperature change varies from season to season. It is the way in which temperature in the rural area changes, that governs the strength and timing of the urban heat island (Oke, 1977). The rural rate is in turn controlled by such factors as city size, degree of urban industrialization, amount of vegetation, and geography of the area (Oke and Maxwell, 1975).

The exact contribution to the urban heat island from anthropogenic heat sources is difficult to assess. A comprehensive listing of all of the contributors would be much too complicated and costly. Even though this is true, heat emission inventories are the only way to accurately estimate the contribution of anthropogenic heat sources in the H.I.S.

One such heat emission inventory was conducted in St. Louis as part of the RAPS/RAMS project. This study, conducted using 1976 data, took into account all point and area sources, stationary and mobile. Specific source data were used for all point sources; annual records were used for the area sources.

The annual curve for both rural and urban emissions are shown in Figure 4.6. The data are confusing and difficult to explain. The midnight maximum in emissions and the 0800 CST minimum are contrary to the activity pattern of industry or the population. In addition, none of the seasonal curves have any features that can be identified as a traffic peak (a peak in the heat emission curve caused by rush-hour traffic), even though 30 percent of the total sources are mobile. A fall maximum at 1600 CST, a spring minimum at 1800 CST, and an unexpected minimum at 0500 CST in the summer also present problems in data interpretation.

Details of the heat emission inventory data were reviewed. The diurnal variations of anthropogenic heat output, which are on the order of 5 percent, cannot be responsible for the diurnal fluctuations on the order of  $2^{\circ}\text{C}$  in the annual average H.I.S.

Clearly, the diurnal fluctuations in the H.I.S. curves are due to some other factor or combination of factors.

The influence of anthropogenic heat output on the urban heat island is overshadowed by the effect of solar radiation during the day. However, anthropogenic heat output at night becomes an important factor in the formation and strengthening of the urban heat island (Bowling and Benson, 1978).

While individual diurnal fluctuations are negligible, the anthropogenic heat output is the correct order of magnitude and exhibits the expected seasonal variation. When substituted into Summers' model (Summers, 1965) in order to predict the contribution of anthropogenic heat sources to the H.I.S., the heat emission data suggest a contribution of about  $1.5^{\circ}\text{C}$  to the urban heat island (under a wind speed of  $2\text{m/s}$ ). The contribution changes with the season becoming less than  $1.4^{\circ}\text{C}$  in the summer. In percentages, these figures represent 110 percent and 56 percent contributions (winter and summer, respectively) of anthropogenic heat sources relative to the solar contribution (see Table 4.2). Obviously, the anthropogenic heat output does not contribute 110 percent to the winter urban heat island. This result is a statistical anomaly caused by comparing the maximum contribution made by anthropogenic heat as a percentage of the average winter H.I.S.

The amount of moisture trapped within the soil exerts some control on the urban heat island, but unfortunately the soil's moisture content was not one of the parameters recorded during the study. A qualitative assessment of the importance of this variable can still be made using temperature measurements taken during a period of drying. This can be accomplished by recording and then analyzing the diurnal temperature cycle for the urban and rural areas. Decreased moisture within the urban area should have little effect on the diurnal temperature cycle, since up to 50 percent of the urban fabric is composed of materials that are impervious to moisture and thus greatly reduce evapotranspiration (Landsberg, 1968).

Table 4.3 shows the amplitude of the urban and rural diurnal temperature traces for July 8 and 11, 1976 as well as the H.I.S. This four day period was relatively dry with no precipitation and only scattered clouds. The data show no trend towards an increasing diurnal amplitude in temperatures for the rural area. In addition, the H.I.S. does not increase significantly. These results contradict those of Lyall (1977) for London and environs.

Table 4.4 compares seasonally and annually averaged rural and urban wind speeds. The increased roughness length found in the urban area slows the wind speeds by as much as 18 percent. This maximum reduction occurs in the spring; the annual

reduction averages to 11 percent. These results are in agreement with those presented by Lowry (1972), who states that a 20 to 30 percent drop in the wind speed is observed in the urban area. At these lower wind speeds, the air has a greater residence time in the urban canyon enabling it to absorb more of the heat stored by the buildings and other urban surfaces (called the 'canyon effect'). This increases the H.I.S.

It appears possible to draw five basic conclusions from this analysis of the climatology of the St. Louis urban heat island.

- 1) The daytime H.I.S. remains constant (at about  $0.6^{\circ}\text{C}$ ); changes in season, wind speed, and cloud cover have little effect on it.
- 2) The nocturnal heat island strength varies significantly with season, amount of cloud cover, and changes in wind speed. Of the latter two, increased wind speed has a greater effect on the nocturnal heat island strength, causing a rapid reduction.
- 3) The 1976 RAPS Heat Emission Inventory needs further scrutinizing. The data, while not in a very useful form, are of the correct order of magnitude and give some indication of the importance of anthropogenic heat emissions to the formation of the urban heat island. While diurnal fluctuations are negligible, and the contribution during the day seems insignificant, anthropogenic heat sources do contribute to the nocturnal H.I.S. The exact proportion of their contribution in St. Louis needs further study.
- 4) The effect of moisture on the urban heat island is unclear. The results presented here disagree with the results presented elsewhere. Enhanced cooling was not observed in the rural areas surrounding the St. Louis metropolitan area. However, the data set used was limited and the results inconclusive.
- 5) The RAPS/RAMS data need and deserve more study. The experiment continued from 1974 to 1977, amassing a huge quantity of data, meteorological as well as ambient air concentrations of certain pollutants. Very little of its full potential has been realized. Analyses similar to those attempted in this study should be undertaken with the full data set. This should further refine the conclusions of this study and make them of real value in understanding and modeling the urban heat island.

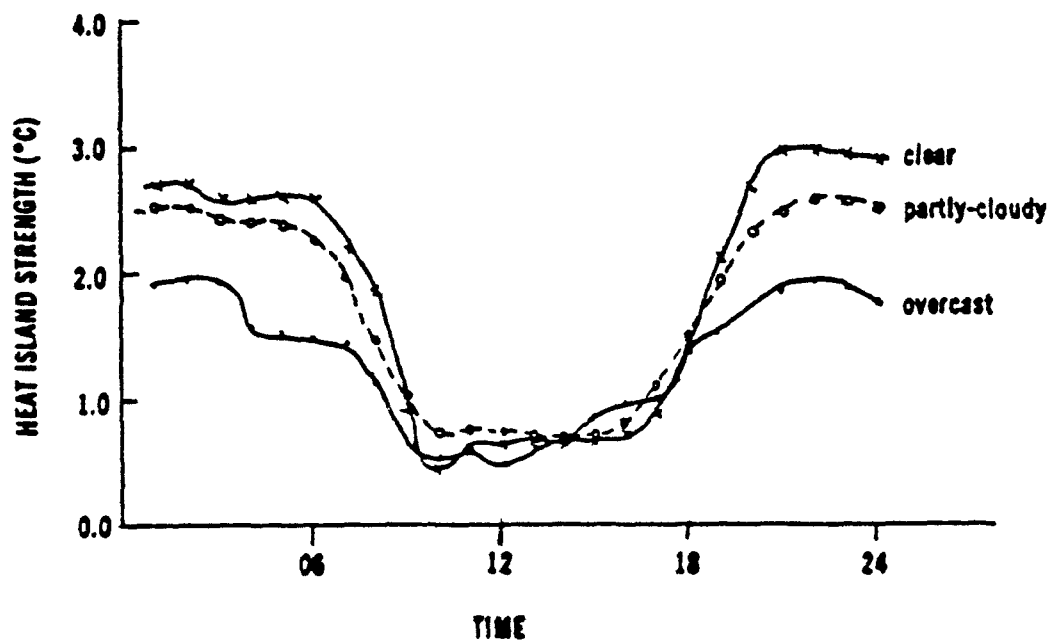


Figure 4.1 Heat island strength by cloud cover category.

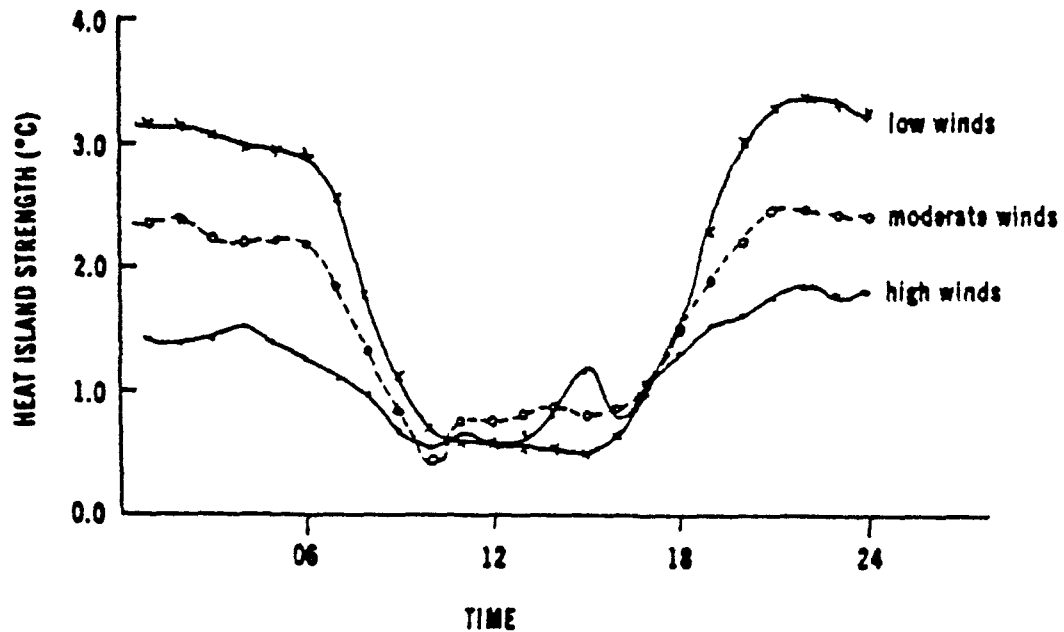


Figure 4.2 Heat island strength by wind speed category.

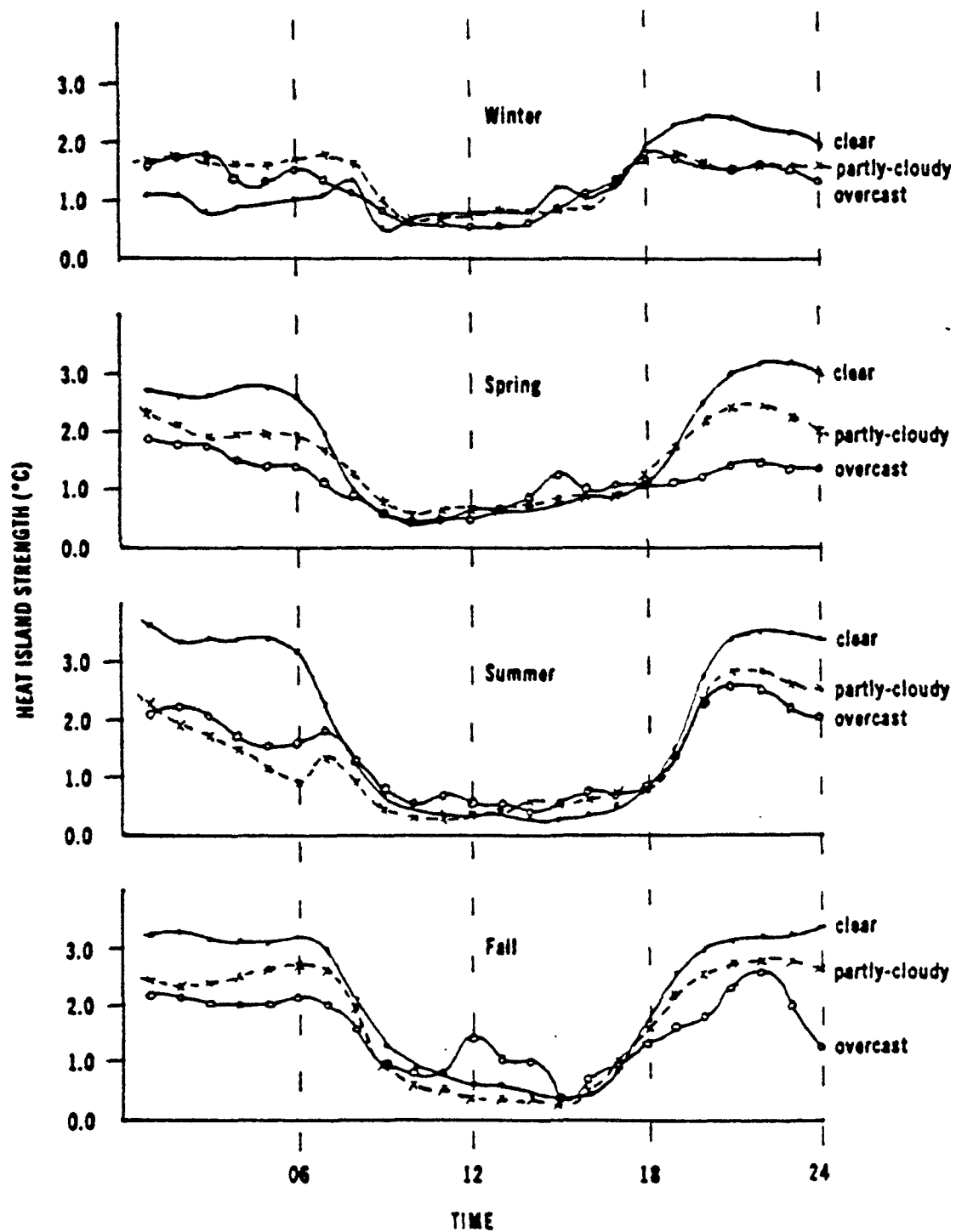


Figure 4.3 Heat island strength by cloud cover category and season.



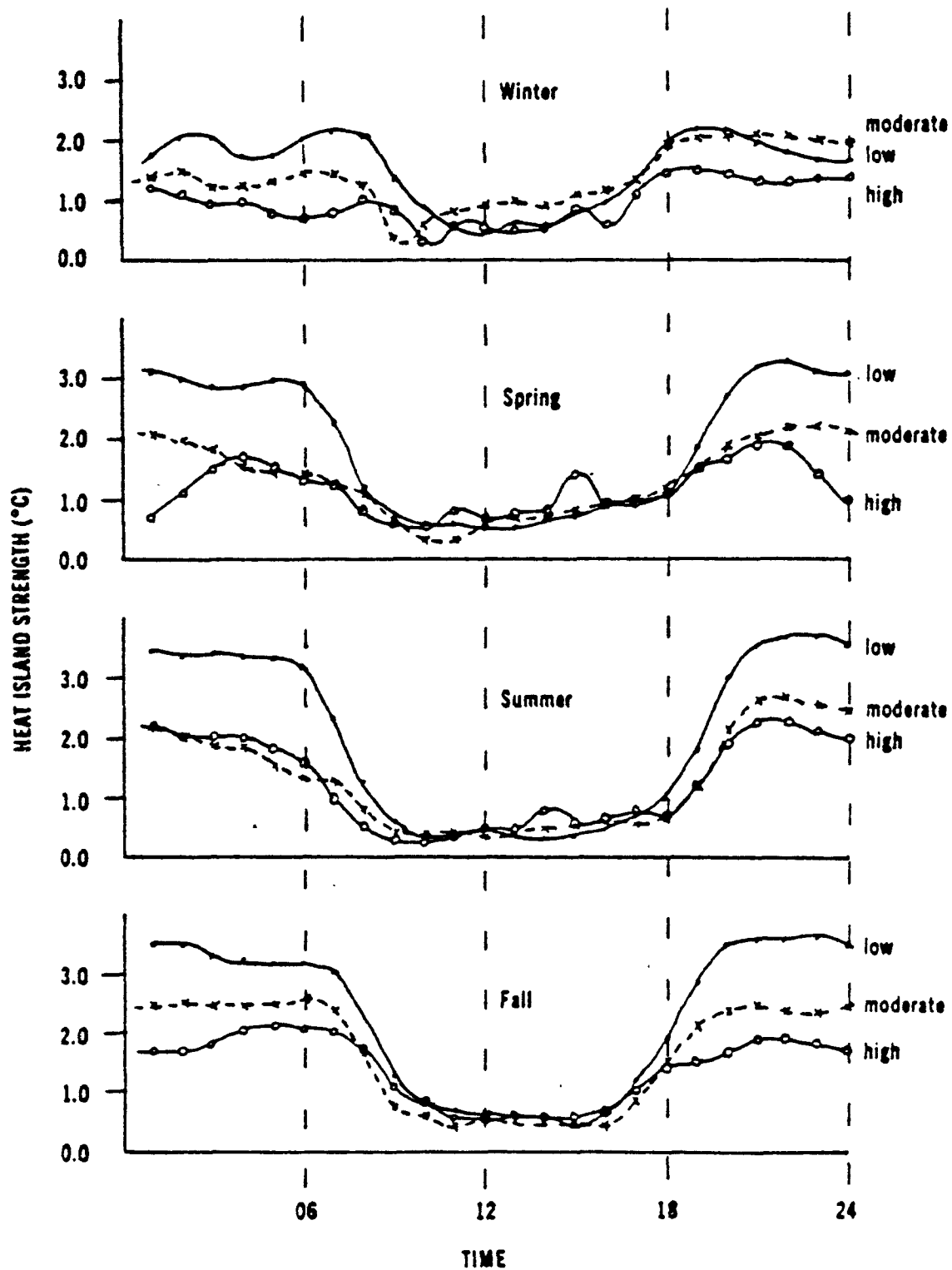


Figure 4.4 Heat island strength by wind speed category and season.

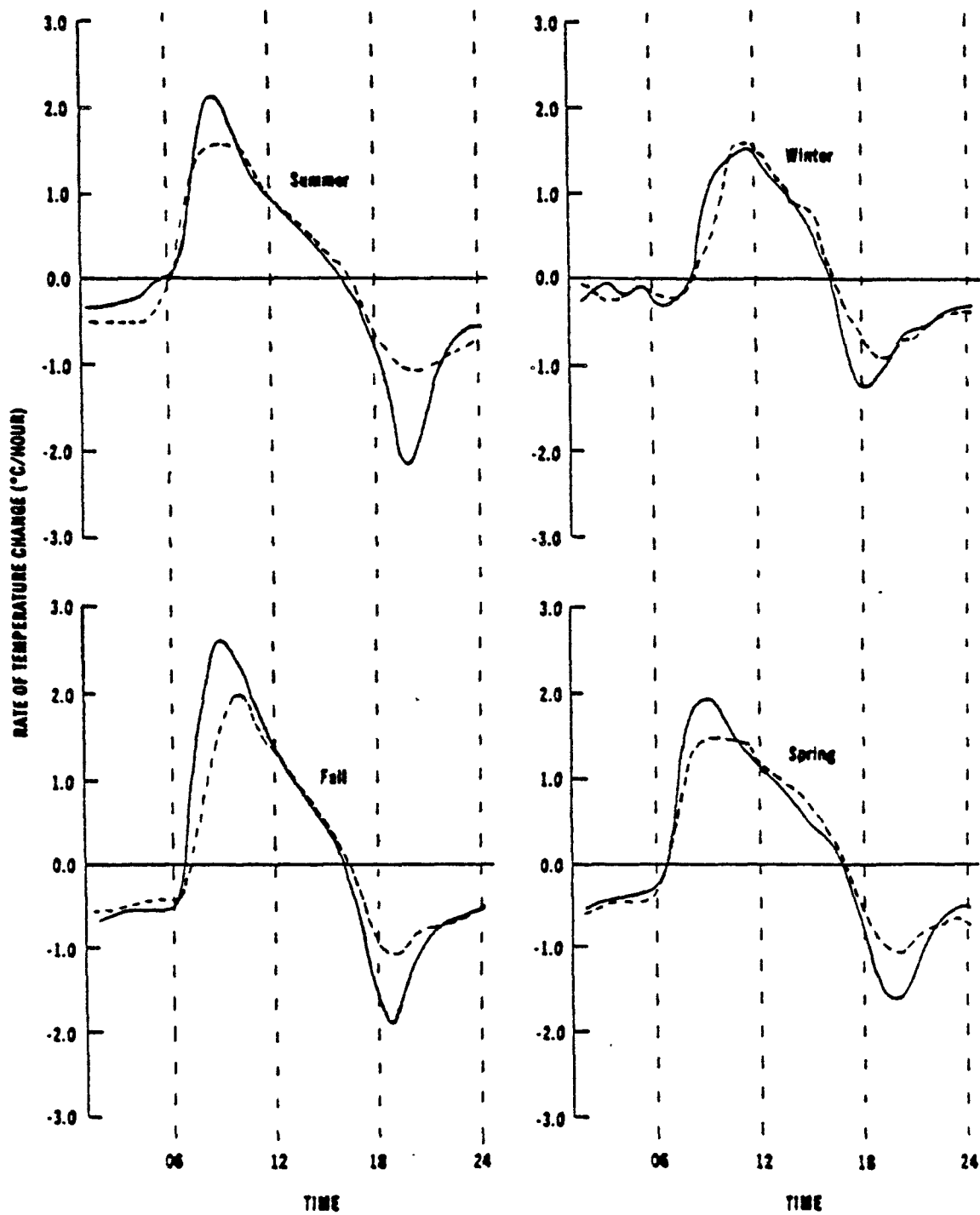


Figure 4.5: Rate of change of temperature .. seasonal averages. Solid line .. rural temperatures; dashed line .. urban temperatures.

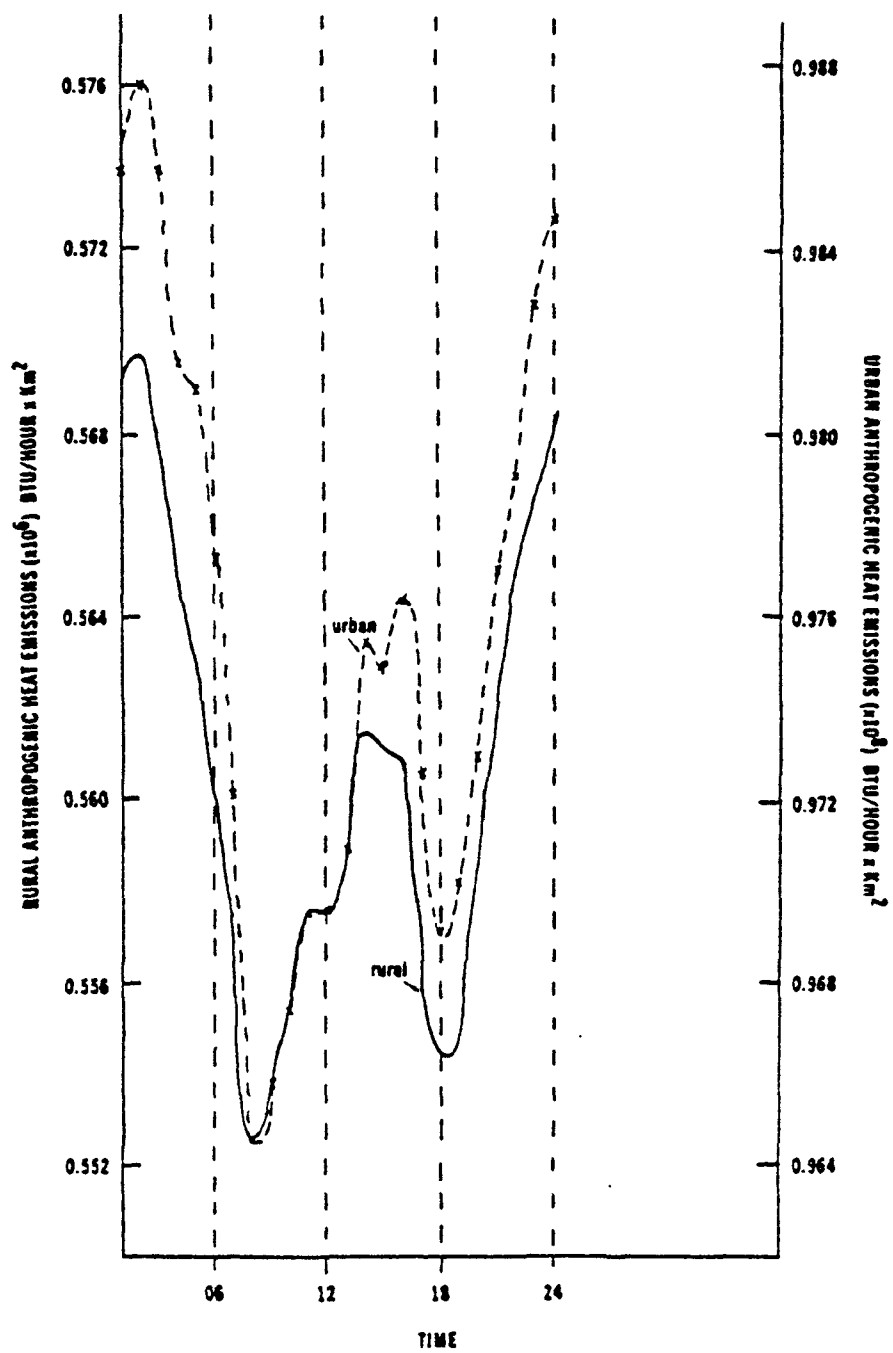


FIGURE 4.6: Anthropogenic heat output .. annual average.

Table 4.1 Heat Island Strength --- Annual and Seasonal Averages.

	<u>Day</u>	<u>Night</u>
Annual	0.60°C	2.60°C
Winter	0.75°C	1.60°C
Spring	0.70°C	2.20°C
Summer	0.45°C	2.50°C
Fall	0.45°C	2.90°C

Table 4.2 Maximum Contribution from Anthropogenic Heat Emissions. Predictions From Summers' (1965) Model.

<u>Season</u>	<u>Maximum contribution</u>	<u>Percentage of average</u>
Winter	1.77°C	110%
Spring	1.54°C	70%
Summer	1.39°C	56%
Fall	1.55°C	53%

Table 4.3 Diurnal Temperature Amplitudes. (July 8 - 11, 1976). (M= morning; E= evening).

	Rural		Urban		H.I.S.	
	<u>M</u>	<u>E</u>	<u>M</u>	<u>E</u>	<u>M</u>	<u>E</u>
July 8	11.2	10.5	10.0	7.8	1.2	2.7
July 9	11.2	10.6	8.2	9.2	3.0	1.4
July 10	13.5	13.0	12.5	11.0	1.0	2.0
Average	12.0	11.4	10.2	9.3	1.7	2.0

Table 4.4 Wind Speed --- Annual Average.

			Percent
	<u>Rural (m/s)</u>	<u>Urban (m/s)</u>	<u>reduction</u>
Annual	4.25	3.77	11.0
Winter	5.29	4.47	15.5
Spring	5.03	4.13	17.9
Summer	3.34	3.22	3.6
Fall	3.41	3.33	2.4

## SECTION 5

### A STUDY OF THE VERTICAL DISTRIBUTION OF OZONE AND THE VARIABILITY OF THE WIND FIELD ABOVE A NOCTURNAL RADIATION INVERSION

Donald R. Hood and A. J. Riordan

#### Abstract

The vertical distribution of ozone prior to the morning breakdown of the radiation inversion is related to the changes in the nocturnal wind field and the trajectory of the layer containing the ozone. Helicopter and hourly pilot-balloon data collected on five days during August 1976, in St. Louis, Missouri, were analyzed.

The ozone was assumed to be uniformly mixed throughout the boundary layer at sunset the previous evening. The study indicates that the similarities and differences between the vertical distribution of ozone assumed at sunset and observed the following morning are related to the variability of the nocturnal wind field.

Analysis of height-time cross sections of the nocturnal wind field indicated that the winds exhibited both vertical and temporal variability above an observation point. Most of the temporal variability in the nocturnal wind field occurs between scheduled radiosonde launch times and will not be completely detected. Therefore, the trajectory computations will not entirely represent the changes which occur. The study also indicates that due to the vertical variability of the wind field, more representative trajectories can be obtained by computing the trajectories for several thin layers versus computing a single trajectory for a thick layer.

## INTRODUCTION

The formation, destruction, and transport of ozone can be investigated through examination of air pollution and meteorological parameters measured in St. Louis, Missouri, as part of the Regional Air Pollution Study (RAPS). RAPS was a multi-year research program conducted by the Environmental Protection Agency (EPA) in St. Louis, in which air quality and meteorological parameters were measured both at the surface and in the lower troposphere from 1974 through 1976. As part of the RAPS, a network of air monitoring stations, called the Regional Air Monitoring System (RAMS), was established to provide a large body of ground level air monitoring data (Figure 5.1). Figure 5.1 also locates four upper air network sites (UAN) numbered 141, 142, 143, and 144, whose purpose was to provide upper air wind data using pilot-balloons (PIBALs) and radiosondes. In addition, during data-intensive periods, helicopter flights originating at Smartt Field were used to obtain the vertical distribution of ozone, total oxides of nitrogen, carbon monoxide, sulfur dioxide, particulate light scattering, temperature and dewpoint as a function of time and altitude. Also during data intensive periods PIBALs were launched each hour from all four UAN sites, with the exception of 0400, 1000, 1600, and 2200 CST, at which times radiosondes were launched from all four UAN sites.

The case studies to follow will use data collected during the summer 1976 data intensive period. The helicopter spirals used in the case studies were observed over Smartt Field which is located in a rural setting approximately 35 km north-north-west of the center of St. Louis. The case studies will also use PIBAL observations taken at UAN site 144 which is located approximately 25 km to the east-southeast of Smartt Field.

The purpose of this study is to describe the early morning vertical distribution of ozone (the ozone profile) above Smartt Field and to relate the shape of the ozone profile to the changes in the wind field that have occurred since sunset on the previous evening and to the trajectory of the air containing the ozone prior to its arrival over Smartt Field.

## RESULTS AND CONCLUSIONS

Five case studies detailing the changes in the wind field above a nocturnal radiation inversion and the effect of these changes on the shape of an early morning ozone profile are presented.

The five days were chosen based on the following criteria:

(1) Either a surface-based radiation inversion or a low-level elevated inversion were present at the time of the helicopter spiral so that the profile was protected from scavenging from below.

(2) No frontal system was present in the St. Louis area from sunset the previous evening to the time of the helicopter spiral.

(3) The helicopter spiral was high enough to detect the subsidence inversion above Smartt Airfield. Thus, the changes in the wind field between the top of the radiation inversion and the base of the subsidence inversion can be related to the shape of the ozone profile.

(4) The helicopter spiral occurred within 3 hours after sunrise so that changes in the shape of the profile due to photochemical activity will be at a minimum.

Using the above criteria the 2nd, 3rd, 4th, 7th, and 8th of August 1976 were chosen from a total of eleven days with morning helicopter spirals for which edited helicopter data were available. Throughout the case studies these five days will be referred to as day 215, 216, 217, 220, and 221, respectively.

The height-time sections for each of the five case-study days have shown that the nocturnal wind field between the top of the radiation inversion and the base of the subsidence inversion is highly variable. The wind field not only exhibits variability with time but also exhibits a large amount of vertical variability above an observation site at a given time. Figures 5.2 and 5.3 for day 216 serve as examples. In addition, the height-time sections have shown that most of the variability in wind speed and direction occurs between the scheduled launch times (1800 CST and 0600 CST) of radiosondes routinely used to obtain wind observations.

The vertical variability of wind direction is most evident on days 216, 217, and 221. On days 215 and 220 the winds were fairly uniform at the time of the helicopter spiral, but the winds had exhibited changes in direction earlier in the night.



The structure of the wind field seems closely related to the shape of the ozone profile. On day 216, for example, a well-developed jet persisted at 200-300 m above the ground for the 8 hours previous to the ozone measurement. A sharp spike in ozone concentration was then found just above the level of the jet maximum. Concentrations decreased rapidly from 400 to 800 m in a zone of over 90 degrees of wind shear which descended from much higher elevations during the night as the low-level jet became concentrated in the lowest layers. Thus, the morning ozone profile has probably been shaped by important structures and variations in the nocturnal wind field. More ozone measurements would certainly have aided in quantifying the relationship.

In all five cases examined the trajectory computed for the original layer (maximum top 2000 m) followed almost the same path as the trajectory for the 900-1100 m AGL layer. Compare, for example, Figures 5.4 and 5.5 for day 216. This agreement might be expected since the 900-1100 m AGL layer is approximately in the middle of the original layer (maximum top 2000 m AGL) depending on the top and base of the layer chosen by the trajectory model. The maximum height of the layer base was 5000 m AGL.

The 200 m-layer trajectories outline the region which could be considered the source region for the pollutants arriving over Smartt Field. The trajectories for days 215 and 216 indicated the least variance in the size of the source region for the entire 60-hour trajectory while day 220 showed the greatest variance between layers, and thus possibly the largest source region.

The Heffter-Taylor Trajectory Model is intended for use as a regional scale trajectory model (Heffter et al., 1975). Therefore, it may not be entirely correct to compare the results of the model to the 12-hour hand computed trajectory, since the hand computed trajectory uses only the winds obtained over one site. However, the comparison is important since it gives an idea of the error that may be present in the first 12-hour segment due to the variability of the nocturnal wind field. The end point of the first segment is the starting point of the second segment; thus, the errors would be cumulative with time.

The morning ozone profiles for days 216 (Figure 5.6) and 221 have almost the same shape between the top of the radiation inversion and the base of the subsidence inversion. The ozone profiles for both days exhibit a sharp "spike" of ozone above the top of the radiation inversion with uniform ozone concentrations between the point where the ozone concentrations decrease to a minimum (possibly natural background levels) and the base of the subsidence inversion. On day 221 layers of

ozone are present above the top of the subsidence inversion as opposed to uniform ozone concentration above the subsidence inversion on day 216.

The time of day when the trajectory passes over an urban-industrial area is a primary determinant of the pollutant burden that will be carried away from the area (Ludwig, 1979b; Hester et al., 1977; White et al., 1977). If the trajectory passes over an urban area at night or in the early morning hours (prior to rush hour traffic), the pollutant burden of the trajectory will not be increased as much as it will be if passage occurs between mid-morning and sunset. This is especially true if a radiation inversion is present in the morning when passage occurs. The term "pollutant burden" refers not only to ozone but also to the precursors from which ozone will form downwind of the urban-industrial area.

Table 5.1 indicates that the area around southern Lake Michigan is most likely to make a significant contribution to the pollutant burden on days 215 and 220 and least likely to make a significant contribution on days 216 and 221, while the contribution to the pollutant burden on day 217 is uncertain.

The following conclusions can be drawn from analysis of the trajectories and the height-time sections:

(1) The height-time sections of wind speed and direction have shown that the nocturnal wind fields are highly variable with time and that significant changes can occur between scheduled launch times of radiosondes routinely used to obtain wind observations.

(2) Since the radiosonde observations do not detect changes in the nocturnal wind field which occur between scheduled launch times, these changes cannot be reflected in the trajectory computations.

(3) The height-time sections of wind speed and direction also indicate that the wind field exhibits a large amount of vertical variability above an observation point at a given time. The vertical variability of the wind field in a layer can be represented, at least in part, by choosing smaller layers within the original layer and computing trajectories for the smaller layers. The need for better time-resolution mentioned in (2) is vital here.

(4) Even with the possibility that vertical motion might be taking place, the choice of several small layers as opposed to one overall layer appears to give a better indication of the source region from which the trajectory may have obtained its pollutant burden.

The shape of the morning ozone profile observed in the case studies is highly variable and is sometimes radically different from the morning ozone profile predicted by Ludwig (1979a). If the ozone profile at sunset on the previous evening is assumed to be a Type D profile, which is described by Ludwig as a profile in which the precursors and the ozone that has formed from them are mixed throughout the boundary layer, then the case studies indicate that the shape of the ozone profile on the following morning could be due to one of or a combination of the following:

(1) The variability of the nocturnal wind field, including the variability of the wind speed and direction, and including both the variability with time and vertical variability above an observation point.

(2) The transport of air parcels containing different pollutant burdens in different layers, with little mixing occurring between the layers, over Smartt Field at the time of the helicopter spiral.

(3) The transport of air parcels containing different pollutant burdens by the nocturnal jet.

(4) The proximity of the source region to major urban-industrial areas and the time of day when the trajectory passes the source region.

(5) The formation of, and the change in height of, nocturnal radiation inversions and the more persistent subsidence inversions. These changes could also affect the nocturnal wind field.

(6) The natural background levels present in the trajectory air mass. This would determine the minimum levels of ozone that could be observed if the air came from "clean" remote areas.

The five case studies indicate that the most plausible explanation for the shape of the ozone profile observed over Smartt Field at the time of the helicopter spiral, is the transport of air containing different pollutant burdens in different layers. However, a major problem with the case studies has been a lack of knowledge of the shape of the ozone profile at sunset on the evening prior to the observation of the ozone profile and the changes that occurred in the profile moving with the trajectory prior to the arrival of the trajectory over Smartt Field. Due to the variability of the nocturnal wind field, it does not seem that this problem can be solved easily. Therefore, the best approach to follow would be to observe hourly profiles of ozone, NO, NO<sub>x</sub>, and temperature in conjunction with hourly wind observations over a chosen point to

determine the changes which are taking place in each of the quantities and the possible relationship between the changes.

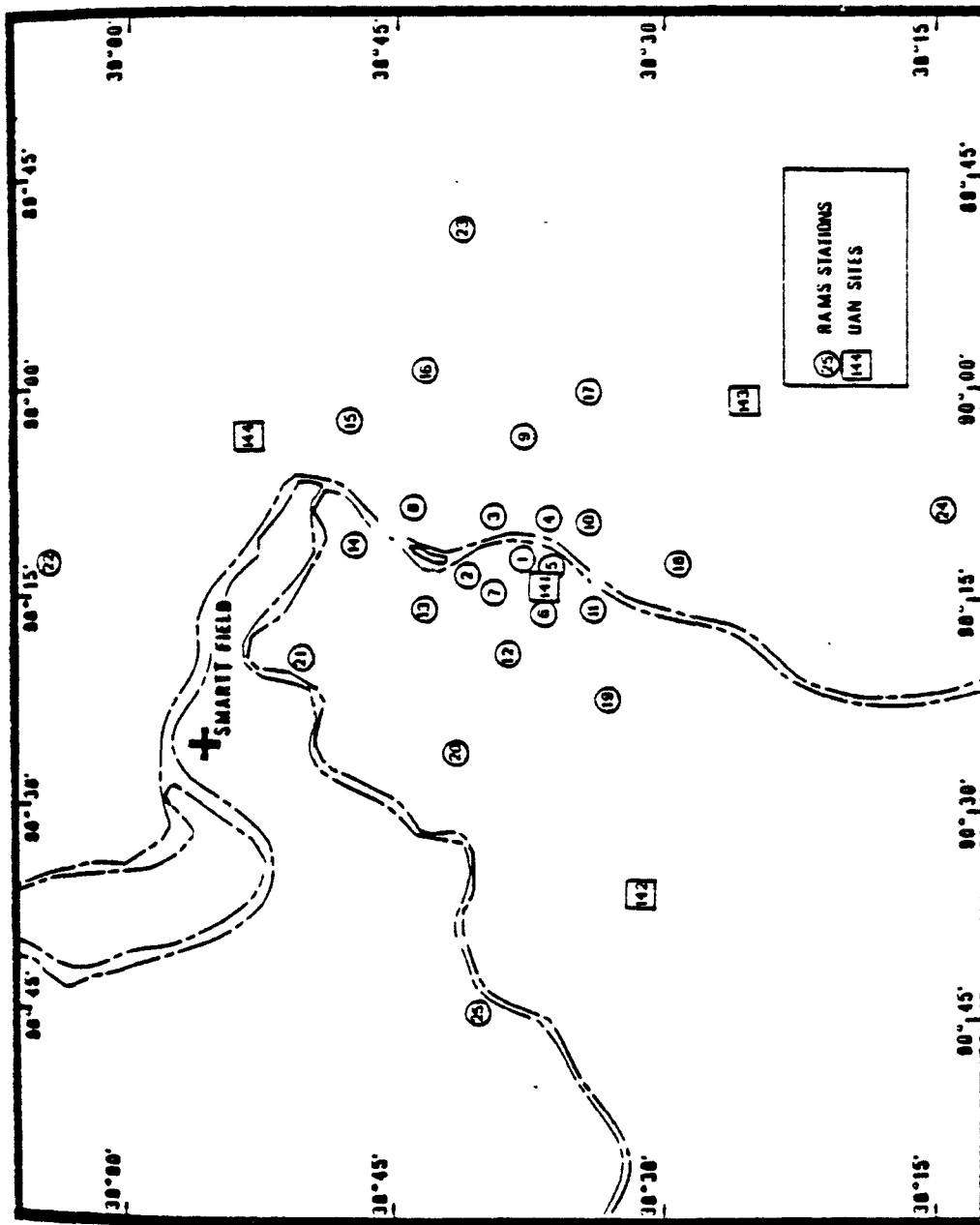


Figure 5.1 Map depicting RAPS facilities in St. Louis, Missouri.

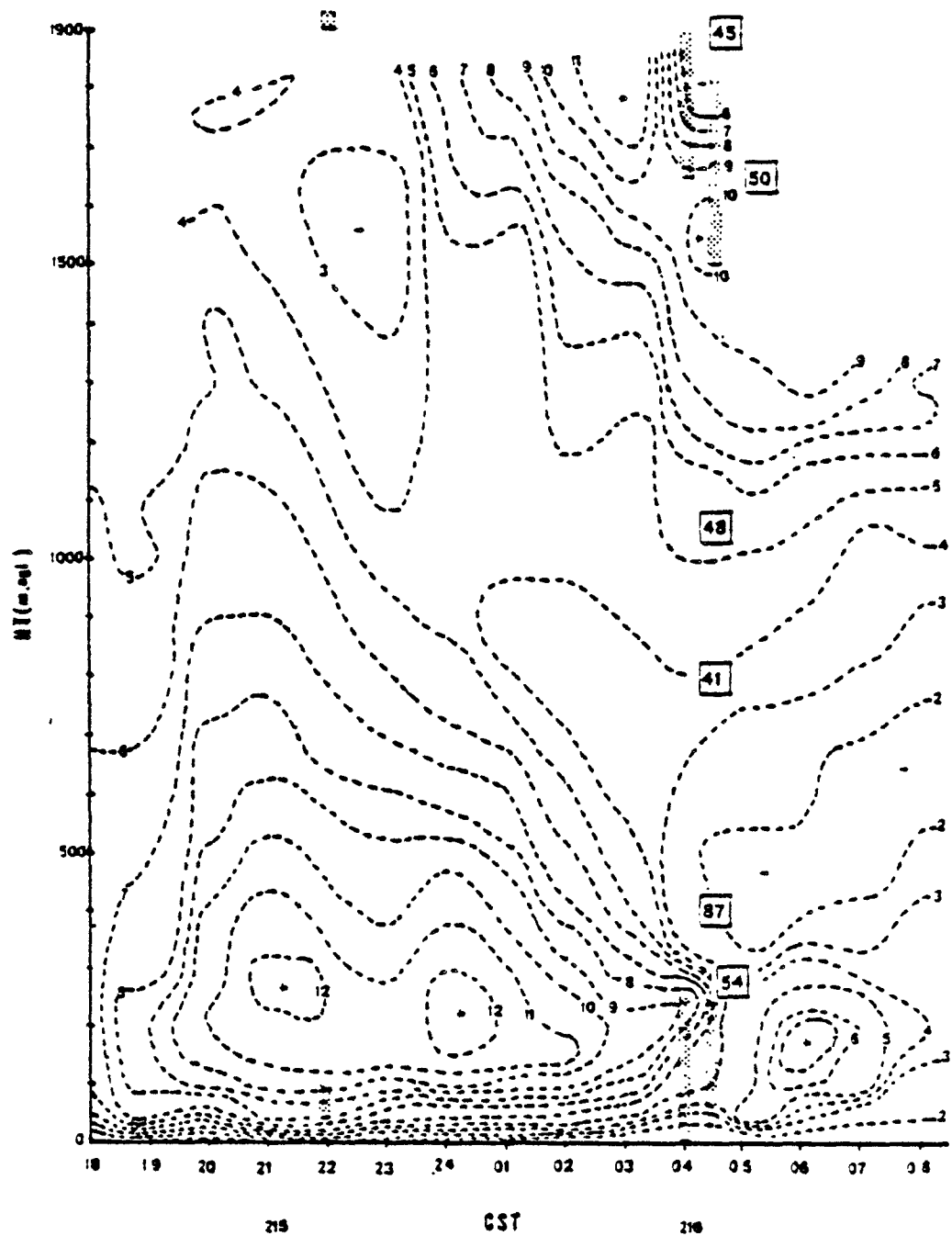


Figure 5.2 Height-time section of wind speed ( $\text{m s}^{-1}$ ) for day 216. Shaded area represents an inversion. A "+" indicates a wind speed maximum. A "-" indicates a wind speed minimum.  $\square$  indicates ozone concentration in ppb.

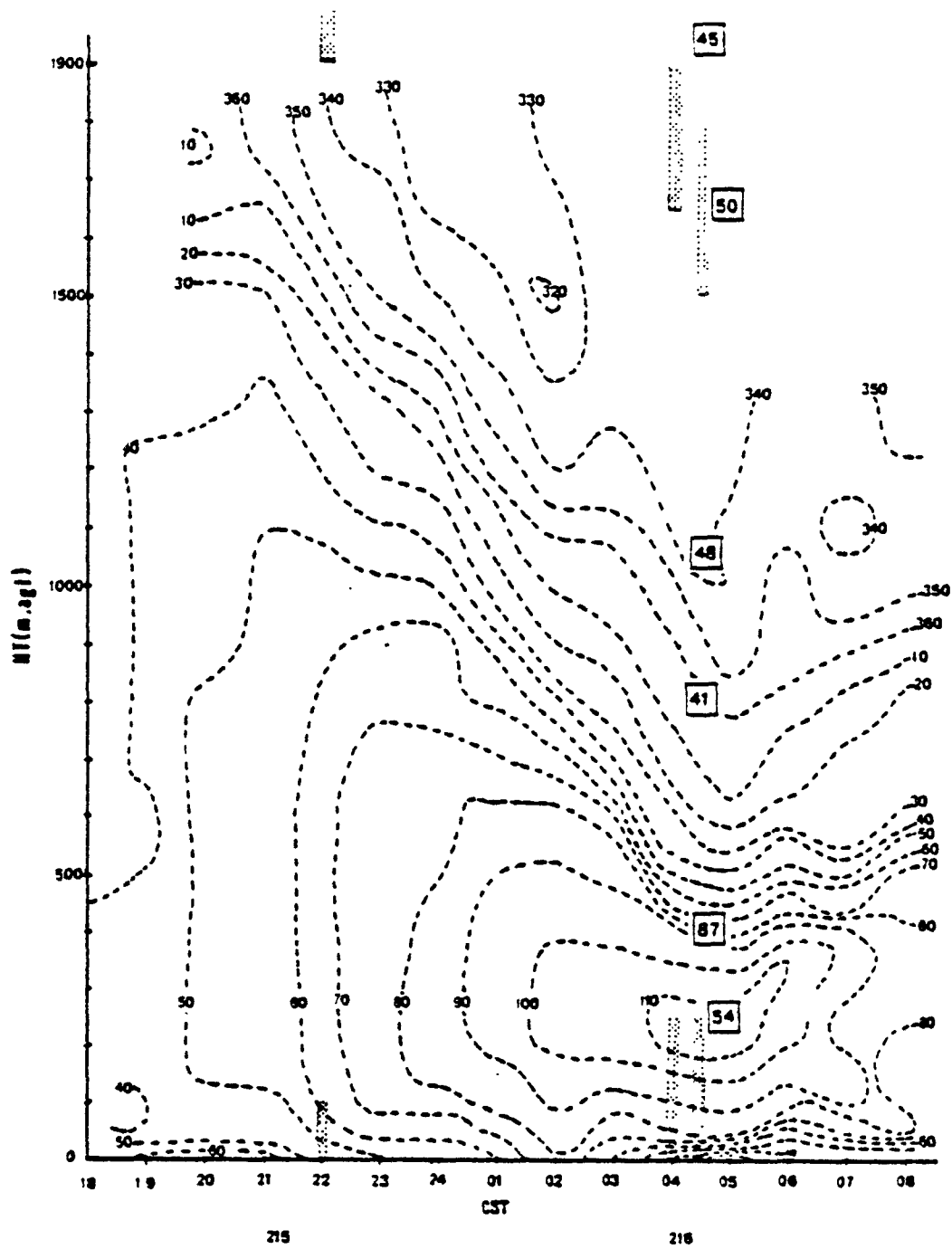


Figure 5.3 Same as Figure 5.2 except for wind direction.

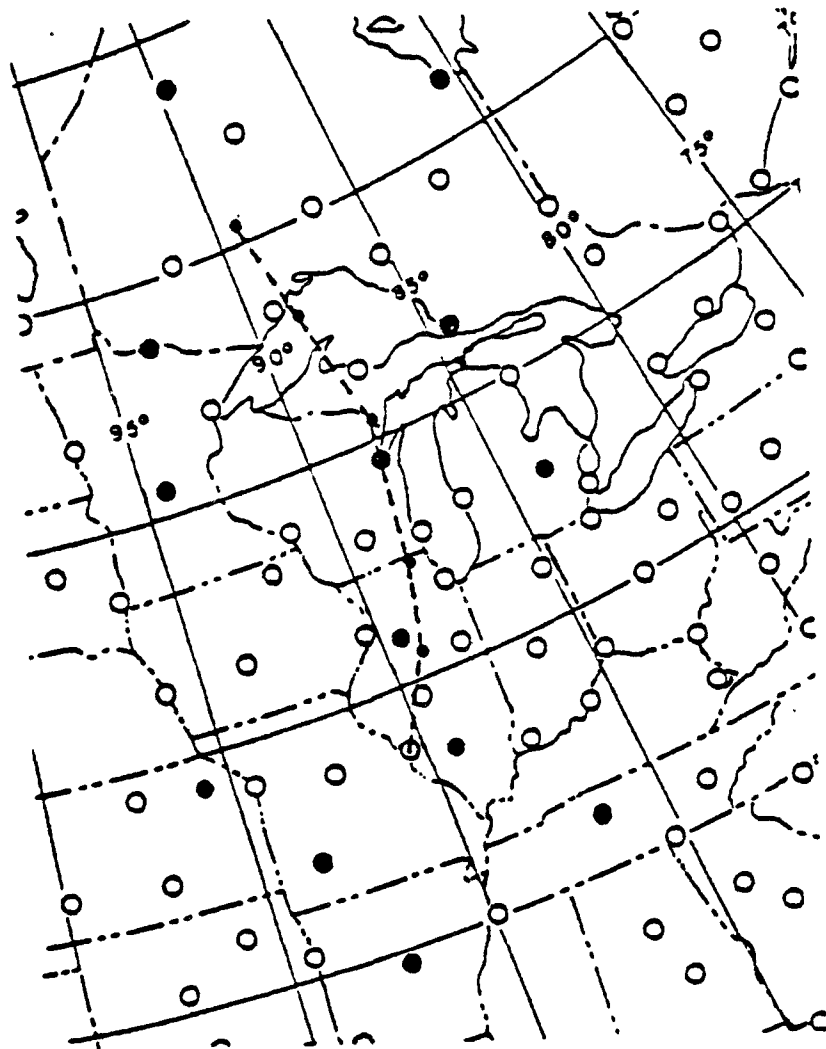


Figure 5.4 Layer-average trajectory for day 216. Maximum top of layer is 2000 m; base of the layer is chosen by the trajectory model. "●" indicates a radiosonde station within 300 nm (approximately 550 km) of trajectory. Each segment represents 12 hours.



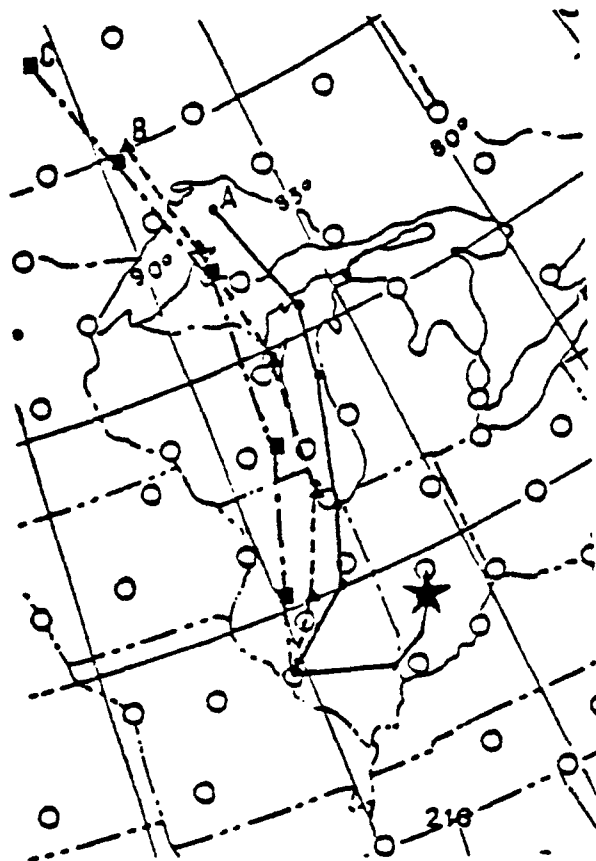


Figure 5.5 200 m layer-average trajectory for day 216. Trajectory A is for 200-400 m AGL layer, Trajectory B is for 900-1100 m AGL layer, and Trajectory C is for 1700-1900 m AGL layer. "★" indicates the end point of the 12-hour computed 200-400 m AGL trajectory. Each segment represents 12 hours.

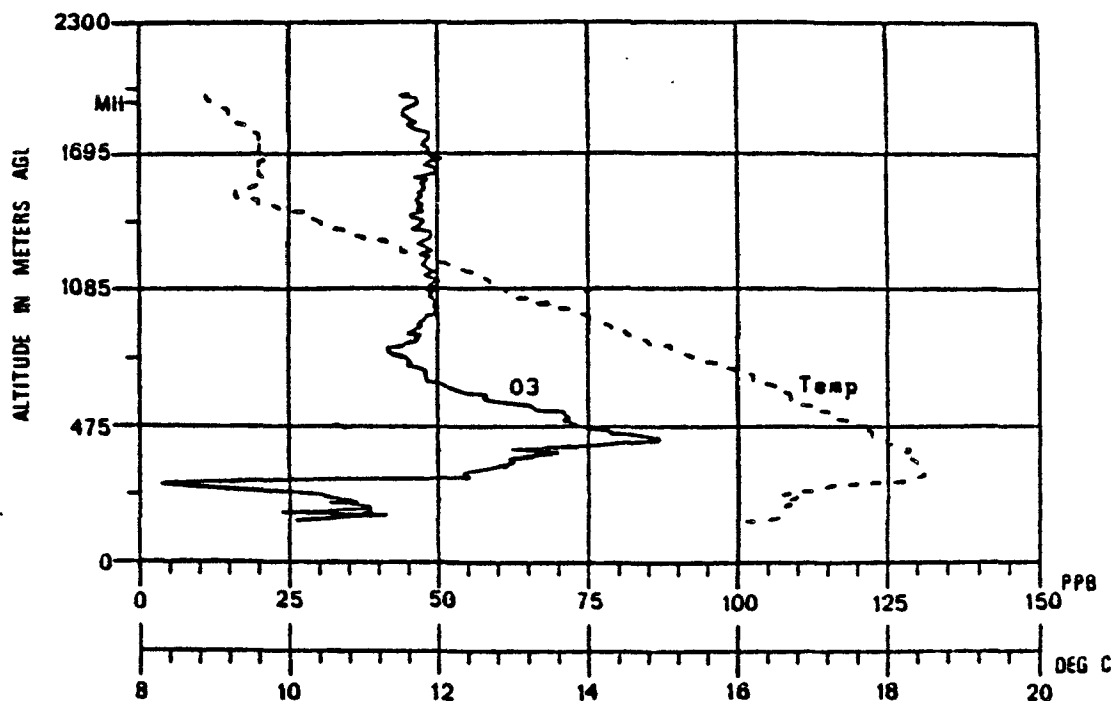


Figure 5.6 Ozone and temperature versus altitude, day 216. Upward spiral over Smartt Field between 0435 and 0448 CST. "MH" indicates mixing height on the previous afternoon upwind of Smartt Field. NO and NO<sub>x</sub> data not available.

Table 5.1 Comparison of the character of the morning profile and estimated time of trajectory passage over southern Lake Michigan.

Day	Character of Morning Ozone over St. Louis	Estimated Time of Passage over Southern Lake Michigan (CST)
216	Sharp Ozone Spike	0300 - 0600
221	Sharp Ozone Spike	0300 - 0600
215	Uniform Profile	0900 - 1500
220	Uniform Profile	0900 - 1500
217	Uniform Profile	Trajectory Uncertain

## SECTION 6

### TEMPORAL VARIATION IN THE SURFACE ENERGY BUDGET COMPONENTS FOR THREE LAND USE PATTERNS

Dennis C. Doll, G.F. Watson, and J.K.S. Ching

#### Abstract

Special St. Louis RAPS data were used to examine the diurnal variation of the net radiation and heat flux components of the surface energy budget for a two-month spring time period for blacktop, concrete, and soil surfaces. Sensible and latent heat fluxes were analyzed from measured and calculated net radiation and ground heat fluxes for each surface.

Ground heat flux for concrete and blacktop was determined for different water contents of the underlying soil layer. A lower water content in the soil layer reduces the magnitude of the total ground flux throughout the blacktop and concrete layer and soil sublayer. An accurate determination of soil water content appears necessary in any ground heat flux evaluation.

The sum of sensible and latent fluxes for the soil surface was found to be nearly twice as large as that for the blacktop layer and approximately three times larger than for the concrete surface during the daytime period of the diurnal cycle. Latent heating appears to be an important component of the surface energy balance for the soil.

Hourly average net radiation and ground heat flux values resulted in an improvement of a parameterization technique based on the ground heat flux to net radiation ratio ( $G/F_n$ ). Diurnal variation in  $G/F_n$  for each surface is distinctly different. For concrete and blacktop,  $G/F_n$  is constant at night but variable during the day. For soil,  $G/F_n$  changes throughout the diurnal period.

## INTRODUCTION

An essential part of determining the behavior of the boundary layer lies in knowing the surface layer fluxes, particularly that of heat, without which one cannot hope to specify pollution transport or mixed layer dynamics (Carlson and Boland, 1978). These surface layer fluxes, particularly heating patterns, are strongly tied to the character of the ground surface temperature and its substrate. The direction of the energy flow across the atmosphere-ground surface interface is primarily determined by the difference between the ground surface temperature and the air temperature above it (Bhumralkar, 1975). Therefore, in studies of atmospheric circulation it is necessary to know the ground surface temperature accurately.

The determination of ground surface temperature within a general circulation or boundary layer model is usually accomplished by solution of the surface energy balance equation (Deardoff, 1978). It is important that the components of the surface energy budget be rather carefully specified if an accurate determination of ground surface temperature is desired. If a model is being considered for a region where different land-use patterns exist, for example urban and rural areas, these same components must be evaluated for each surface type considered in the modeling in order to eventually determine representative surface temperatures. It is important, therefore, that comparisons of the different surface energy budget fluxes be assessed in order to determine how these fluxes vary among the surfaces. These fluxes can be compared for annual or diurnal characteristics depending on the time scale of the modeling effort.

Data collected during the subsurface heat flux experiment of St. Louis Regional Air Pollution Study (RAPS) are the basis for the present evaluations. The field site was the St. Charles County Airport (formerly Smartt Field) about 35 km NW of downtown St. Louis. The concrete runways and adjacent soil/grassy area were to represent urban land use materials. A portion of the runway was painted black to simulate asphalt. Net radiometers were installed directly over each surface, while thermistors embedded at several levels from the surface to 50 cm depth provided measurements for determination of ground heat flux. This particular RAPS experiment was run from January 1976 to May 1977. However, only the last two months (April-May) had

concurrent soil moisture data, and the present study is restricted to this period.

Soil moisture affects both the soil density and heat capacity and is crucial to the accurate determination of the ground heat flux. Soil moisture was directly determined for the soil/grassy surface. However, for the soil sublayer beneath the 12 cm thick concrete runway it was necessary to assume values. An assumed 35% water content by weight was the average of that for neighboring soil, while a 60% value was appropriate to saturation.

As mentioned by Deardorff (1978), the one component of the surface energy balance that is particularly difficult to evaluate in numerical models is the ground heat flux term. Several authors have suggested parameterizing the ground heat flux as a function of the more easily defined net radiation. This parameterization involves defining a proportionality constant for the ratio of ground heat flux ( $G$ ) to net radiation ( $F_n$ ). Nickerson and Smiley (1976), for example, have suggested using the constant 0.19 to represent  $G/F_n$  for daytime periods, and  $G/F_n = 0.32$  at night. Idso et al. (1975) have suggested a range of values for  $G/F_n$  around 0.4 depending on the type and moisture content of the soil.

In this study, then,  $F_n$  and  $G$  are directly measured. The surface energy budget equation  $F_n - G = H + LE$  also provides information on the sum of the sensible ( $H$ ) and latent ( $LE$ ) heat fluxes. The following results are the mean diurnal variation of the various fluxes and ratio  $G/F_n$  over the two-month spring period.

## RESULTS AND CONCLUSIONS

Evaluation of the energy balance components for each surface pattern considered in this analysis showed significant differences between soil and concrete surfaces and soil and blacktop surfaces. Variations noted between the concrete and blacktop were primarily attributed to differences in albedo.

The diurnal variation of mean net radiation for all surfaces (Figure 6.1) showed a very similar pattern with the maximum occurring around 1300 Local Time (LT) near the time of the maximum flux of solar shortwave radiation. Variations in magnitude are primarily attributed to differences in albedo between the concrete, blacktop and soil surfaces. Nighttime values of net radiation showed larger magnitudes for concrete and blacktop as compared to the soil.

Figure 6.2 shows the magnitude of ground heat storage to be

more than twice as large for concrete and blacktop as compared to that for soil. The maximum ground heat flux occurs near the time of maximum solar shortwave radiation for the concrete and blacktop. However, for soil, the time of maximum ground heat flux is shifted nearly two hours earlier to approximately 1000 LT. A large upward flux of heat occurs within concrete and blacktop at night due to the large amount of heat stored during the daylight hours. For soil, there is a much smaller upward flux compared to the concrete and blacktop due to the much smaller amount of heat stored during the daylight hours.

The diurnal variation of sensible heat flux ( $H$ ) plus latent heat flux ( $LE$ ) is found to be much greater in amplitude for the soil compared to the concrete and blacktop. The maximum daytime value for soil is nearly twice as large as that of the blacktop and approximately three times greater than that for concrete (Figure 6.3). Since the magnitude of  $H$  plus  $LE$  can be considered to be primarily due to  $H$  for the concrete and blacktop, it appears that latent heating effects are a major contributor to the large magnitude of  $H$  plus  $LE$  noted for the soil.

Figure 6.3 also shows an important characteristic of the diurnal curve of  $H$  plus  $LE$  for concrete and blacktop, namely, the occurrence of positive values during the nighttime hours. There is thus a continuation of a flux of heat from the surface to the atmosphere. Nighttime values of  $H$  plus  $LE$  for the soil were found to be small in magnitude and only slightly positive.

The diurnal pattern of the quantity  $G/F_n$  for concrete and blacktop in Figure 6.4 reveals that nighttime values are positive and greater than 1.0, indicating that the nighttime ground heat flux is of greater magnitude than the net radiative flux. The nighttime temporal variation of  $G/F_n$  is seen to be rather small. During the daylight hours,  $G/F_n$  varies little, except near the time of the evening transition period around 1700 to 1800 LT when  $G/F_n$  becomes negative. This is due to the change in the sign of ground heat flux that occurs prior to that for net radiation.

The mean diurnal pattern of  $G/F_n$  for soil in Figure 6.5 illustrates a much different pattern than that for concrete and blacktop. However, nighttime values are again found to be positive and greater than 1.0, similar to that for concrete and blacktop, although smaller in magnitude for the soil. Values of  $G/F_n$  just after the sunrise transition period around 0600 LT show values decreasing from approximately 1.0 to nearly 0.0 at about 1500 LT when the sign change in ground heat flux occurs. This is almost three hours earlier than the sign change in net radiation.

In conclusion, it seems clear that soil moisture content

has a very important effect in the heating rate of a soil sublayer. Generally, a moist soil layer will have a greater heat flux than a dry soil layer due to the larger thermal conductivity for the moist layer.

A concrete material over soil transmits heat effectively to the soil sublayer. Concrete generally has a higher thermal conductivity and lower heat capacity than soil allowing a greater heat flux. This greater heat flux for concrete allows a larger storage of heat to occur during the day compared to soil. This results in a greater release of heat during nighttime hours which aids in maintaining the surface temperature of the concrete and blacktop at warmer values than that of the soil.

Although the sensible heat flux ( $H$ ) over the concrete and blacktop may be larger than  $H$  over soil, the total of  $H$  plus the latent heat flux ( $LE$ ) is still larger for the soil than that of concrete and blacktop. This suggests that the latent heat flux is a major component of the energy budget for the soil material.

The contrast of energy budgets for these adjoining materials demonstrates the complexities involved in undertaking energy budget analyses. In mesoscale modeling, it has been demonstrated that land use variability greatly influences the energy budget component magnitudes, and must be considered in any type of mesoscale energy budget analysis.

The parameterization of  $G$  to  $F_n$  ratio is possible under undisturbed weather conditions. A strong diurnal effect of  $G/F_n$  is observed for all three surfaces although hour to hour variations may be small. This suggests that a traditional use of a single value for  $G/F_n$  as applied by some authors during the day and night does not accurately describe the parameterization. The results presented here show  $G$  to be greater than  $F_n$  at night for all three surfaces, although those for soil are less than those for the concrete and blacktop. Also, these results appear larger than those reported in most other studies.

Some suggestions for further research include:

- 1) An attempt to expand this two-month study using data obtained over all seasons so that seasonal variations in the energy budget can be evaluated.
- 2) A repeat of this rural site experiment at a more urbanized area. The magnitudes and characteristics of the energy budget for various surface materials can be contrasted to those found in this study.

- 3) A test to see whether applying the results presented here for the variation of  $G/F_n$  with respect to time of day and land use would in fact provide for more accurate flow predictions in boundary layer models.



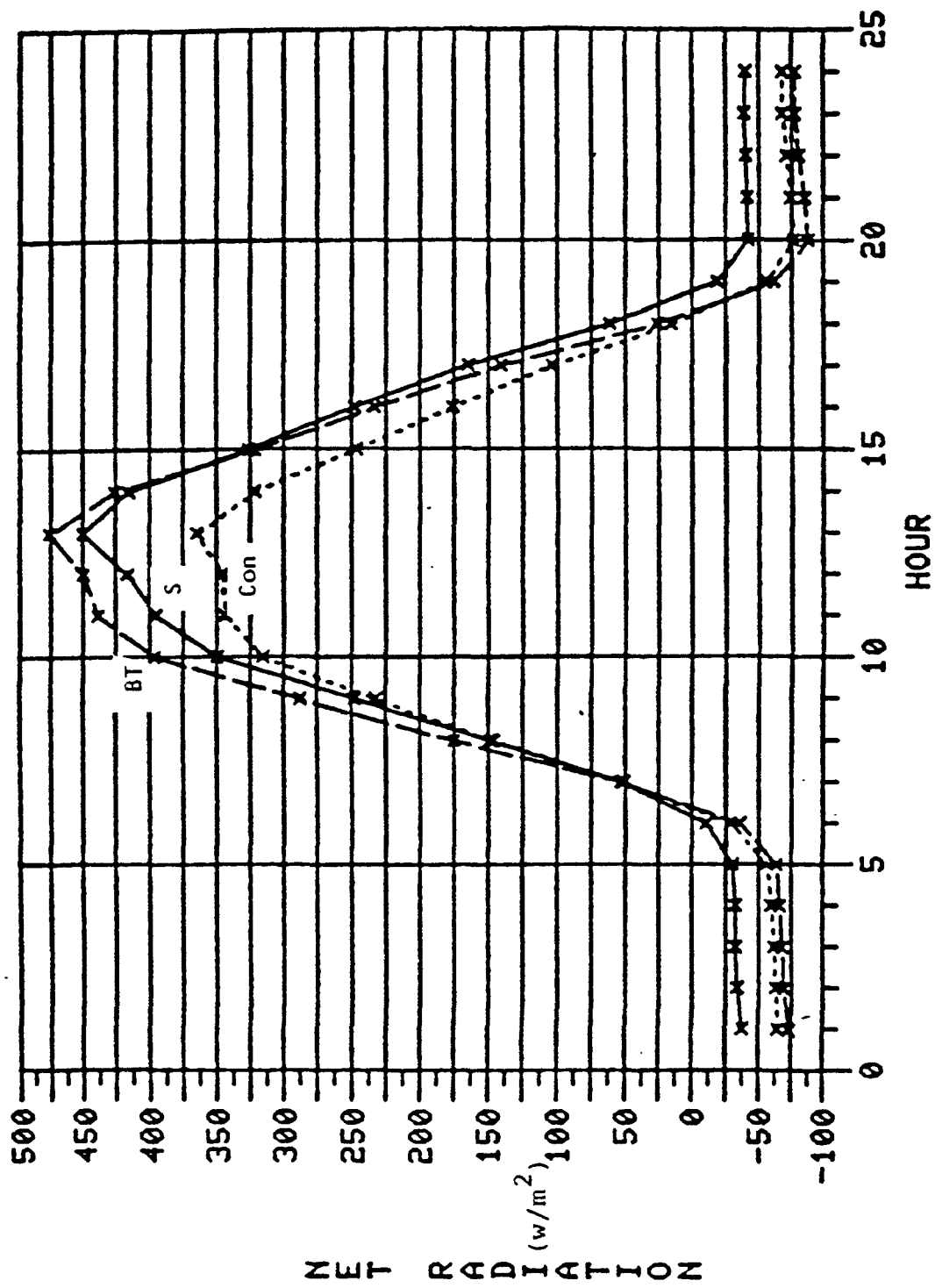


Figure 6.1 Diurnal variation of net radiation (Fn) over blacktop (BT), concrete (Con), and soil (S).

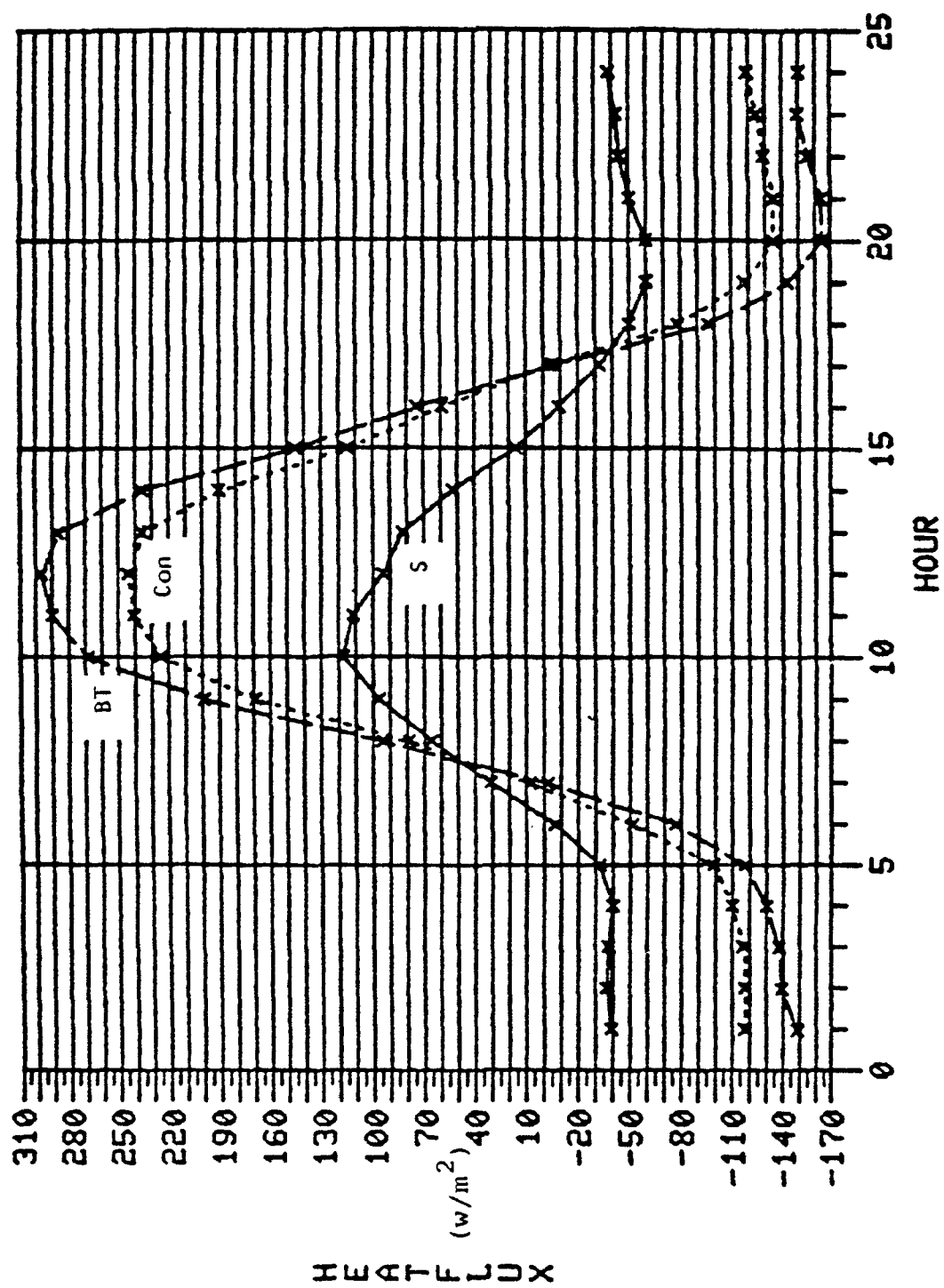


Figure 6.2 Same as Fig. 6.1 but for ground heat storage (G).  
Water content=0.35.

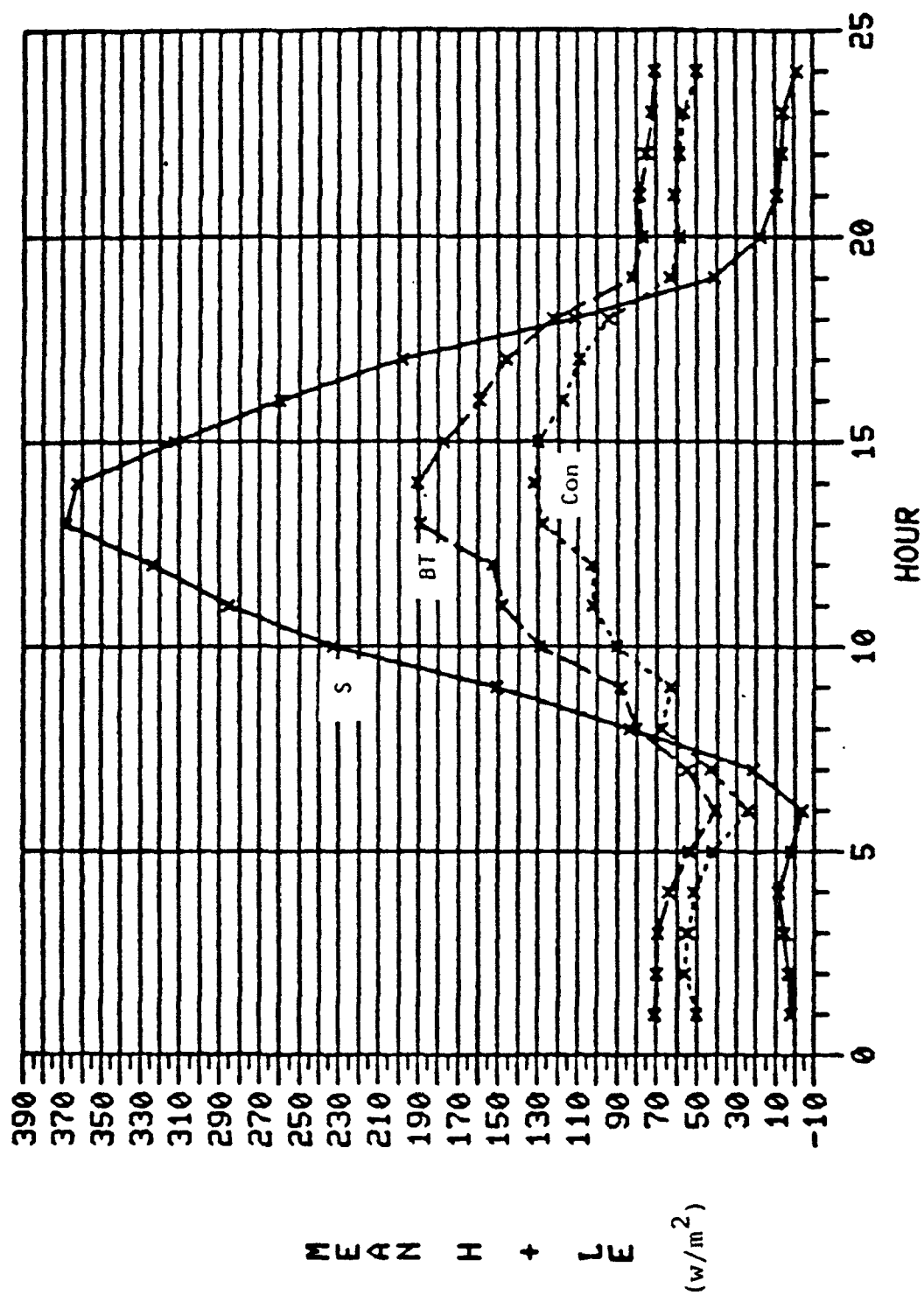


Figure 6.3 Same as Fig. 6.1 but for the sum of the sensible plus latent heat fluxes ( $H+LE$ ). Water content=0.35.

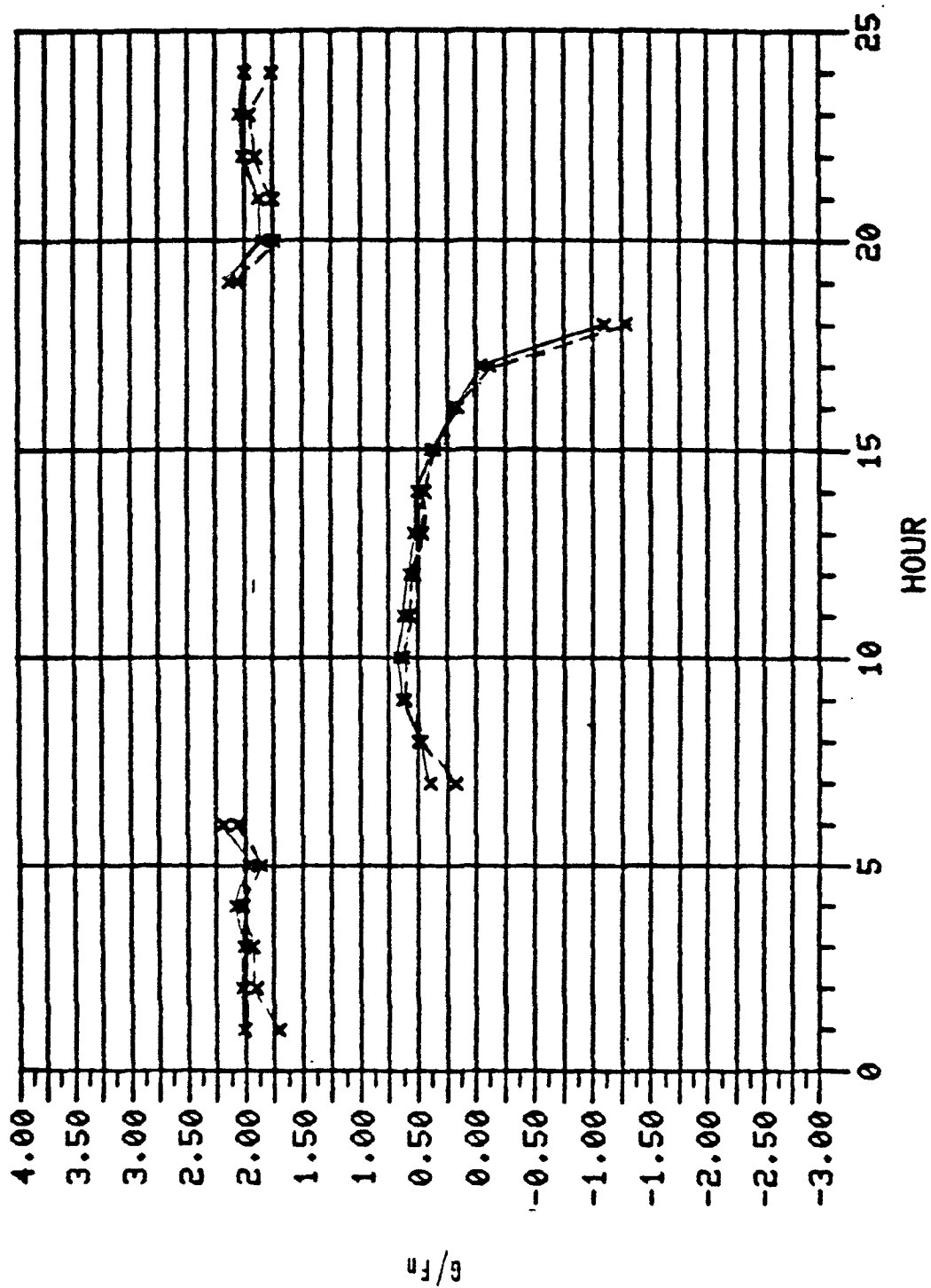


Figure 6.4 Diurnal variation of the ratio  $G/F_n$  for blacktop (solid line) and concrete (dashed line).

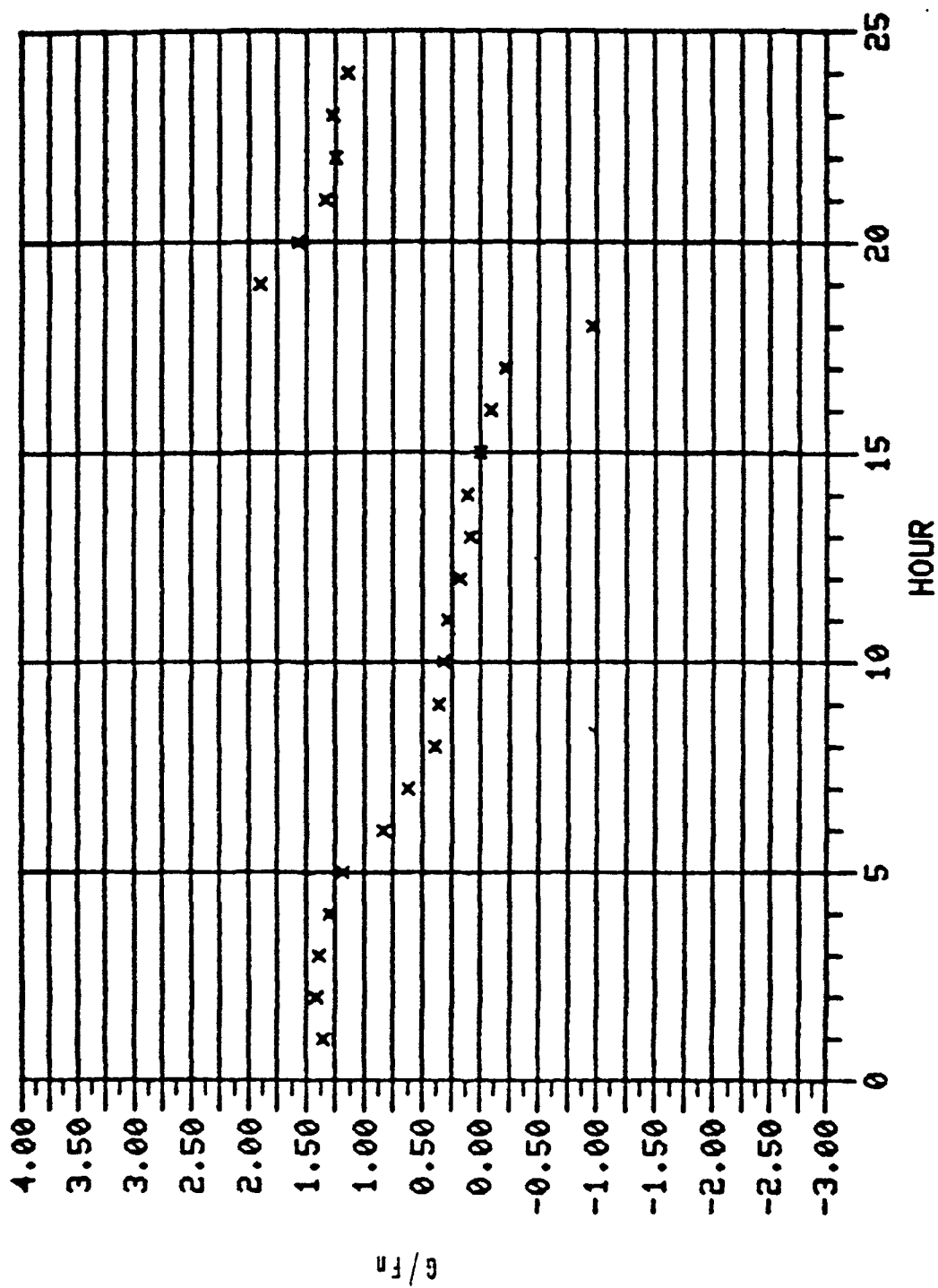


Figure 6.5 Same as Figure 6.4 but for soil.

## SECTION 7

### TRENDS IN ATMOSPHERIC VISIBILITY ACROSS THE UNITED STATES FROM 1955 TO 1972

Jerrold S. Foster, T.L. Tsui, and G.C. Holzworth

#### Abstract

Regular daytime synoptic observations from 14 stations across the United States but excluding those with relative humidity greater than or equal to 90% and those with precipitation or fog present, were used to determine the trend in visibility from 1955 to 1972.

Comparison of statistics at the beginning and the end of the period, and linear regression of the monthly mean visibilities were used to discover relationships between visibility and other meteorological variables such as wind speed, wind direction, and relative humidity. Spectrum and cross-spectrum analysis of the time series of visibility and relative humidity were also performed.

The results of this study indicate: (1) a deterioration of the visibility at all 14 stations, (2) a bimodal (six and twelve month) oscillation in the annual cycle of visibility, and (3) an inverse correlation of relative humidity with the annual cycle of visibility.

## INTRODUCTION

Growing concern for the quality of our air, not only with regard to health, but also for aircraft safety and for the aesthetic beauty of our environment has motivated this study. The concentration of various constituents of the atmosphere, such as water droplets, dust, smoke and other pollution particles, condensation nuclei, and the air molecules themselves, determines the optical transparency. Therefore, 'visibility' is often used in evaluating the quality of our air, especially in aviation operations. Consequently, it is of interest to aircraft safety and air clarity to understand how visibility changes and the relationship between visibility and other meteorological variables.

However, because of the human factor involved in the estimation of visibility, it is sometimes difficult to evaluate the changes in visibility. That is why a very large data set, 18 years, is used in this study. Such a large sample should override most of the subjectivity inherent in the data. In addition, subjectivity can be overcome by using some sort of smoothing technique, such as averaging, in order to make each member of the data set less dependent on the preceding one.

In meteorological usage, the term 'visibility' means both the condition of being visible and the "visual range." The latter term was introduced by Bennett in 1930 to indicate the distance at which something can be seen, i.e., the clearness with which objects stand out from their surroundings. Since then the definition of visibility has undergone many revisions. Throughout the period covered by this study "prevailing visibility" has been defined to be the greatest visibility, equaled or exceeded throughout at least half the horizon circle, which need not be continuous. One difficulty in the analysis was the use of the "+" in reporting the visibility. This symbol was used when the observer judged the prevailing visibility to be more than seven miles and also more than twice the distance to the most distant marker visible. The observer then encoded the visibility as twice the distance to that marker, or seven miles, whichever was greater. If the visibility was greater than the coded value, then a "+" was added. This symbol was deleted from the observations when they were archived thus making it impossible to determine if, and by how much, the visibility exceeded the recorded value. Therefore, any study of visibility trends becomes more problematic, and may be somewhat biased.

Complete airways observations from National Weather Service reporting stations, archived on magnetic tape at the National Climatic Center at Asheville, North Carolina were used in this study. Observations from 1955 through 1972 for sites with continuous records and which had not significantly changed location were selected. Of these 14 stations only observations between 0900 and 1600 local time for which precipitation, fog, or relative humidity of 90% or more were not reported were included.

Trend analysis methods by Holzworth and Maga (1960) and standard time series and cross-spectrum analysis were used to examine the changes of visibility and its relation to variations in wind speed, wind direction, and relative humidity at each reporting site.

Research in visibility as an indicator of air quality has been going on most of this century. One technique described by Holzworth (1959) and common to many studies is to determine the percent frequency of occurrence of the visibility in a few (four or five) categories within the range of the visibility at the station in question. The percent frequency is calculated at the beginning and the end of the period being studied. Holzworth (1959) used this technique and found that the visibility near Sacramento, California had deteriorated from 1935 to 1956. The author also related poor visibility to wind directions which brought pollutants from urban areas. Holzworth (1962) determined that the visibility at various cities was lower from 1955 to 1959 than from 1929 to 1938 because of an increase in the frequency of visibility less than seven miles. This decrease was found to relate to the wind speed and direction relative to pollution sources. Miller *et al.* (1972), using comparisons of statistics at the beginning and the end of the period coupled with multiple regression showed that the summer daytime visibility in Ohio, Kentucky, and Tennessee deteriorated from 1962 to 1969, and that wind direction and relative humidity were significantly related to visibility.

The southwest United States is an area of great interest in visibility studies today. Because of the typically large visibilities, over 100 miles, reported by stations in this area, a decrease of only 10 or 15 per cent in the prevailing visibility is considered a large change, and is of more concern than a similar percentage decrease in the more populated eastern United States. A recent study by Trijonis and Yuan (1977) showed the visibility throughout the southwest United States to be decreasing. The concern over the deterioration of the visibility in this area, as well as over the remainder of the United States, points to the need for continuing research of visibility trends.

Because of these findings, the present visibility study was



undertaken to verify whether deteriorating visibility was common to many stations across the country. If this is the case then what meteorological elements, or their combinations, are responsible? Linear regression and time series analysis will seek relationships between visibility and other meteorological variables.

## RESULTS AND CONCLUSIONS

Some of the difficulties inherent to an investigation of visibility were brought out in this study. Problems were lessened by using a large data base of 18 years. One particular problem encountered by this study was the use of the "+" in reporting visibility. Unfortunately the "+" symbol was not in the archived data and the results biased by changes in the usage of the "+" symbol cannot be estimated. If the "+" symbol did impose an influence on the outcome of the trend analysis, the trend deduced should have been discontinuous. This was shown in the Austin, Texas visibility data. In general, the "+" symbol has not seriously affected this study.

The first major finding was the downward trend in visibility at all 14 stations listed in Table 7.1. This was shown by the linear regression method (for example, Figure 7.1), and more dramatically by the method developed by Holzworth and Maga (1960). This result may be due to new urban and/or industrial developments around the airports or to an increase in the amount of aircraft traffic. The deterioration of visibility from 1964 to 1970 may also be due to an increase in the sulfate percentage of the total particulate matter in the air.

Another finding of this study was a bimodal annual oscillation in the mean monthly visibility cycle. Spectral analysis indicated that two major components of the total variance occur with periods of approximately six and twelve months. The spectrum for Raleigh-Durham, NC is displayed in Figure 7.2. The positive correlation of the visibility time series was high among stations within similar geographical areas, indicating that geographical region is one major factor in determining the periodicity of the visibility.

Further examination of this result determined that the monthly mean relative humidity also exhibits a bimodal annual oscillation, but 180 degrees out of phase with the visibility. This relationship is illustrated for two stations in Figures 7.3 and 7.4. There seems little doubt that seasonal variability in relative humidity is a major, if not the dominant, cause of the bimodal oscillation in the annual visibility cycle. Other factors such as wind speed, wind direction, the number of daily observations used in this study, and station location may also play an important role in the periodic variability of visibility.

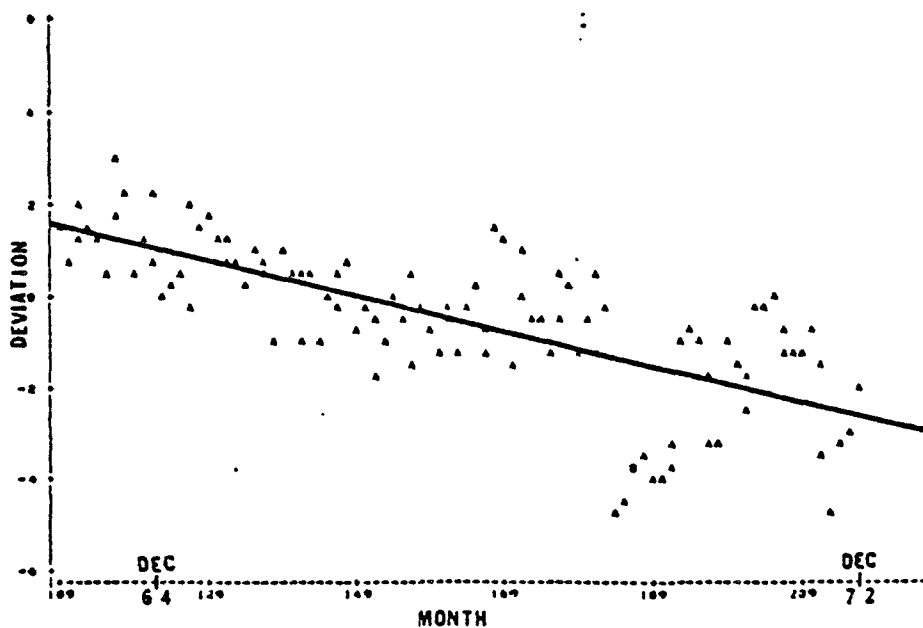
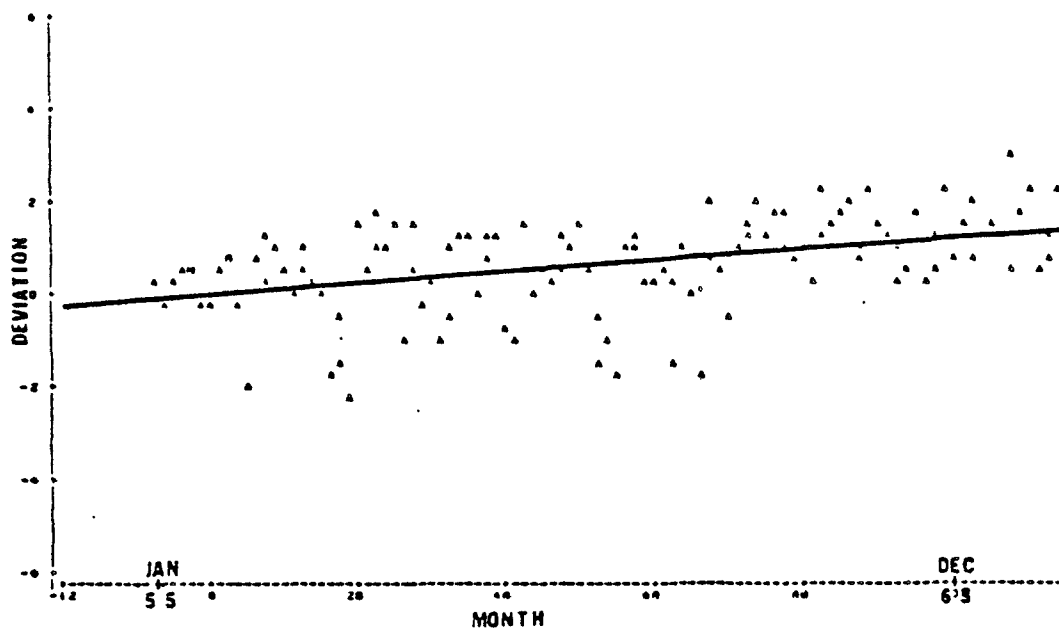


Figure 7.1 Trend determined from deviations in visibility (miles) from the respective monthly mean (1955-1972) at Birmingham, AL. Note the general decrease in visibility in the latter half of the period.

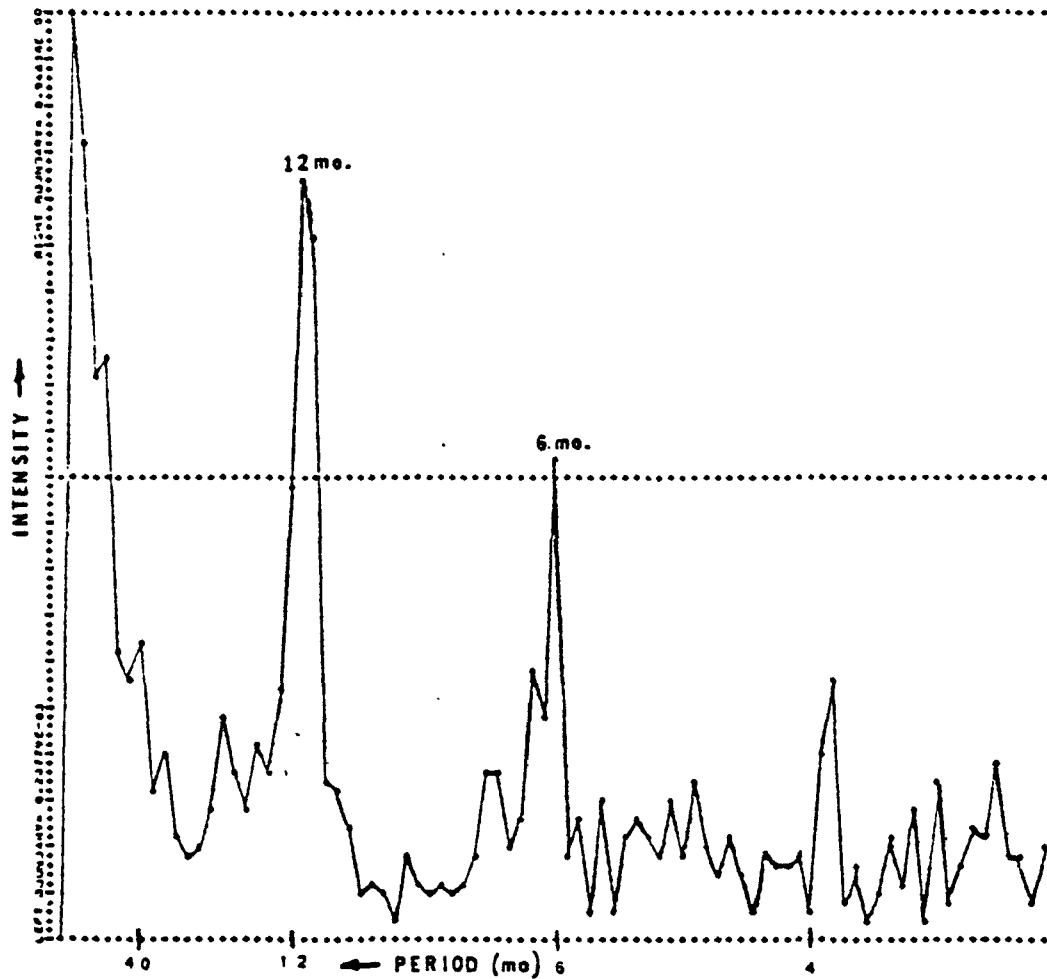


Figure 7.2 Fast Fourier Transform of Visibility  
Time Series of Raleigh-Durham, N.C.

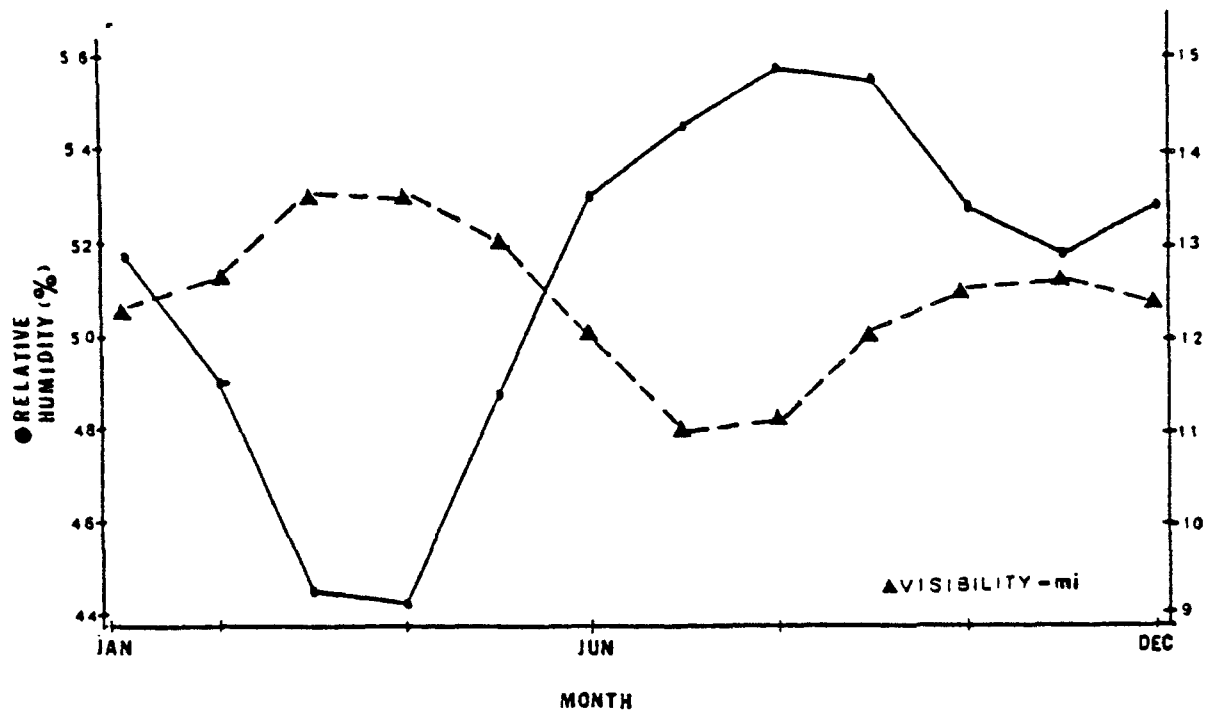


Figure 7.3 Bimodal annual oscillation of visibility and relative humidity at National Airport (D.C.).

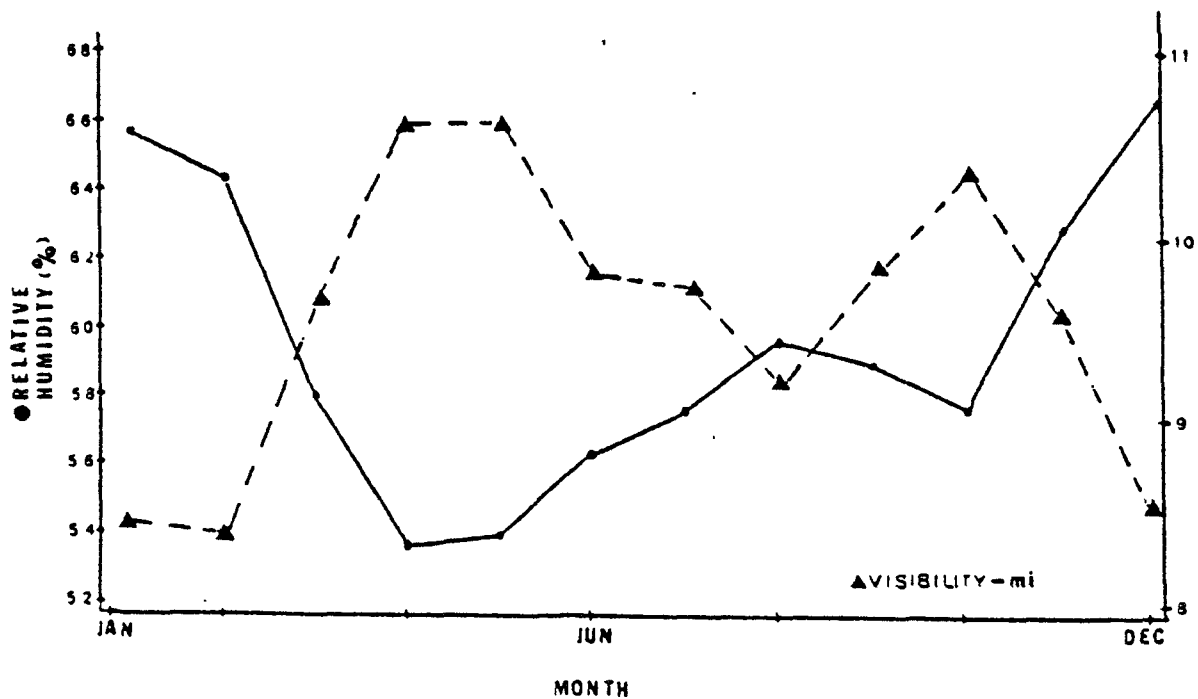


Figure 7.4 Bimodal annual oscillation of visibility and relative humidity at Cleveland, OH.

Table 7.1 Stations used in this study and grouped according to geographical region.

Station	Distance and direction of airport from city	Elevation (ft)
1. Washington, D. C. (National)	3 mi. S	65
Raleigh-Durham, N. C.	10 mi. NW	441
Atlanta, Ga.	7 mi. SW	1034
Birmingham, Ala.	6 mi. NE	630
2. Houston, Tx.	7 mi. SE	662
Austin, Tx.	3 mi. E	621
3. Tucson, Az.	-	2555
Phoenix, Az.	3 mi. E	1107
4. St. Louis, Mo.	13 mi. NW	564
Peoria, Ill.	6 mi. SW	662
Milwaukee, Wis.	7 mi. S	663
Ft. Wayne, Ind.	5 mi. S.	828
Cleveland, Ohio	10 mi. SW	805
Youngstown, Ohio	8 mi. N	1186

## SECTION 8

### A VISIBILITY STUDY IN THE EASTERN HALF OF TEXAS FROM 1949 TO 1968

Alfonse J. Mazurowski, A.J. Riordan, and G.C. Holzworth

#### Abstract

Hourly weather observations for times 0900-1500 CST were used to examine visibility trends, obstructions to vision, and the effects of different parameters on visibility for eight stations in the eastern half of Texas from 1949 to 1968.

Observations with any obstruction to vision, along with the individual obstructions by haze, smoke, and dust, were examined to determine their effect on visibility. Mean visibility categorized by wind direction was employed to investigate the influence of winds from industrial areas and cities on visibility at airports. Trend analyses of mean visibility data, both annual and seasonal, were performed using mean ridits and shifts in frequency from one visibility range to another. The effects on visibility of population growth and distance of stations from the Gulf of Mexico were also analyzed.

The main results of this study are: (1) a deteriorating trend in annual visibilities was apparent for seven of the eight stations, (2) smoke was a major factor in the reduction of visibility in Houston, (3) smoke appeared to be a result of local transport of air pollution while haze and dust seem to be associated with long-range transport processes, (4) daily resultant winds from nearby industrial areas produced the lowest mean visibilities, (5) mean visibility increased significantly as the distance of stations from the Gulf of Mexico increased.

## INTRODUCTION

Visibility has been considered a valuable tool in determining the quality of the air for many years. Since its inception, the aviation industry has been concerned with visibility, but recently individuals and groups have become involved with investigating the apparent degradation of the air quality. This involvement has resulted in an increased awareness of the trend of declining visibility throughout the United States. As a result, visibility studies have become more numerous in the interest of aircraft safety and air quality improvements.

Visibility studies have been conducted at various locations in the United States. References cited in the previous section of this report (SECTION 7) are also relevant to this study, and these are not repeated. Some additional references include Holzworth (1962) who examined the percent frequency of all visibilities less than 7 miles at stations scattered throughout the United States in the period 1929 to 1961. Results indicated that visibility was improving in many of these urban areas. Holzworth suggested that the possible reduction of the emission of visibility-reducing materials to the atmosphere, such as the smoke from coal combustion, may have been responsible for the visibility increases. Faulkenberry and Craig (1976) showed that a trend of declining visibility was apparent for Salem, Oregon in January and August from 1950 to 1971. But at the same time, no significant trends were indicated at Portland and Eugene, Oregon.

The long range transport of air pollution has been studied by following areas of reduced visibility during periods of increased air stagnation. Hall et al. (1973) used surface visibilities and an 850-mb wind trajectory analysis to show that air pollution advanced as much as 1100 km from the central midwest into the upper midwest and Great Plains in August 1970. Visibility contour maps, daily weather maps, and long-range trajectory analyses were employed by Husar et al. (1976) to monitor the long range transport of pollutants in June and July 1975 in the eastern half of the United States. They found that haziness may be caused by long range transport from sources 1000 km or more away.

This report examines visibility at eight stations in the eastern half of Texas (Table 8.1). The area stretches from the Gulf of Mexico to the Oklahoma border. The region is of interest because it has had large population increases since the 1940's, and the effect of topography appears negligible.

The eight stations were selected based on continuity of location, and data were examined for trends or discontinuities in visibility relating to changes of the observation site. The largest change was 5.6 km at Corpus Christi, but there was no significant change in visibility associated with that re-location. Data after 1968 were not included for any site because after this some sites began reporting maximum visibilities as 7+ rather than 15 miles (see Section 7). Finally, only observations for 0900 to 1500 CST without precipitation or fog were included. Prior to 1965 observations were hourly, but from 1965 through 1968 they were archived only for 3-hour intervals.

The influence of the Gulf of Mexico on the stations is investigated as are the obstructions to vision that are associated with air pollution problems. The existence of visibility trends, the effect of various non-meteorological parameters on visibility, and the influence of long range and local transport of air pollutants on visibility also are examined.

## RESULTS AND CONCLUSIONS

The predominant resultant winds on an annual basis are from the direction of the Gulf of Mexico for all eight stations. The Gulf of Mexico, therefore, has a large influence on the climate of the area. These resultant winds from the Gulf of Mexico are also conducive to unstable conditions over land, giving large mixing heights and decreased potential for air pollution problems.

Houston has by far the greatest number of days with obstructions to vision reported. The remaining stations have considerably fewer such days (Table 8.2). Every station, except Fort Worth, has significant negative correlation between mean annual visibilities and the number of days per year with obstructions to vision (Table 8.3).

Table 8.4 shows that smoke appears to be a major factor in reducing the mean visibility in Houston. In Dallas and Houston, smoke is reported a greater percentage of the time when resultant winds are from the nearby industrial areas. Figure 8.1, and others, suggest that smoke is a local rather than a regional problem.



Days with haze occur most frequently in the South Central and Gulf Coastal regions, but differences among all the stations are small (Table 8.5). The uniformity of the number of days with haze at all the stations suggests that haze is generally a regional problem. Further evidence is provided by Figure 8.2 in which the predominant wind direction associated with haze occurrence at Houston is not from the industrial area.

Observations with dust are widespread over the eastern half of Texas, with small differences in the number of days with dust noted among the stations. Drought conditions in the 1950's were responsible for the majority of the dust reported in the study period, and a case study during this period showed that large-scale transport processes contributed to the dust observed.

The most important result of the present study is the apparent trend of deteriorating visibility (Table 8.8) on an annual basis at every station, except Brownsville. Seasonal analysis shows that Houston is the only station with a trend of declining visibility in all seasons. Two contrasting methods are utilized for determining the visibility trends. Both give similar results. The Holzworth and Maga (1960) method employs the resultant shift between visibility ranges to determine trends, while the method introduced by Faulkenberry and Craig (1976) uses mean ridity. Ridity analysis (Bross, 1958) is appropriate when the response variable has numerical values but the measurement system is heavily dependent on the technical skill of the scientist. Because visibility observations involve a subjective decision by an observer, the results reported depend on the skills of the observer.

Increases in city population, when correlated with the number of days with mean visibility in the 13-15 mile range, are found to decrease significantly the frequency of visibilities in this range at all stations except Brownsville. Another factor that influences visibility is the distance of a station from the Gulf of Mexico. As this distance increases, the mean visibilities for the study period increase significantly. Tables 8.6 and 8.7 document, respectively, visibility dependence on population trends and distance from the Gulf.

Because of the continued migration of people and industries to the "Sun Belt" states, future visibility studies should be considered in this portion of the country to monitor the effects of this migration. Detailed case studies would be especially beneficial in determining the transport processes of both haze and smoke, and to determine if the smoke observed in Houston might be affecting the visibility in nearby cities.

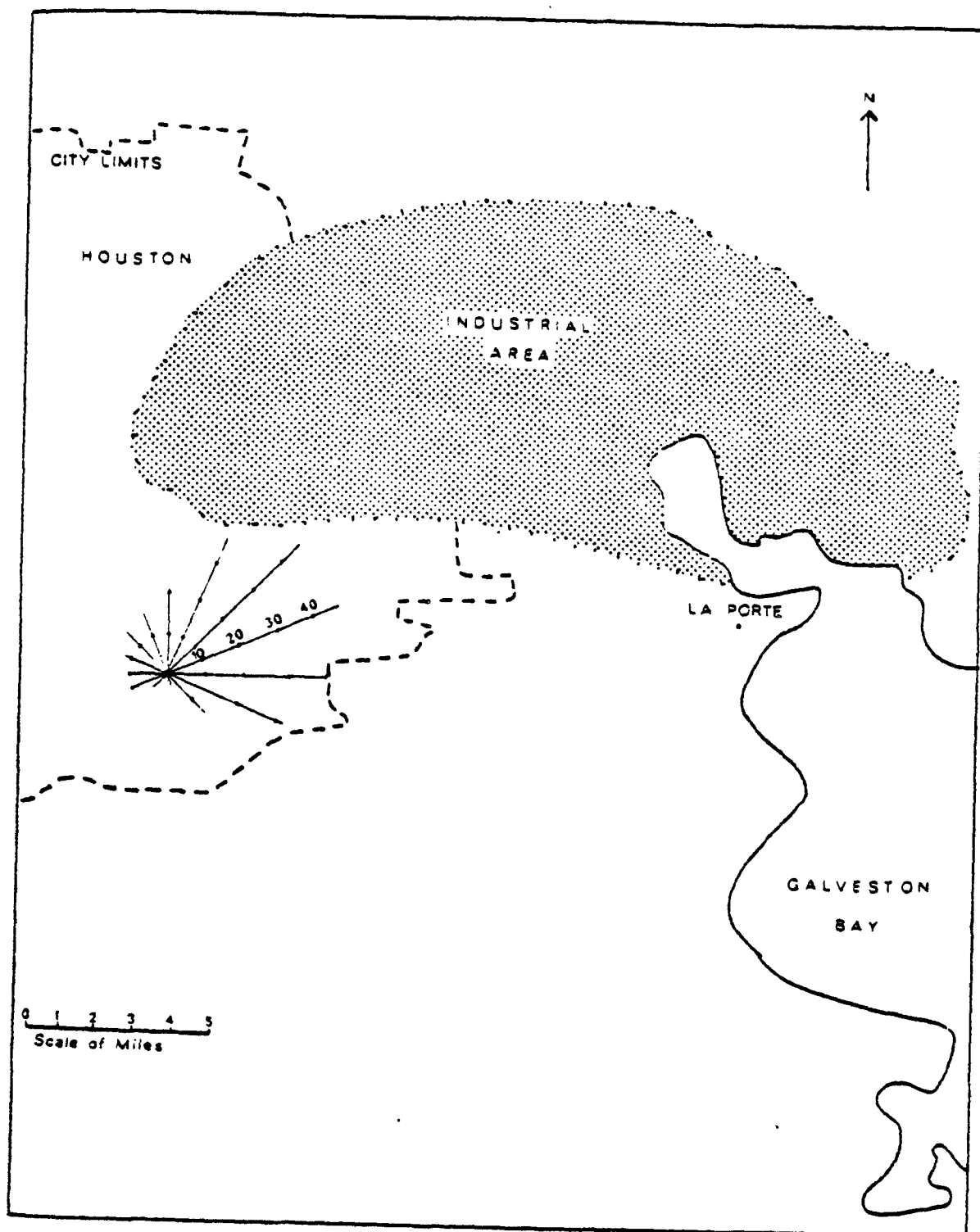


Figure 8.1 Percent frequency of the ratio of the number of smoke days from a particular resultant wind direction to the total number of days with the same resultant wind direction at Houston, 1949-1968.

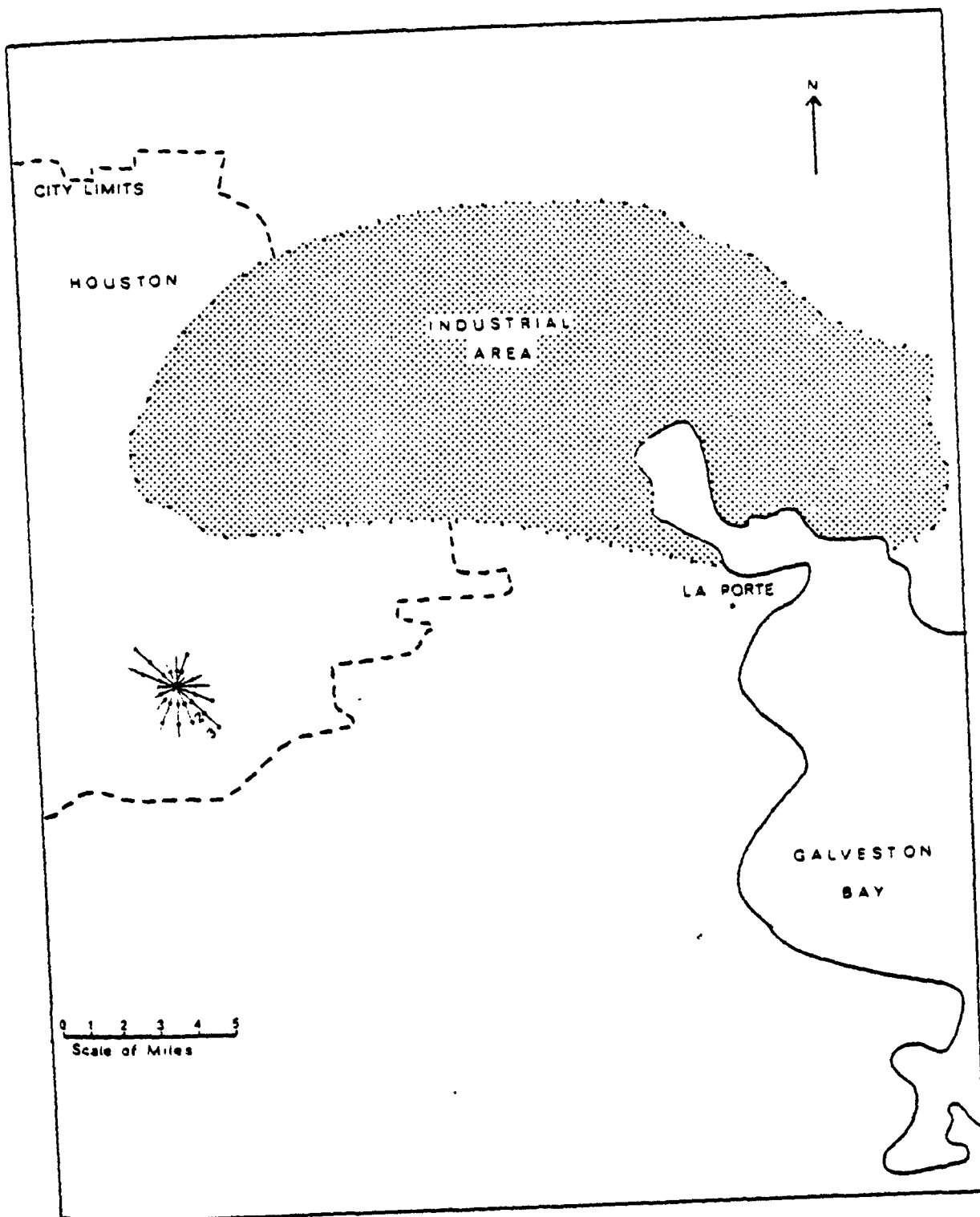


Figure 8.2 Same as Figure 8.1 except for haze days.

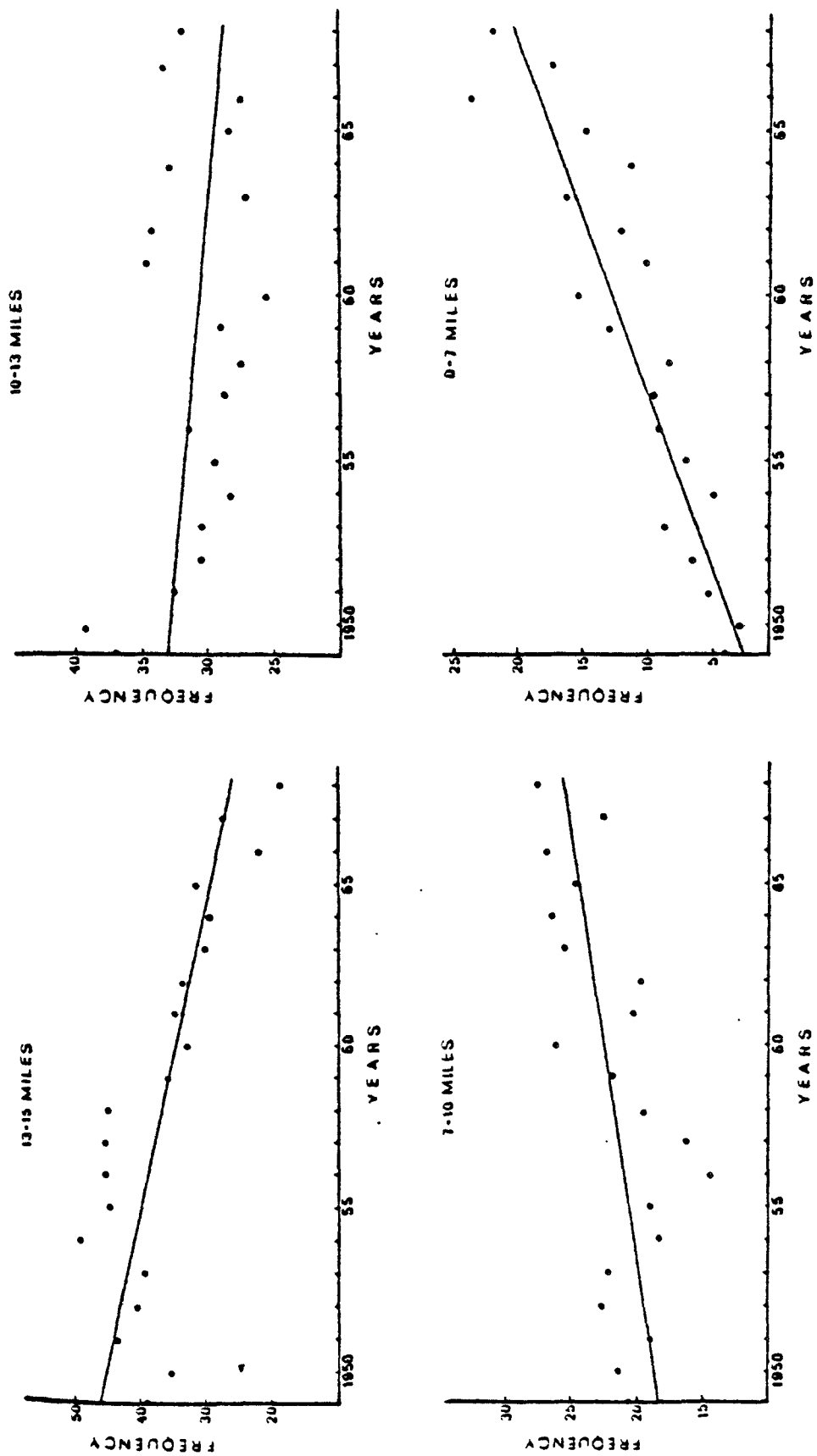


Figure 8.3 Annual visibility frequencies (%) and linear trend lines in the four visibility ranges for Houston, 1949-1968.

Table 8.1 Station information and data years used.

STATION	LOCATION IDENTIFIER	DATA YEARS USED	DIRECTION & DISTANCE FROM CITY	ELEVATION
Houston Intl. Aprt.	HOU	1949-1968	16 km SE	15 m
Dallas Love Field	DAL	1949-1968	9 km NW	145 m
San Antonio Intl. Aprt.	SAT	1949-1968	13 km N	241 m
Greater Southwest Intl. Aprt. (Fort Worth)	GSW	1954-1968	27 km ENE	166 m
Austin Municipal Aprt.	AUS	1949-1968	4 km ENE	187 m
Corpus Christi Intl. Aprt.	CRP	1949-1968	8 km W	13 m
Wichita Falls Municipal Aprt.	SPS	1949-1968	11 km N	305 m
RGV Intl. Aprt. (Brownsville)	BRO	1949-1968	5 km E	5 m

Table 8.2 Number of days with obstructions to vision and mean daily visibility.

STATION	NUMBER OF DAYS WITH OBSTRUCTIONS (1949-1968)	MEAN DAILY VISIBILITY (MILES) (1949-1968)
Houston	1748	11.2
San Antonio	496	13.2
Dallas	484 (379)*	13.8
Corpus Christi	361	12.9**
Brownsville	344	12.8
Austin	303	12.9
Fort Worth	184*	13.9*
Wichita Falls	166	14.1

\* 1954-1968

\*\* 1952-1968

Table 8.3 Results of the correlation between annual mean visibilities and the number of days with obstructions, 1949-1968.

STATION	CORRELATION COEFFICIENT	SIGNIFICANT AT THE 5% LEVEL
Houston	-.860	X
Dallas	-.806	X
San Antonio	-.854	X
Fort Worth *	-.422	
Austin	-.593	X
Corpus Christi **	-.685	X
Wichita Falls	-.472	X
Brownsville	-.451	X

\* 1954-1968

\*\* 1952-1968

Table 8.4 The number of days with smoke and the mean population for all locations.

STATION	NUMBER OF SMOKE DAYS (1949-1968)	MEAN POPULATION (1949-1968)
HOU	1344	879,018
DAL	243 (175)*	628,937
CRP	73	154,759
SAT	70	540,638
AUS	30	180,491
GSH	12*	354,349
SPS	6	89,914
BRO	3	44,885

\* 1954-1968

Table 8.5 Number of days with haze.

STATION	NUMBER OF DAYS WITH HAZE (1949-1968)
SAT	341
BRO	238
AUS	203
CRP	186
HOU	153
DAL	123 (100*)
GSW	116*
SPS	43

\* 1954-1968

Table 8.6 Correlation coefficients between population growth and (a) the frequency of days with mean visibility less than 7 miles and (b) visibilities in the 13 to 15 mile range for all locations.

STATION	CORRELATION COEFFICIENT		POPULATION GROWTH 1949-1968	PERCENT GROWTH
	(a)	(b)		
Houston	.399*	-.739*	598,887	51%
Dallas	-.012	-.621*	390,968	48%
San Antonio	.531*	-.601*	247,883	39%
Austin	-.013	-.616*	110,749	46%
Corpus Christi	.230	-.320*	93,970	48%
Fort Worth	-.392	-.723*	76,260**	20%**
Wichita Falls	-.081	-.564*	32,647	33%
Brownsville	-.207	.028	16,958	33%

\* Statistically significant at the 5% level

\*\* 1954-1968

Table 8.7 Distance and direction from the Gulf of Mexico and mean visibility for all locations.

STATION	DISTANCE (KM) AND DIRECTION FROM THE GULF OF MEXICO		MEAN VISIBILITY (Miles) 1949-1968
Corpus Christi	23	WNW	12.9*
Brownsville	29	W	12.8
Houston	64	NW	11.2
San Antonio	225	NW	13.2
Austin	259	NW	12.9
Dallas	450	NNW	13.8
Fort Worth	475	NW	13.9**
Wichita Falls	644	NW	14.1

\* 1952-1968

\*\* 1954-1968



Table 8.8 Visibility trend analysis using the method of Holzworth and Maga (1960). Given is the net percentage change in the frequency of the 13 to 15 mile visibility range for seasons and locations with a downward trend during the period 1949 to 1968.

STATION	ANNUAL	WINTER	SPRING	SUMMER	FALL
Houston	-19.64	-13.24	-24.98	-20.11	-25.45
Dallas	-14.36		-13.44	-16.49	-22.54
San Antonio	-18.43		-28.56	-16.07	-29.05
Fort Worth	-16.13		-14.91	-19.68	-25.16
Austin	-18.69		-24.77		-25.66
Corpus Christi	-23.34	-30.22	-33.75	-13.20	
Wichita Falls	- 6.70				-12.08
Brownsville					

## SECTION 9

### SYNOPTIC-SCALE VARIABILITY IN ATMOSPHERIC SUSPENDED SULFATE CONCENTRATIONS

Brian W. Galusha, G.F. Watson, and G.C. Holzworth

#### Abstract

The spatial variation in atmospheric suspended sulfate concentrations is studied for evidence of meteorologically linked sulfate transformation and transportation. Low frequency (every 12-14 days) data from 41 National Air Surveillance Network stations as well as higher frequency (every 2-3 days) data available from two special studies are examined. Variations in high frequency data with wind direction for St. Louis, Missouri, are compared to local and regional sources of precursor pollutants for two one-year periods; January-December 1969 and April 1975-March 1976. Spatial variations in low frequency sulfate concentrations during the spring season (March-May) for the six-year period 1969-1974 are compared with synoptic weather and wind circulation patterns. These comparisons indicate that regional and local sulfate transport can largely account for large-scale sulfate variations. Sulfate transformation due to humidity, temperature, and sunlight intensity do not adequately explain observed variations, but may be of secondary importance.

The existence of regionally high concentrations of sulfate in the northeastern United States and of a general summertime peak in sulfate values is confirmed.

## INTRODUCTION

Atmospheric suspended sulfates have been identified as a significant pollution problem by the Environmental Protection Agency (EPA). These sulfates have been related to adverse health effects (EPA, 1974c), reduced visibilities (Wilson et al., 1977), and the corrosion, discoloration, and deterioration of materials (EPA, 1975).

The term "sulfates" applies collectively to a large class of sulfur compounds. Any single physical property which characterizes all is difficult to define. One of the major distinctions is that some sulfates are hygroscopic and others are not. Although some researchers have found it convenient or necessary to assume homogeneity, generalizations about sulfates are often invalid. Thus, results of studies conducted in one section of the country may not be applicable to other regions. Adding complexity to the problem is the fact that sulfates are usually secondary pollutants transformed chemically from the precursor agents such as sulfur dioxide ( $\text{SO}_2$ ) and hydrogen sulfide ( $\text{H}_2\text{S}$ ).

The present study is undertaken with the hope that a more detailed meteorological investigation can provide a better understanding of the mechanisms involved in sulfate transport and transformation. In particular, this study proposes to determine whether the sulfate concentrations display well-defined patterns over areas resolvable by the normal meteorological surface observation network. This implies areal extents of a few hundred kilometers (synoptic-scale).

Patterns in sulfate distribution on this scale will be determined from data collected by the National Air Surveillance Network (NASN). There are about 100 more or less continuously reporting stations in the NASN with sampling frequency about once each 12 days. In this study only urban sampling sites in close proximity to National Weather Service (NWS) stations and in the eastern United States are employed. Further restrictions include: (i) samples must be chemically analyzed by the same (methylthymol blue) method; (ii) each station must have at least five samples from each season during any year; iii) each station must have four valid years of data out of the six-year period. The 41 NASN stations satisfying these criteria are shown in Figure 9.1.

Synoptic scale patterns in sulfate distribution will next be presented and related to patterns of meteorological variables.

## RESULTS AND CONCLUSIONS

The presence of significant synoptic-scale variability in sulfate concentrations in NASN data is illustrated by that at Nashville, TN in Figure 9.2. Seasonal mean values at a number of stations (Figure 9.3) show the summer maximum and generally higher values in the northeast states.

This study has arrived at a number of conclusions. Some conclusions must be considered tentative due to the marginally acceptable sulfate data presently available. Future researchers, utilizing data of better quality and quantity, may be able to determine whether these conclusions remain valid.

When sulfate values are represented as deviations from seasonal means and plotted on maps, synoptic-scale patterns emerge as in Figure 9.4. This figure, and others analyzed for the weather active spring season, show coherent patterns of + and - deviations. However, a systematic relationship of these patterns to those of weather variables is not obvious. For example, the large positive values over the Carolinas and Virginia on May 11, 1974 are associated with cloudy skies and warm temperatures. On March 10, 1969 positive values in the same area are related to mostly clear skies and near-freezing temperatures. Large negative values over Nebraska and Kansas are related to clear skies and warm temperatures on May 11, but to cloudier skies and sub-freezing temperatures on March 10. Although expected correlations with temperature, moisture, and sunshine were not clearly evident, these are still thought to exist. Apparently, such relationships are overshadowed by sulfate transport.

The importance of sulfate transport was most readily demonstrated at St. Louis, Missouri where sufficient data were available and sources of sulfate or precursor agents are nonuniformly distributed around the horizon (see Figure 9.5). Similar results were apparent at other stations with relatively high frequency observations. Recognition of the dominance of the transport process led to a re-examination of previously puzzling sulfate distributions in which no obvious correlation with other meteorological variables was evident. Figure 9.6 represents a reconsideration of the patterns in Figure 9.4. If streamlines are used to infer transport, the positive deviations over the Carolinas on May 11 are evidently the result of transport from the sulfate producing northeast states. On March 10 the mid-Atlantic states are experiencing higher than normal sulfate concentrations as a result of winds passing over the

Ohio Valley source region. The large negative deviations over the mid-west mentioned in connection with Figure 9.4 can now be understood as arising in the northwest air flow coming from the relatively sulfate-free north central states. Reinterpretation of these distributions in terms of regional sulfate distribution and wind circulation convincingly demonstrates the primary role of long-range transport. This confirms and strengthens the conclusions of Spirtas and Levin (1970).

The strength of the sulfate source/wind relationship can be expected to depend on the general sulfate environment of a station. Stations in a rather extensive area of more or less uniform sulfate background might show less variability with wind direction than, say, St. Louis. Such a station might allow the unmasking of relationships with other meteorological variables.

Some complications to any interpretation of sulfate variability include such local effects as terrain and proximity to water bodies. For example, Lyons (1977) showed that large bodies of water can affect low-level atmospheric stability which in turn produces unexpected pollution problems. Additional problems can occur in analyzing sulfate pollution near the sea since sea salt nuclei may contain sulfate.

Because large scale sulfate concentrations depend upon wind direction, annual means, and interannual trends, inferences about intrinsic sulfate variability based on such data (Frank, 1974) should be reevaluated. The present monitoring network with 12 or so days between measurements may not be adequate to remove through averaging preferential wind directions which in turn may bias the derived annual mean. Furthermore, such means may be expected to vary from year to year because of shifting storm tracks and flow patterns associated with the planet's general circulation.

The results of this study suggest topics for further research. In some instances these new efforts may not be practicable without an improved sulfate sampling network or firmer knowledge of sulfate chemistry.

The direct measurement of sulfate concentration needs to be performed as a separate sampling process, not merely as a by-product of the total particulate evaluation. A separate sampling method for sulfate would eliminate much of the systematic error incurred by artifact production on the intake filter in the presence of other pollutants. Furthermore, the laboratory analysis would be simpler and more reliable if it were not first necessary to separate sulfates from the mixture of various substances. If and when this improvement becomes available shorter sampling periods and more frequent observations would be justified. Such data would help resolve some of the weather/sulfate relationships suspected but not

detected in this study.

Research into appropriate ways of filtering out the influence of wind direction in annual means and variability is needed if underlying variations due to source effluxes are to be determined. This might be accomplished by taking into account changes in annual wind roses and significant changes in regional sulfate sources. These filtered data would aid the Environmental Protection Agency in establishing meaningful sulfate standards, as well as providing data that could be subjected to analysis for relationships with other meteorological variables.

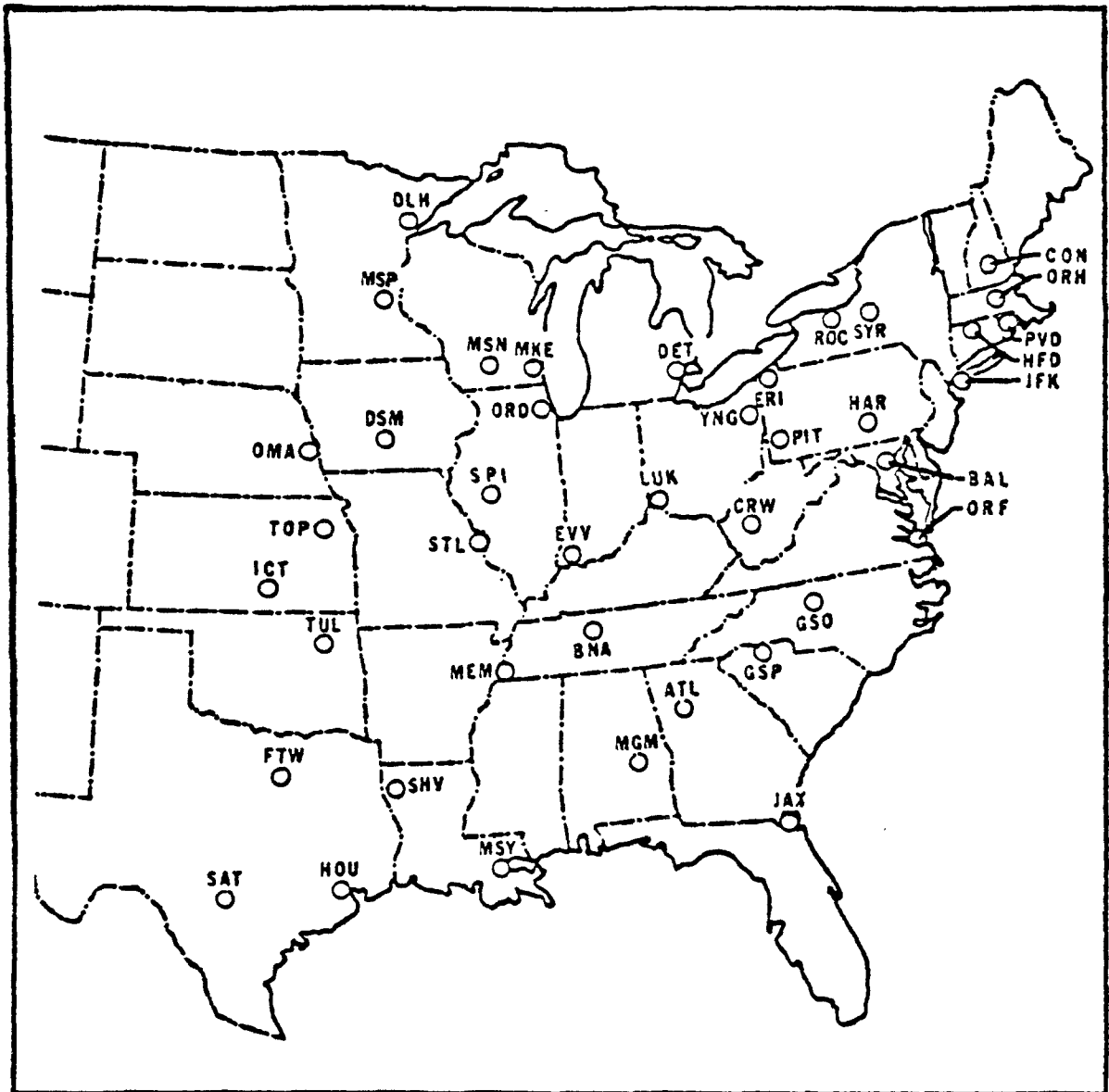


Figure 9.1 National Air Surveillance Network (NASN) stations whose data are employed in the present research.

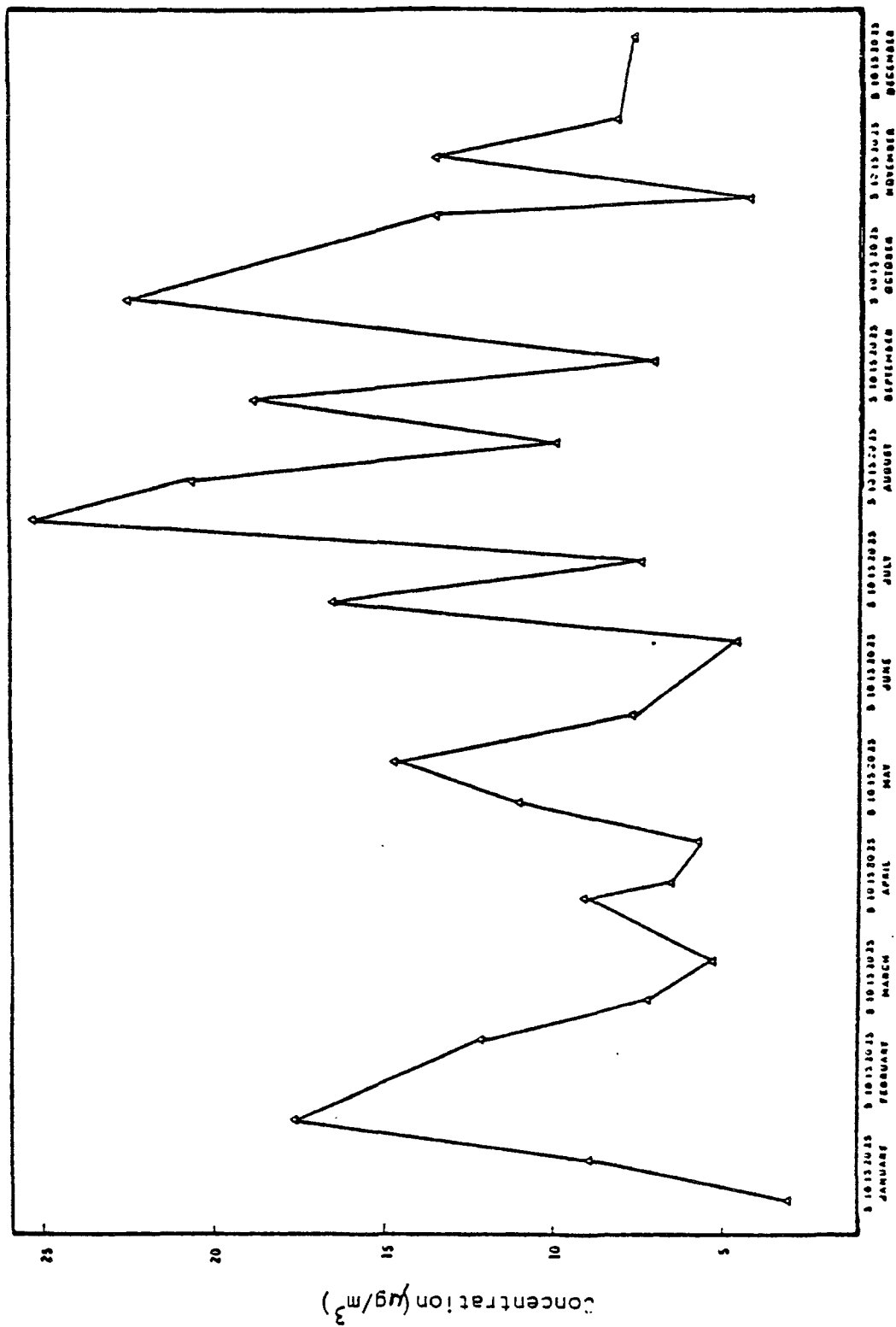


Figure 9.2 Time Series of one year's sulfate data (1972) for Nashville, TN.



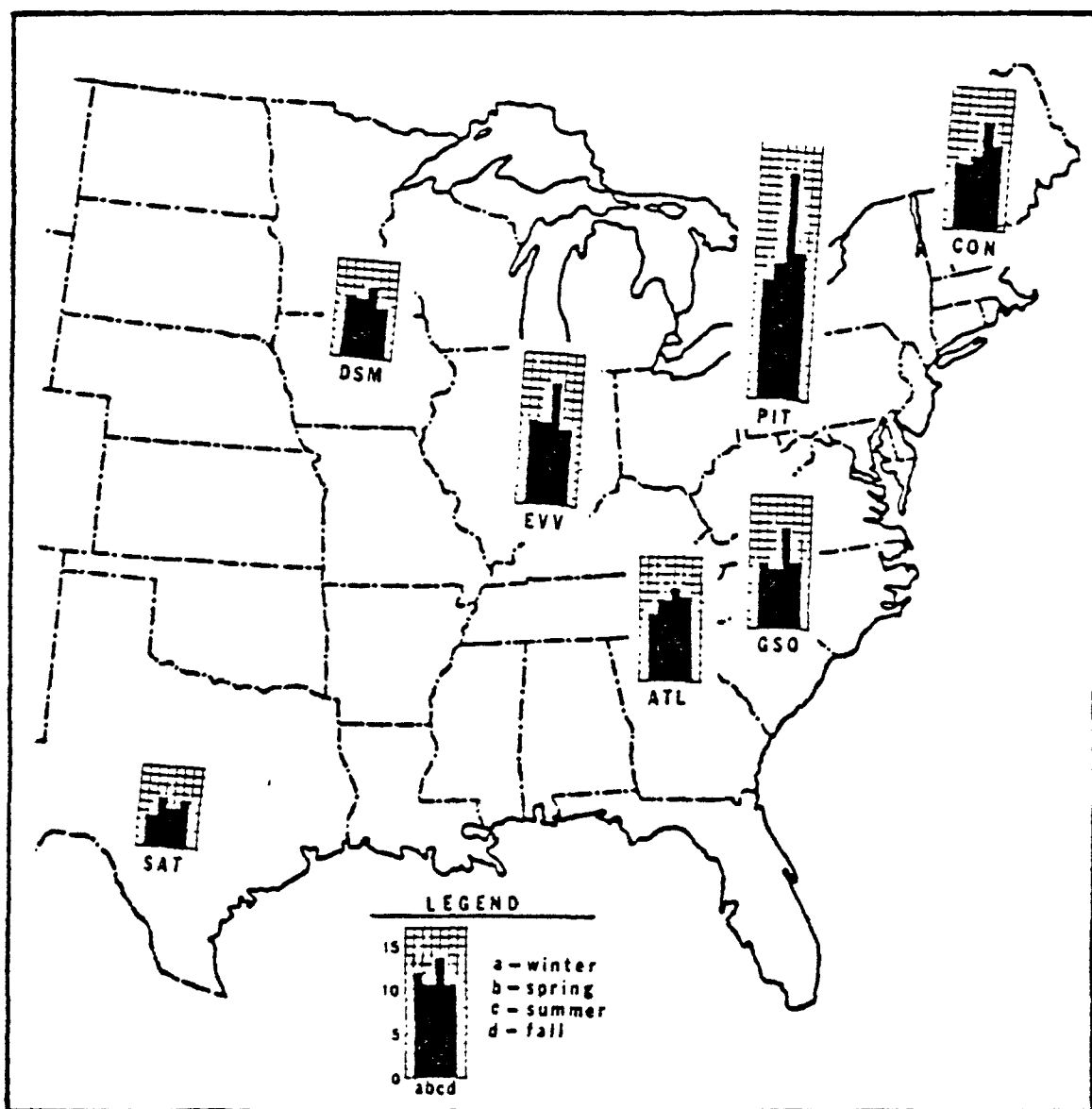


Figure 9.3 Regionally representative seasonal means (1969-1974). Each bar in the graph represents a mean seasonal value. Vertical scales are in units of  $\mu\text{g}/\text{m}^3$ .

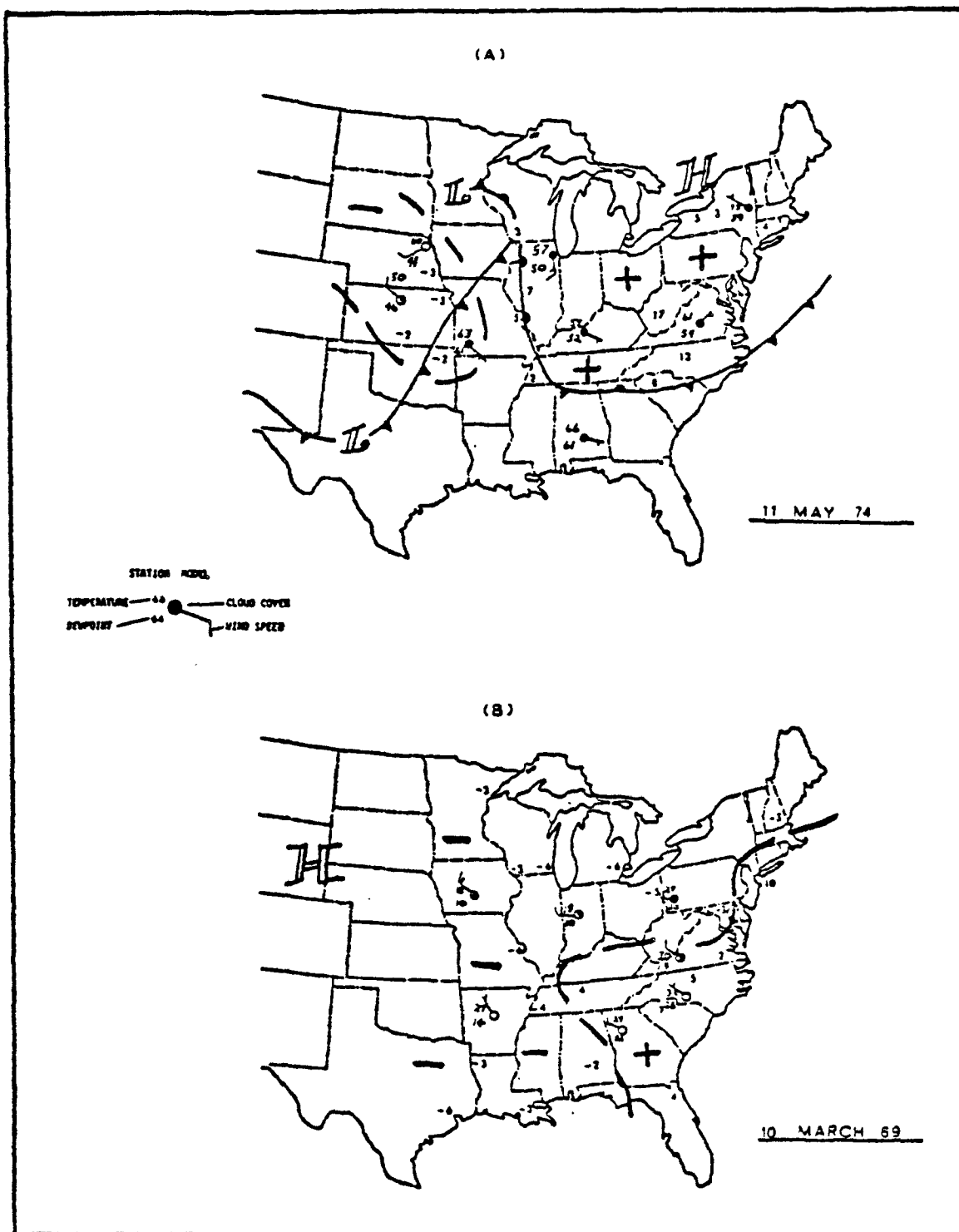


Figure 9.4 Patterns of synoptic weather (12GMT) and sulfate concentration. Sulfate concentrations are expressed as deviations from the seasonal mean. Only deviations greater than  $1 \mu\text{g}/\text{m}^3$  are plotted.

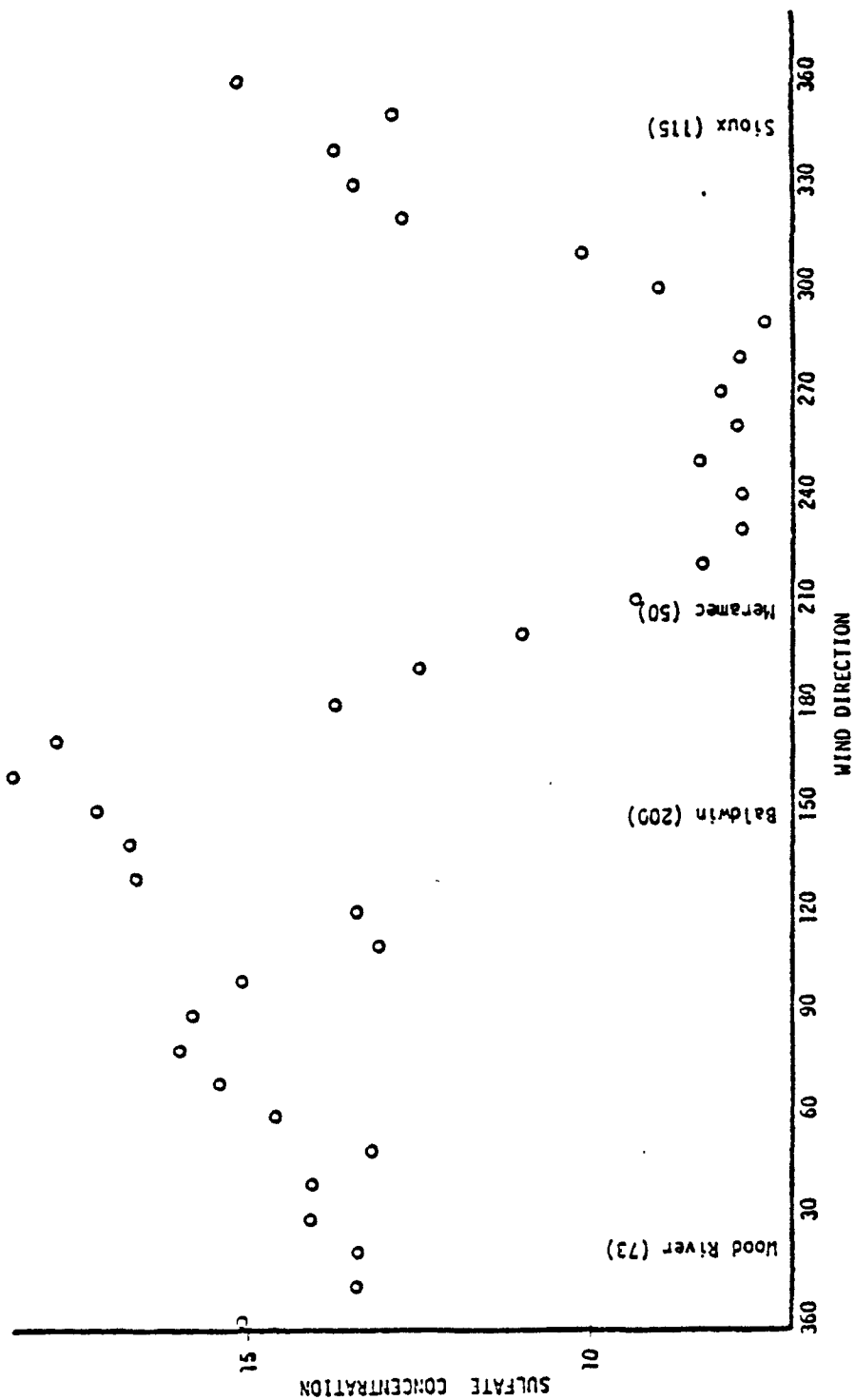


Figure 9.5 Sulfate concentration ( $\mu\text{g}/\text{m}^3$ ) versus wind direction at St. Louis, MO January-December 1969. The concentrations shown are 5-point running averages for those days with wind persistence  $> 85$  per cent. Annual  $\text{SO}_2$  emissions in 1000 tn/yr (in parentheses) are noted with source name.

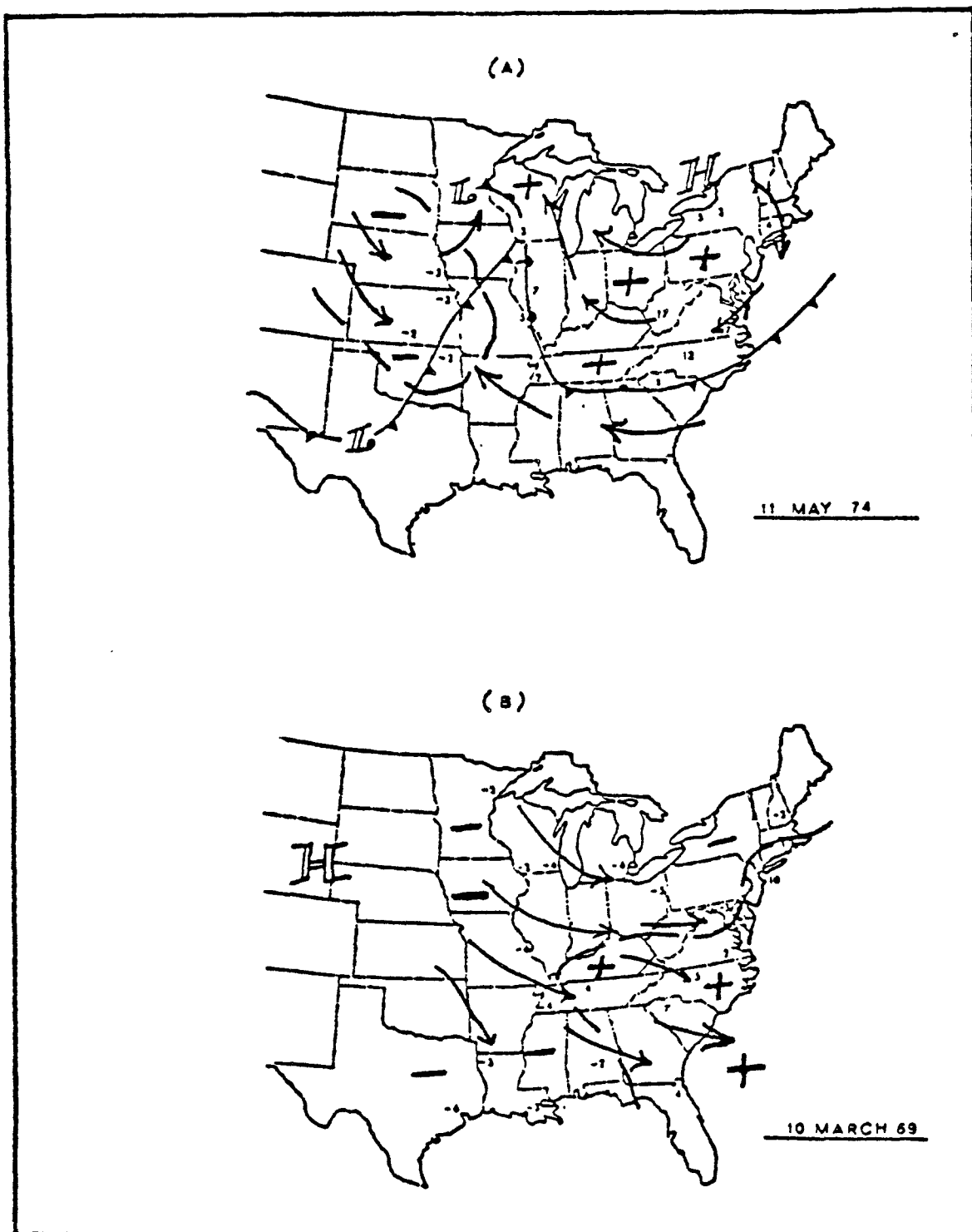


Figure 9.6 Patterns of synoptic weather (12 GMT) and sulfate concentrations. Streamlines (arrows) suggest sulfate transport. Synoptic stations are the same as in Figure 9.4, but have been omitted for figure clarity.

## SECTION 10

### DIURNAL VARIATION OF WIND PROFILES ACROSS MOUNTAINOUS TERRAIN DURING AN AIR STAGNATION PERIOD

Julius A. Jackson, W.J. Saucier, and W.D. Bach

#### Abstract

The diurnal variation of wind profiles across mountainous terrain during an air stagnation period was evaluated for seven days in the summer of 1957. The study was conducted across the north-central Appalachian Mountains, an area of heavy pollution concentration. The study was divided into easterly (16-18 July, 1957) and westerly (19-22 July, 1957) flow across the mountains.

Examination over the seven days showed a diurnal variation in boundary layer winds on the eastern side of the mountain range with a maximum amplitude of about 3 to 4 m sec<sup>-1</sup> at 1000-1500 m MSL in both the easterly and westerly flows. On the western side of the mountain range, a diurnal variation with a maximum amplitude of about 4 m sec<sup>-1</sup> at 600-1100 m MSL occurred in both flows.

This oscillation in the lower levels showed the presence of a low-level jet, which was unexpected in that this study was conducted during an air stagnation period. The low-level jet in the easterly flow across the mountains reaches a maximum wind speed at approximately 0600 GMT at about 300 m above ground level. In the westerly flow, the low-level jet occurs at approximately 1200 GMT at 600-800 m above the ground. This low-level jet is due to an inertial-type oscillation driven by the diurnal variation of the frictional forces aided by thermal forcing.

## INTRODUCTION

Stagnating anticyclones are often associated with incidents of heavy air pollution in urban areas. These anticyclones usually linger over an area for a protracted period (four days or more). During this period, surface wind speeds may be very low, and visibility and vertical mixing are often restricted. Thus, the circulation is often thought to be insufficient to disperse the accumulated pollutants of the atmosphere. The resulting accumulation may cause distressful and possibly hazardous conditions for inhabitants of the area.

The stagnating anticyclones that produce the major air pollution episodes are usually found in the eastern United States (Korshover, 1975), and are most likely to occur in late summer and autumn.

The northeast United States is very susceptible to air pollution episodes due to the heavy concentration of industry and population centers. Figure 10.1 shows the annual SO<sub>2</sub> emission density in the northeast and Ohio Valley areas. These pollution episodes not only affect the urban areas, but the non-urban areas are affected due to dispersion and transport of pollutants.

The purpose of this study is to investigate the effects of the mountains on the wind profile in the boundary layer during an air stagnation period, as well as the effects of boundary layer winds on air pollution dispersion and transport in a stagnation period over mountainous terrain. Various studies have been completed on diurnal wind variation in the boundary layer, but none (as could be found) during air stagnation period.

Bonner and Paegle (1970) found that boundary layer winds oscillate diurnally, reaching a maximum speed at night and a minimum during the day at elevations between 50 and 2000 m above the ground. The wind variation is especially pronounced with southerly flow over the central plains to the east of the Rocky Mountains. The amplitude of this oscillation is 2 to 3 m sec<sup>-1</sup> at levels of 0.5 and 2.0 km above the ground (Hering and Borden, 1962).

Boundary layer wind oscillations may arise from periodic variation in the horizontal pressure gradient force as in

mountain wind circulation, or they may be driven by day-to-night variation in the frictional force. A number of theories have been put forward to explain this diurnal wind oscillation which is often associated with the low-level jet. Blackadar (1957), argues that the jet results from a free inertial oscillation superimposed on the geostrophic basic flow, initiated by the rapid nocturnal breakdown of the frictional restraining force in the boundary layer. As the eddy diffusivity decreases during the onset of stable stratification in the evening hours, the motion in the upper part of the boundary layer becomes uncoupled from the frictional force and undergoes an inertial clockwise oscillation about the gradient wind vector. For the latitude of Washington, D.C., a maximum at lowest levels is most likely 9 hours after the oscillation begins. Attempts (Blackadar and Buajitti, 1957) to simulate this behavior indicated that both the mean value of the eddy viscosity and the amplitude of its diurnal variation must decrease rapidly with height. Numerical experiments with constant geostrophic wind and diurnally varying eddy viscosity duplicate reasonably well the observed oscillation over the central plains.

The present study attempts to describe the diurnal variation of wind profiles across the north-central Appalachian Mountains, and to find what effects the mountains have on the boundary layer wind profile. The six stations used in this study, which lie along an axis approximately perpendicular to the mountains, are listed in Table 10.1 and located in Figure 10.2.

## RESULTS AND CONCLUSIONS

Wind profiles across the Appalachian Mountains and available at six-hourly intervals showed the presence of a low-level jet during two air stagnation periods. These periods included July 19-22, 1957 when the flow was generally westerly, and July 16-18, 1957 when easterly flow prevailed. A representative 12 GMT surface analysis for each of the two periods is shown in Figure 10.3. Both periods are dominated by weak high pressure systems. Diurnal variability in profile shape is significant, but typically the wind maximum occurred at 0.5 to 1 km above ground. Wind speeds decreased rapidly above this level and then remained about constant to 3 km. Some of these features can be noted in the average wind profiles for two stations presented in Figures 10.4 and 10.5.

Diurnal oscillations about the daily mean in the zonal (U) and (V) wind components, at the same stations are portrayed in Figures 10.6 and 10.7. Amplitudes at jet level range from 1.5 to 3.0 m sec<sup>-1</sup>.

The analysis of the flow over the terrain has shown that the low-level jet is at different altitudes depending on the wind direction across the mountains. The time of the day is also a factor in the occurrence of the low-level jet. The easterly maximum low-level wind flow occurs at 0600 GMT (about 6 hours after sunset), and in the westerly flow it occurs at 1200 GMT (about 2 hours after sunrise) (Figures 10.8 and 10.9).

Inertial oscillations above the terrain as revealed by hodographs (for example, Figure 10.10) indicate that below the mountain top, on the windward side, the mountains tend partially to divert the component of the mean motion normal to the mountains to that parallel to the mountains. It also aids in explaining the wind maximum in the low-levels as an inertial-type oscillation driven by the diurnal variation of the frictional force aided by thermal effects.

Extensive analysis of the diurnal winds across the north central Appalachian Mountains has shown that a low-level jet exists across mountainous terrain during air stagnation periods. This jet is similar to that over the Great Plains, but is reduced in magnitude. Nevertheless, the low-level wind maximum described in this study can be effective in transporting and dispersing pollutants across the Appalachians.



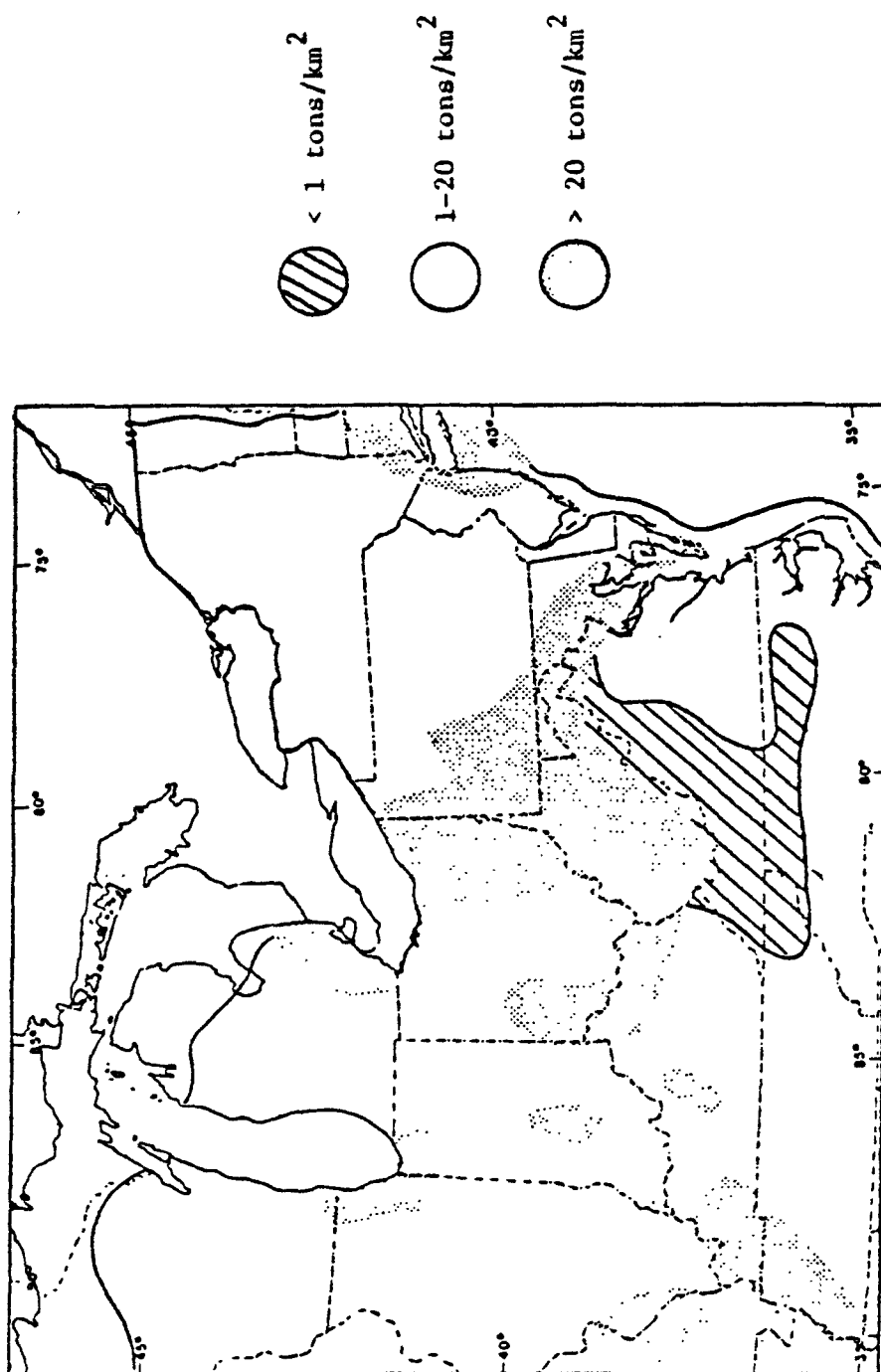


Figure 10.1 Geographic variation in annual SO<sub>2</sub> emission density  
(after EPA report 450/2-75-007).

Table 10.1 Station identifiers and elevations.

Station	Identifier	Elevations above MSL(m)
Washington, D. C.	DCA	20
Harrisburg, Pa.	HAR	107
Pittsburgh, Pa.	PIT	373
Akron, Oh.	AKN	377
Toledo, Oh.	TOL	211
Flint, Mich.	FNT	233

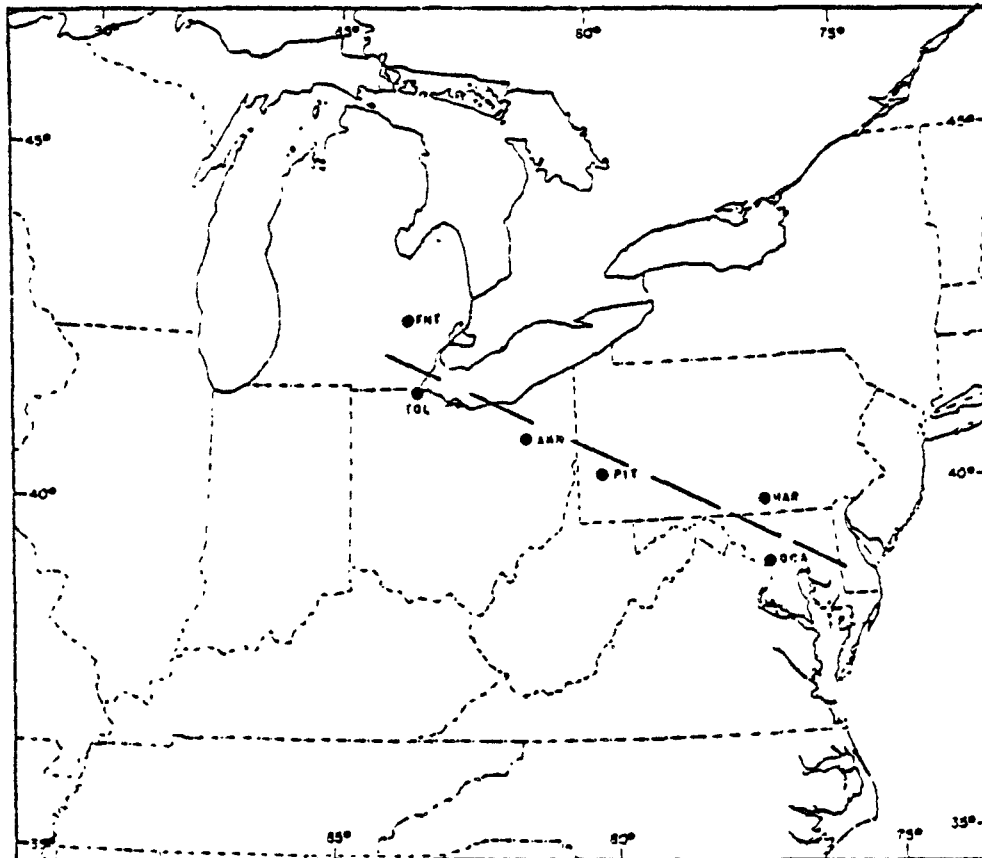


Figure 10.2 Area and stations analyzed.

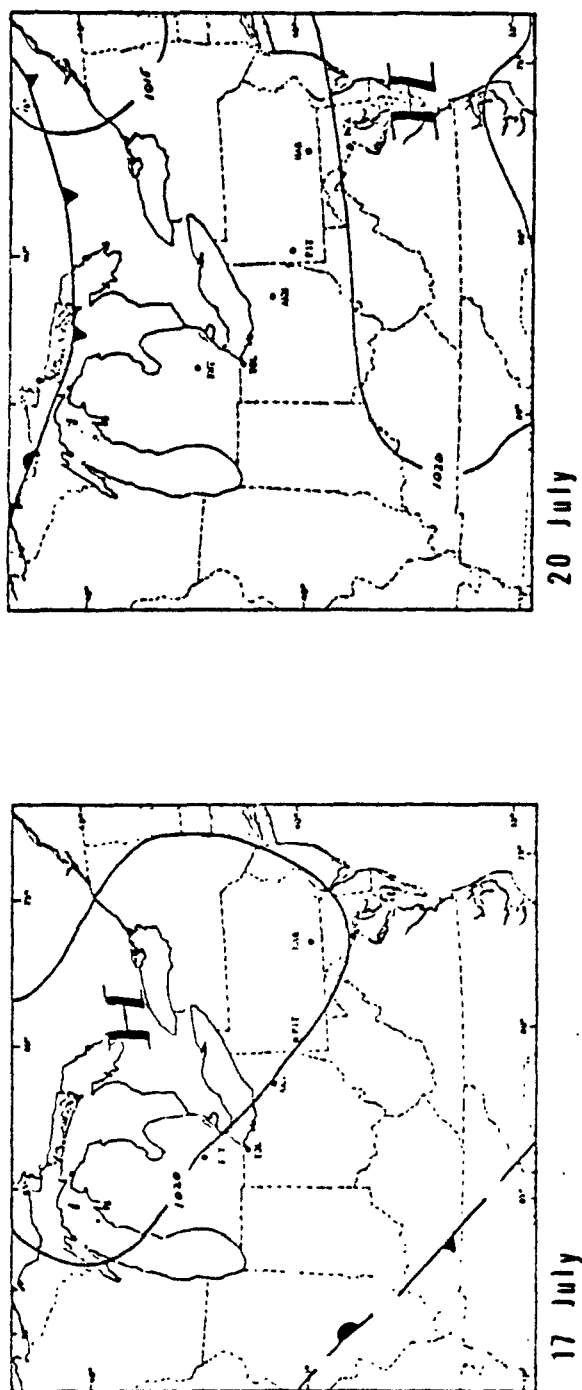


Figure 10.3 Representative sea level pressure analyses during the air stagnation period 16-22 July 1957 featuring light easterly winds (17 July) and light westerly winds (20 July) over the study area.

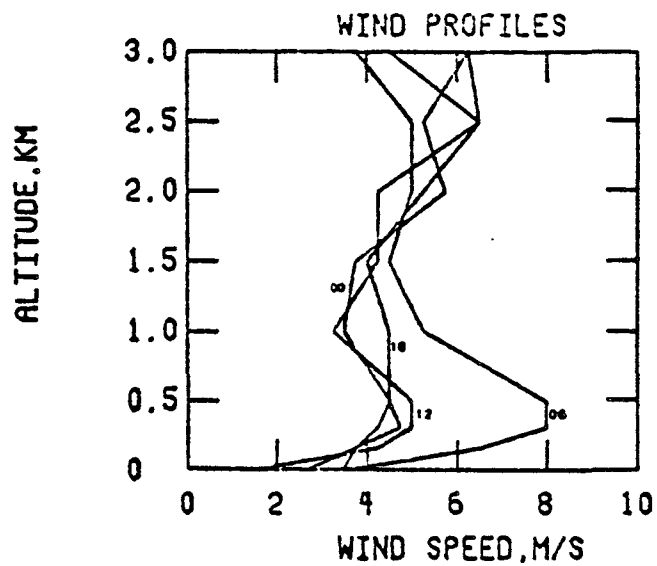


Figure 10.4 Average wind speed profile for westerly flow at Washington, D.C.

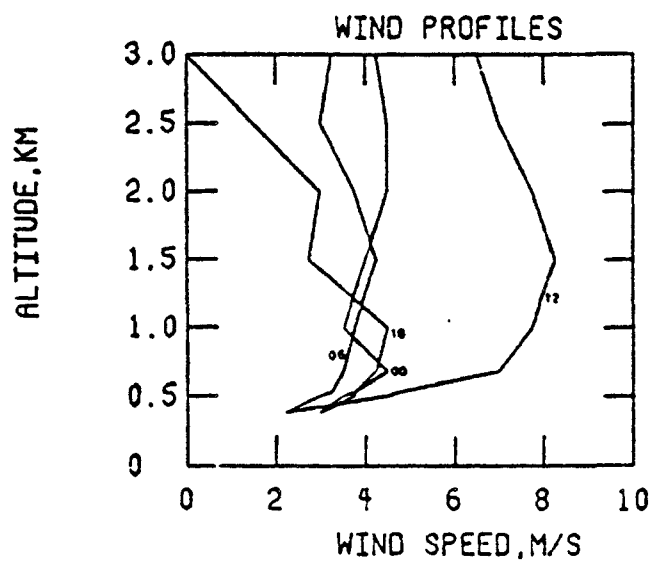


Figure 10.5 Average wind speed profile for westerly flow at Akron, Ohio.

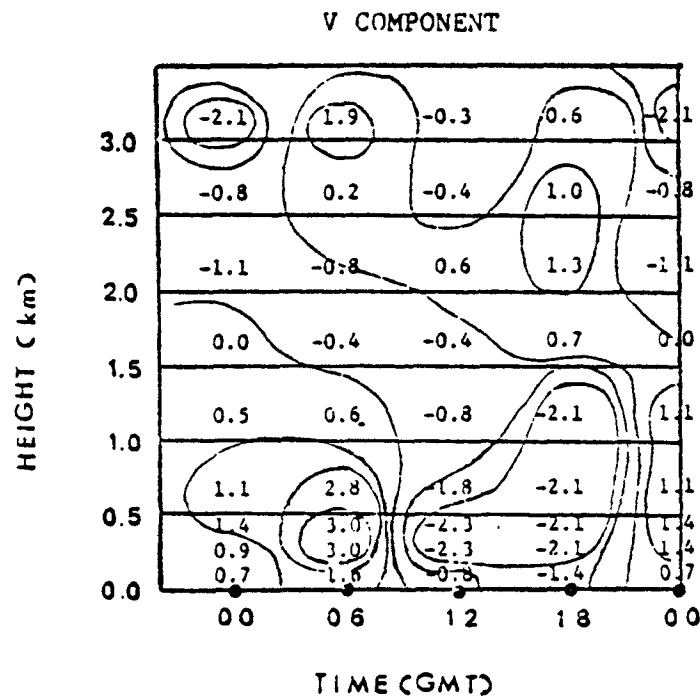
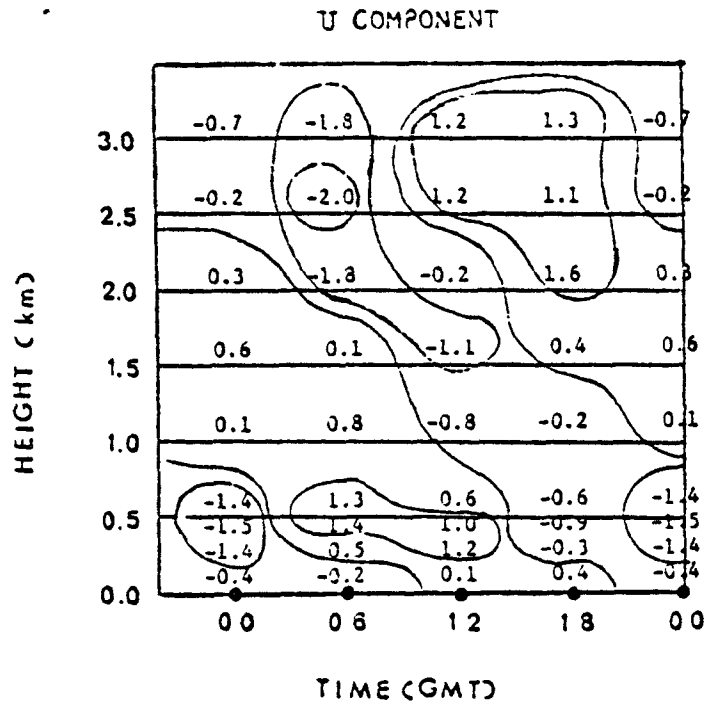


Figure 10.6 Time variation of the deviation in westerly wind from its daily mean at Washington, D.C. Values are in meters per second; times are in GMT.

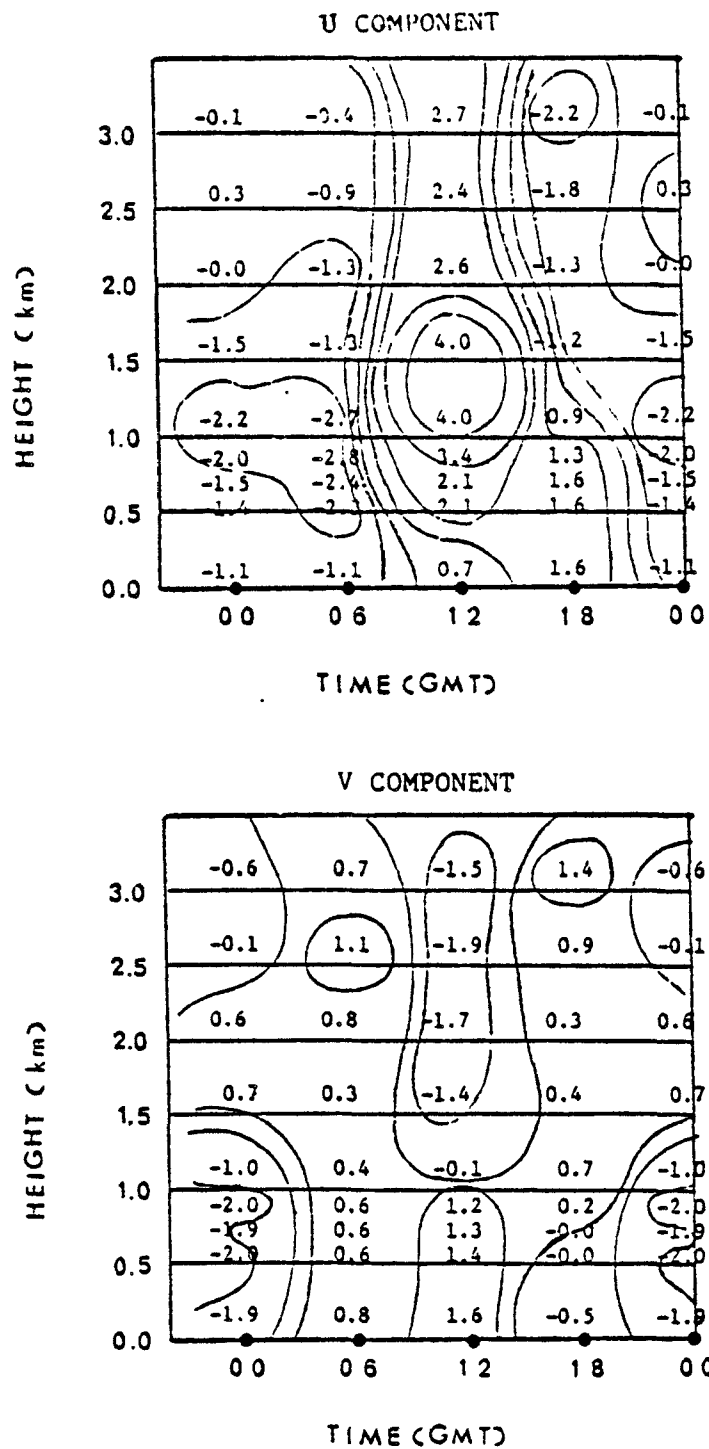


Figure 10.7 Time variation of the deviation in westerly wind from its daily mean at Akron, Ohio. Values are in meters per second; times are in GMT.

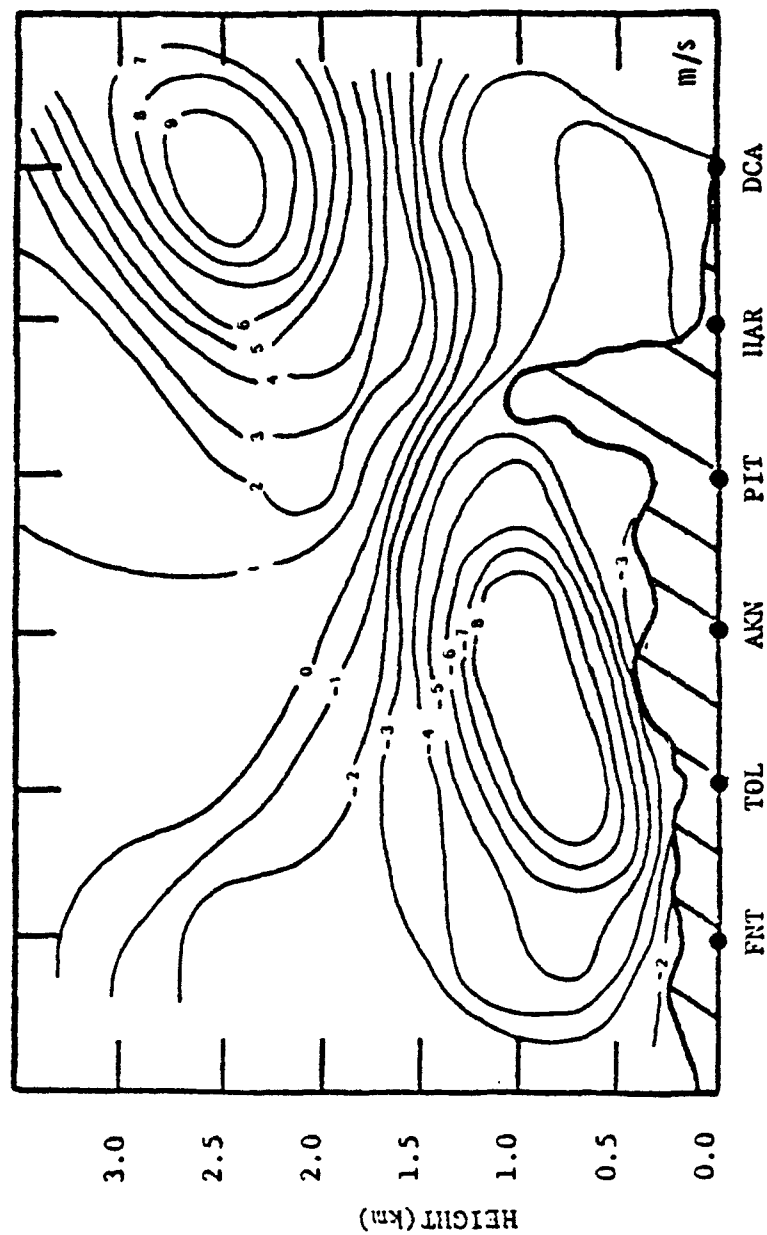


Figure 10.8 Cross-section of 0600 GMT easterly flow  
(U component) across terrain.

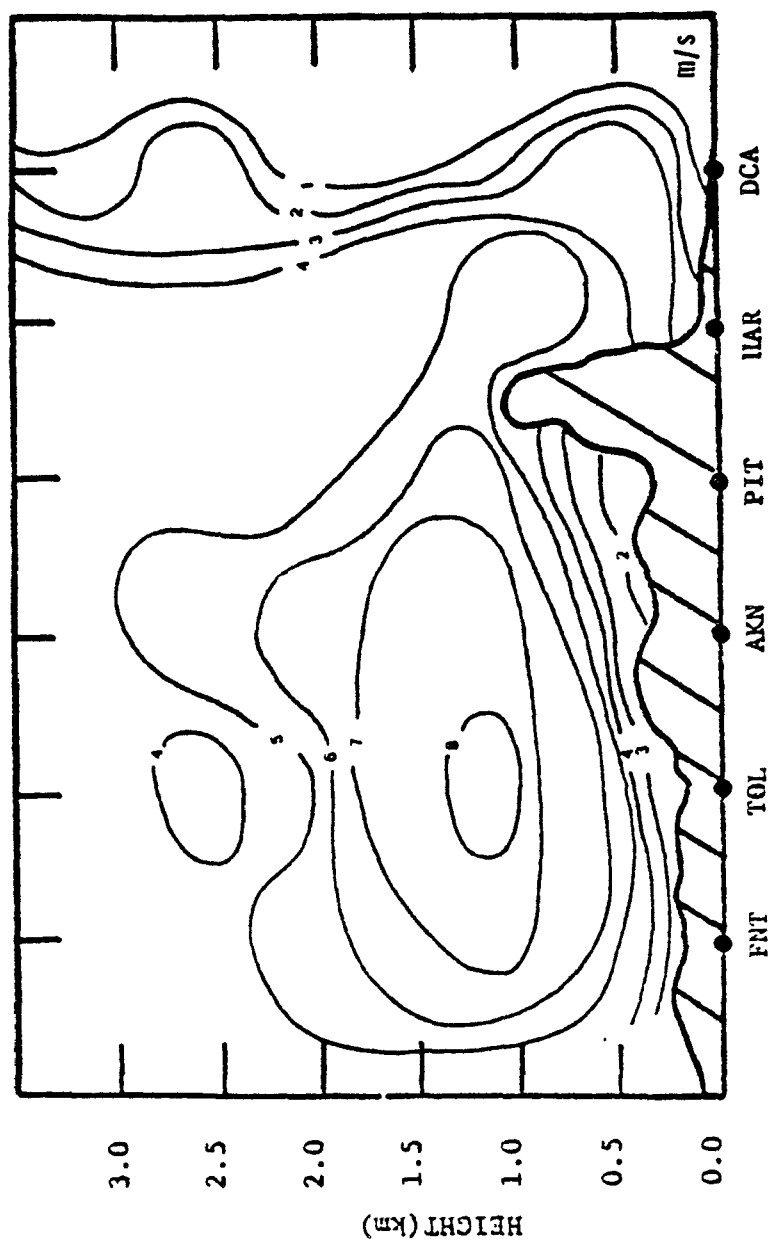
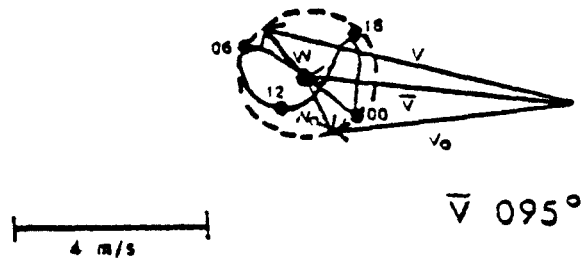


Figure 10.9 Cross-section of 1200 GMT westerly flow  
(U component) across terrain.



EASTERLY (0.5 km)



WESTERLY (0.5 km)

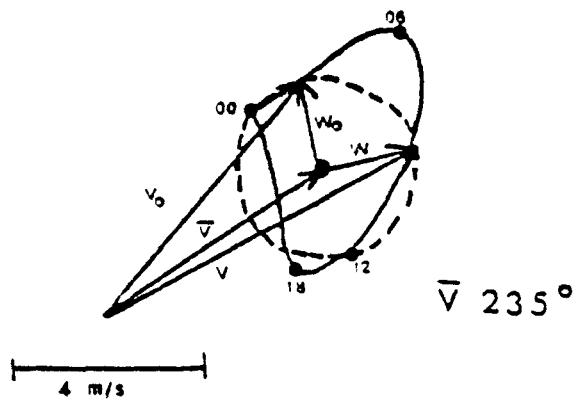


Figure 10.10 Hodographs of the wind variation at DCA in the easterly and westerly flow. Heights are MSL; times are GMT.

## SECTION 11

### A MESOSCALE ANALYSIS OF AIR FLOW IN COMPLEX TERRAIN

Christofer Maxwell, W.J. Saucier, T. L. Tsui and G.C. Holzworth

#### Abstract

Analyses of wind data are presented which examine the coupling of the surface and 850mb wind directions in a region of complex terrain. The data were grouped based on periods when the 850 mb wind directions were parallel or perpendicular to the major valley axis. The diurnal and pressure gradient influences were also examined.

The analyses show that the surface and 850mb wind directions agree best when the 850mb winds are about parallel to the valley axis. The agreements are best during daytime periods when the 850mb wind speeds are strong. In addition, wind measurement sites in valleys agreed better with the 850mb winds than did sites located on ridges. When the 850mb winds were perpendicular to the valley axis, the wind measurement sites on ridges tended to agree better with the 850mb winds than did the valley sites.

Further analyses show that 30m tower wind sensors can be discriminately used to predict the direction of power plant plume travel in complex terrain regions. The tower sensors are unreliable during nighttime hours and are best during daytime hours when the 850mb winds are parallel to the valley axis.

## INTRODUCTION

The structure of wind fields over flat terrain is well understood. Both the statistical and turbulent quantities have been examined and are fairly well expressed mathematically. Recently, however, attention has been shifted toward learning more about air flow in complex terrain. The reasons for the shift are varied but strong influence comes from atmospheric pollution control agencies as well as energy and defense concerns.

Very few locations in the United States conform to the terrain and source characteristics of the places where empirical determinations were made of the atmospheric dispersion parameters. The terrain in areas where there is an interest in calculating the pollution potential will exhibit varying degrees of complexity, either a step change in roughness, variations in temperature fields, or actual terrain variations. Early studies of air flow in irregular terrain were limited (Defant, 1951; Forchtgott, 1949; Gleeson, 1951), and even at present relatively few investigations are being conducted to study the flow characteristics in complex terrain. Consequently, there is a strong need to learn more about the basic influences of terrain on the winds.

A simplistic description of the diurnally varying circulations resulting from the variably-sloped terrain within a valley was presented by Defant (1951) (Figure 11.1). Using a symmetrical valley with an axis running east to west, Defant showed the diurnal changes in winds due only to heating by the sun passing directly overhead and due to the subsequent radiative cooling at night.

Defant's description explains the basic principle of the diurnal pattern of slope and valley winds but considers an ideal valley. Other researchers expand and add to Defant's description of mountain/valley winds. Gleeson (1951) developed Defant's description further by explaining the single cellular pattern that would result when the sun warms one valley slope and not the other. Instead of air sinking down the middle of

the valley, the air tends to sink along the slope that is not in sunlight. Forchtgott (1949) and Musaelyan (1964) discussed vortices produced in the lee of ridges due to winds blowing perpendicular to the ridges. Forchtgott noted that vertical and horizontal extent of the lee side vortices increased with increasing wind speeds. More recently, Nappo (1977) presented analyses of the three-dimensional wind fields over a large area of eastern Tennessee mountains. In particular, he compared the vertical wind field structure of complex terrain to uniform terrain.

The analyses to be presented here examine the statistical relationships between the surface and upper level winds within a mountainous or complex terrain region. The terrain influence will be measured by examining wind direction differences between the surface and upper levels during periods when the upper level winds are perpendicular and parallel to the valley or ridge axis. In addition, the turning of the near-surface winds to those at 850 millibars (mb) will be examined.

The data used in the analyses are from the Power Plant Stack Plumes in Complex Terrain study conducted by GEOMET, Inc. for the U.S. Environmental Protection Agency. The purpose of the study was to collect a reliable data base for meteorological studies in complex terrain and to examine the effects of complex terrain on the dispersion of power plant plumes. The study was conducted in the mountains of southwest Virginia along the Clinch River in the vicinity of Carbo, Virginia.

The terrain within the study area is highly complex. Elevations vary from 1500 feet MSL to better than 3500 feet MSL. The major valley axes extend approximately from southwest to northeast. Most of the study area is covered by forest.

The power plant used for the study is the Clinch River Steam Plant. The plant has a maximum generating capacity of 712 megawatts (MW). The daily-average minimum output is 491 MW between 3 and 4 a.m.. The average daily maximum output is 661 MW between 11 a.m. and 12 noon. The plant burns coal, releases the exhaust through two 453 foot stacks, and is considered a base-load plant.

The Power Plant Stack Plumes in Complex Terrain study spanned a sixteen month period, June 1976 through September 1977, during which meteorological and pollutant data were collected at eight fixed stations. For brevity the names of the fixed stations will be referred to as:

Castlewood-----	Castle (8 km WSW)
Tower-----	Tower (3 km NE)
Nash's Ford----	Nash (11 km ENE)
Lambert-----	Lambert (8 km E)
Munsey-----	Munsey (4 km SE)
Hockey-----	Hockey (6 km SE)
Johnson-----	Johnson (6 km S)

The approximate distance and direction of the seven stations from the Clinch River Plant are noted.

The data collected at each fixed station are listed in Table 1. All data are stored as hourly average values, with the exception of the hourly peak values of the pollutants, on magnetic tape.

Upper-level data consist of 850 and 700 mb winds from three stations surrounding southwestern Virginia; namely, Greensboro, NC; Huntington, WV; and Nashville, TN. The winds were decomposed into east-west (U) and north-south (V) components, and distance-weighted values then interpolated to the study area. Winds were considered parallel to the valley axis if within a 45° sector of the mean valley bearing (60°-240°). Perpendicular winds were those within a 45° sector centered on 150° or 330°. Wind direction at 850 and/or 700 mb fell within these four sectors 64.6% of the time included in the study period; NW perpendicular and SW parallel winds accounted for 60.1% of all winds directions. Directional sectors for surface winds were 60° wide in order to allow for some terrain deflection and frictional effects.

Results presented in the next section were obtained during the one-year period October 1976 through September 1977.

## RESULTS AND CONCLUSIONS

The description of the diurnal cycle of slope and valley winds by Defant is simplified in using a symmetric valley. The orientation of a valley as well as the angle of its slopes and the complexity of its surface will complicate the slope and valley flows. However, the basic physics of Defant's description is good, as can be seen in the day and night wind roses for a valley (Nash) site from the Power Plant Stack Plumes in Complex Terrain study (Figure 11.2). The Nash site is located in a valley with higher elevations to the northeast (Figure 11.3). The wind roses show the tendency of the wind directions to reverse from down-valley at night (Figure 11.2a) to up-valley during the day (Figure 11.2b). In addition, the up-valley winds tend to be faster than the down-valley winds. This may simply reflect the fact that daytime winds are generally faster than

nighttime winds from all directions, as appears to be the case here.

The surface winds in complex terrain regions become further complicated by the channelling effects of the terrain (Start, 1975; Egami, 1974; Nappo, 1977). Channelling effects can be observed readily at the ridge sites of the Power Plant Stack Plumes in Complex Terrain study. Figure 11.4 depicts the night and day wind roses for the Hockey site. The terrain surrounding the Hockey site is shown in Figure 11.5. The wind roses show the preference of winds to come up through the hollows on the side of the ridge and, in particular, up through the wide hollow to the south-southwest of the site. This is observed both day and night. In addition, the speeds of the winds tend to be faster when the winds blow through the hollows.

The analysis schemes used to examine the interaction of the surface and upper-level winds during periods when the upper-level winds were parallel and perpendicular to the valley axis worked well. In general, the terrain influence appeared more significant when the upper-level winds were perpendicular to the valley as opposed to parallel to the valley. Tables 11.2 and 11.3 present many of the relationships described further below.

In the latter table poor ( $< 25\%$ ) and good ( $> 60\%$ ) agreement refer to the percentage of the 12-hour periods centered on the two radiosonde times that the hourly surface winds were in agreement with the sector direction of the upper-level winds. In this way something of the short-term persistence of the surface wind is introduced as another factor in categorizing results.

Examinations of the periods when the upper-level winds were parallel to the valley showed fair to good correlation of wind directions between valley stations and the upper levels. The valley station wind directions were from the same directional sectors as the upper level winds about 50% of the time. The agreement was found to be stronger during the day than at night suggesting a stronger thermal influence on the local winds during the night than during the day. Stations located in broad valleys, on the side of valley slopes, or on ridges had significantly lower percentages of agreement. A 30m tower located in a valley had wind directions within  $\pm 45^\circ$  of the 850mb wind directions 85% of the time during the day. At night the agreement dropped to 76.2% of the time. The tower located on the ridge had lower agreements: 80.0% during the day and 58.3% at night. Intuitively, the magnitude of the agreements decreased when considering sectors  $60^\circ$  ( $\Delta\theta = \pm 30^\circ$ ) wide or when veering cases alone were considered ( $\Delta\theta = +45^\circ, +30^\circ$ ). Faster wind speeds at 850mb tended to improve the agreement in the wind directions between the surface and upper levels during the 1200 GMT radiosonde release periods, but were not as strong a factor

during the 0000 GMT radiosonde release periods.

In general, the agreement of wind directions between the surface and upper levels was lower when the upper level winds were perpendicular to the valley axis instead of parallel to the valley axis. During the perpendicular flow periods, surface stations located on ridges had better agreement of wind directions with the upper levels than the valley sites. Again the agreements were better during the day than at night. The wind directions at the tower located on the ridge were within  $\pm 45^\circ$  of the upper level wind directions 78.9% of the time during the 0000 GMT radiosonde releases and only 33.3% of the 1200 GMT radiosonde releases. The valley site tower had corresponding values of 71.4% during the 0000 GMT releases and only 9.9% of the 1200 GMT releases. Similar to the parallel flow periods, faster 850mb wind speeds improved the agreement between the 850mb wind directions and the 30m level wind directions at Hockey and Tower during the 1200 GMT radiosonde release times, but did not appear to be a strong factor at the times of the 0000 GMT radiosonde releases.

The results of the analyses give insight into the extent of the influence of complex terrain on surface winds. Slope and valley winds apparently account for a large portion of the observed surface winds. Typical valley winds are commonly observed in narrow valley locations and are less frequent in broad valleys. The vertical extent of valley winds is fairly deep. Defant (1951) suggested the valley winds extend to the height of the flanking ridges. During periods when the upper level winds are parallel to the valley, however, the wind directions may be uniform up to the 850mb level. Slope winds affect locations on valley slopes and ridges. The vertical extent of slope winds on the ridges appears small with some data suggesting about 30m.

In the analysis that compared the difference in wind direction between the 850mb wind and the corresponding hourly-average 30m level winds at Hockey and Tower (Table 11.4), the separation of the results into the two radiosonde release times (0000 GMT and 1200 GMT) was significant. The variation between the release times is attributed to the day to night differences of the Tower and Hockey winds. Since most of the release periods studied occurred during the winter and spring, this assumption appears appropriate. The 0000 GMT (0700 LST) radiosonde release which was compared to the 0700-0800 hourly average winds at Hockey and Tower is believed to represent nighttime conditions. Although sunrise usually occurs by 0700 LST, the solar elevation is not large enough to affect the flow in the valleys due to the shading by the surrounding ridges; thus, the nocturnal valley wind circulations continue considerably past the time of sunrise. The length of the delay until the sun will heat the valley surface depends on the

orientation of the valley, the height of the surrounding ridges, and the season. The argument to use the 0000 GMT (1900 LST) radiosonde release is weak for the late fall, winter, and early spring months. During the other months, sunset occurs near to or later than 1900 LST; therefore, the daytime valley wind circulations are still present and the 0000 GMT radiosonde release represents the daytime conditions. During the late fall, winter, and early spring, the sun sets considerably before 1900 LST. Therefore, the nocturnal valley wind structure is developing; however, the up-valley wind from the daytime may still be present and therefore be partially representative of the daytime wind field structure. Consequently, the 0000 GMT radiosonde release generally represents the daytime cases and the 1200 GMT radiosonde release represents the nighttime cases.

The appropriateness of using the 30m level wind directions at the Hockey or Tower sites to predict the direction of plume travel will depend on the time of day and the direction of the 850mb winds. Provided the plume direction of dispersion is needed more in a qualitative rather than a quantitative sense, the Tower and Hockey 30m winds can be used in some cases. The Hockey and Tower winds are inappropriate at night when the 850mb winds are perpendicular to the valley axis. During the day, with the same 850mb winds, the Hockey 30m level winds will give a fair to good indication of plume travel. During all periods when the 850mb winds are parallel to the valley, the 30m level winds at Tower will give a good indication of plume travel. The daytime winds, however, will be more representative than the nighttime winds. In addition, the faster the 850mb winds the better the Tower and Hockey winds will represent the direction of plume dispersion.

Numerous studies of the Power Plant Stack Plumes In Complex Terrain data should be undertaken to determine the basic structure of wind fields in complex terrain. Other studies could readily include the correlation of winds with ground level pollutant concentrations, the temperature field in complex terrain, the distribution of stability categories, and the change in wind speeds with height within the confines of the valley. In all, the data are of good quality and can be used to identify many basic influences of terrain on the wind field.



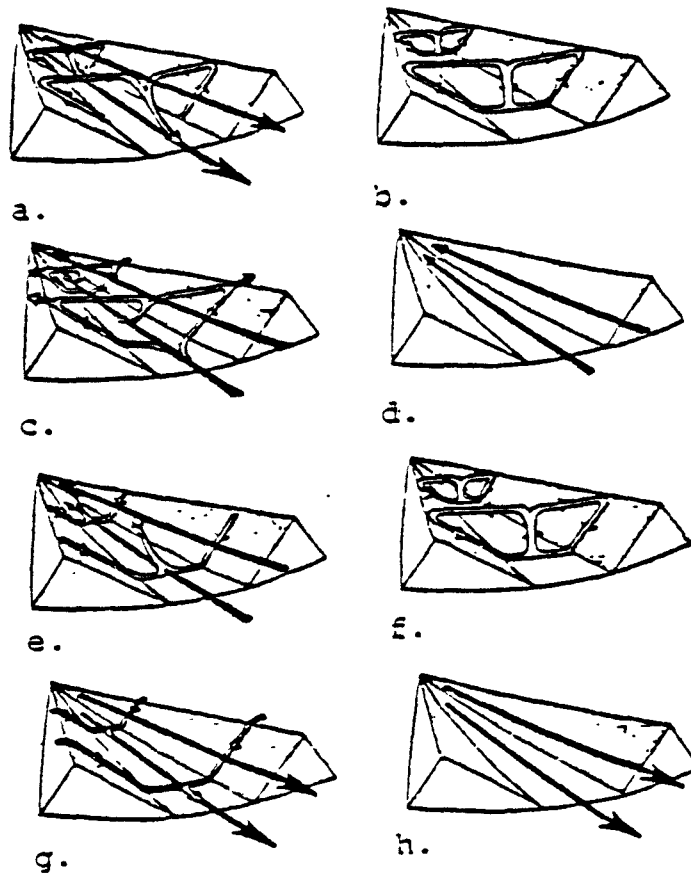


Figure 11.1 Variations in the Windfield Within a Symmetrical Valley Due to the Uneven Heating of the Variably Sloped Terrain (Defant, 1951).

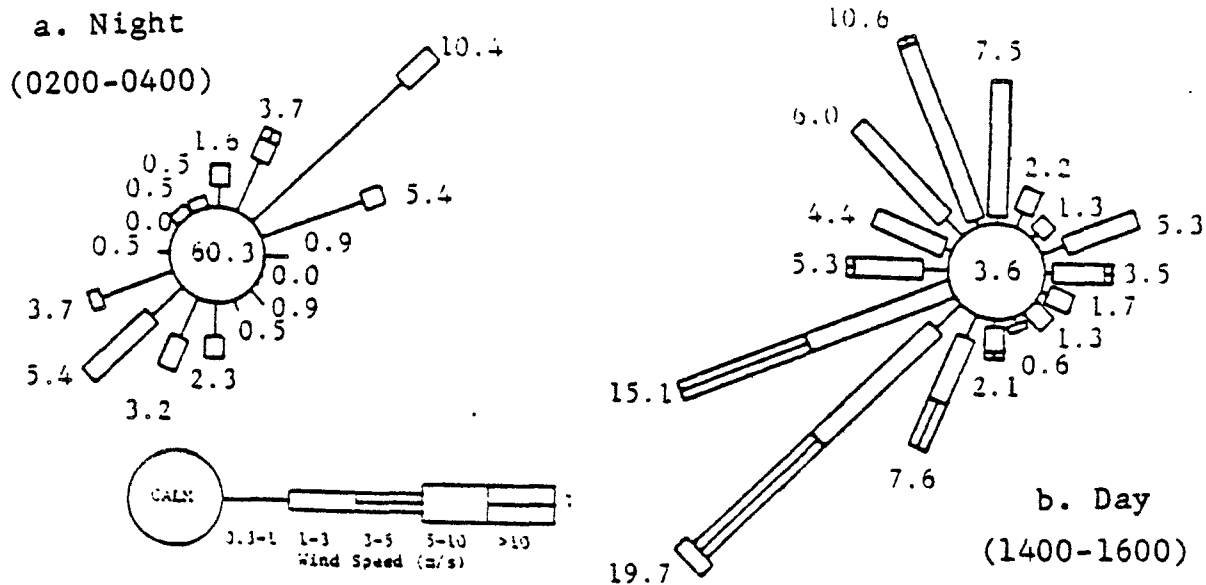


Figure 11.2 Night and Day Wind Roses at a Valley (Nash) Site.

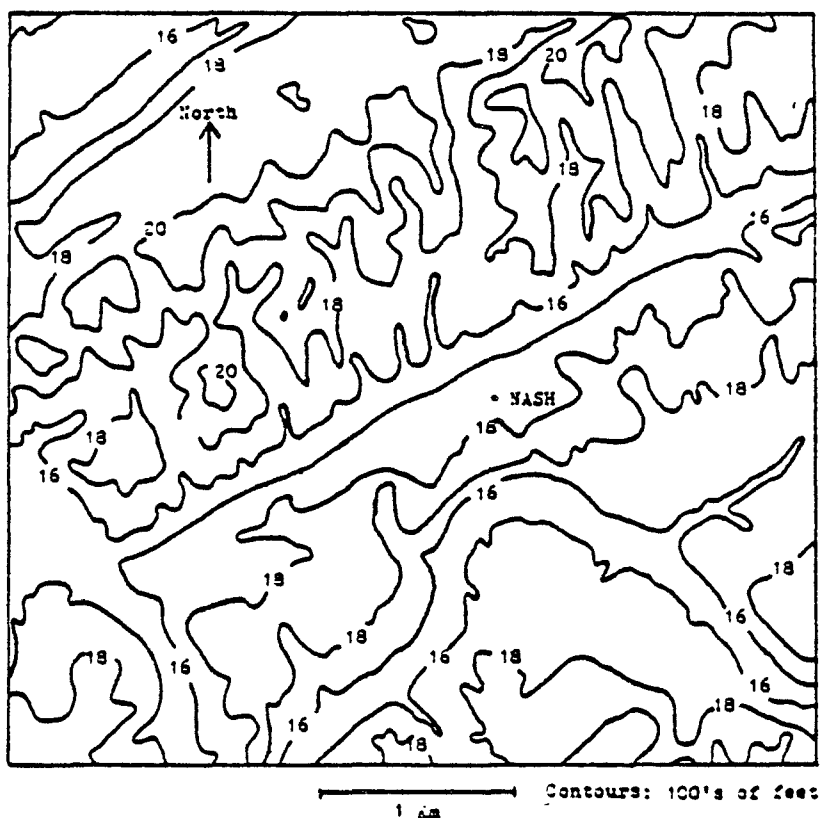


Figure 11.3 Terrain Surrounding the Nash Site.

a. Night (0200-0400)

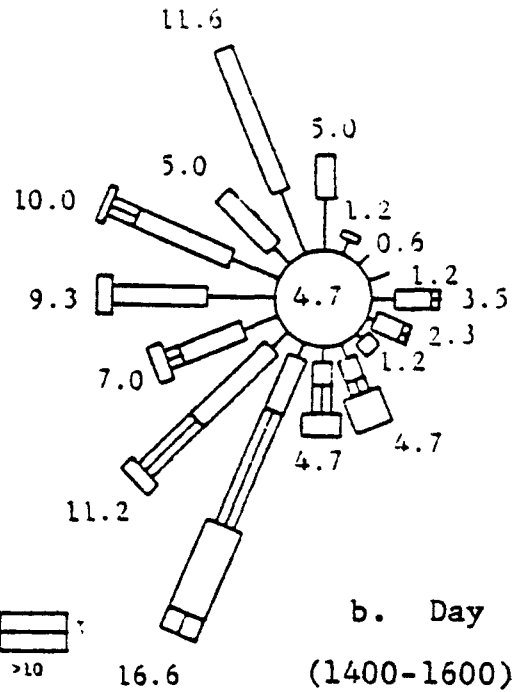
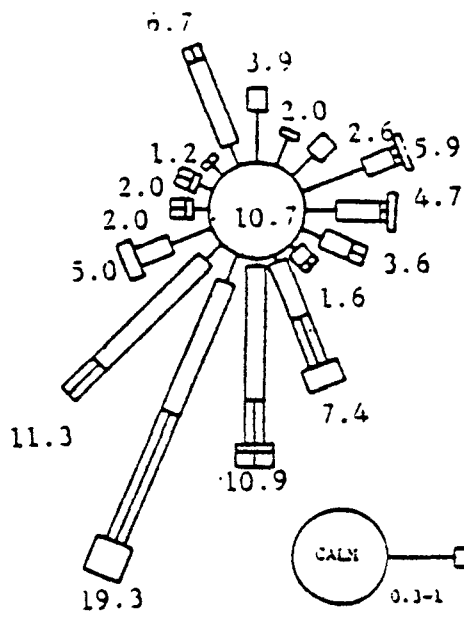


Figure 11.4 Night and Day Wind Roses.

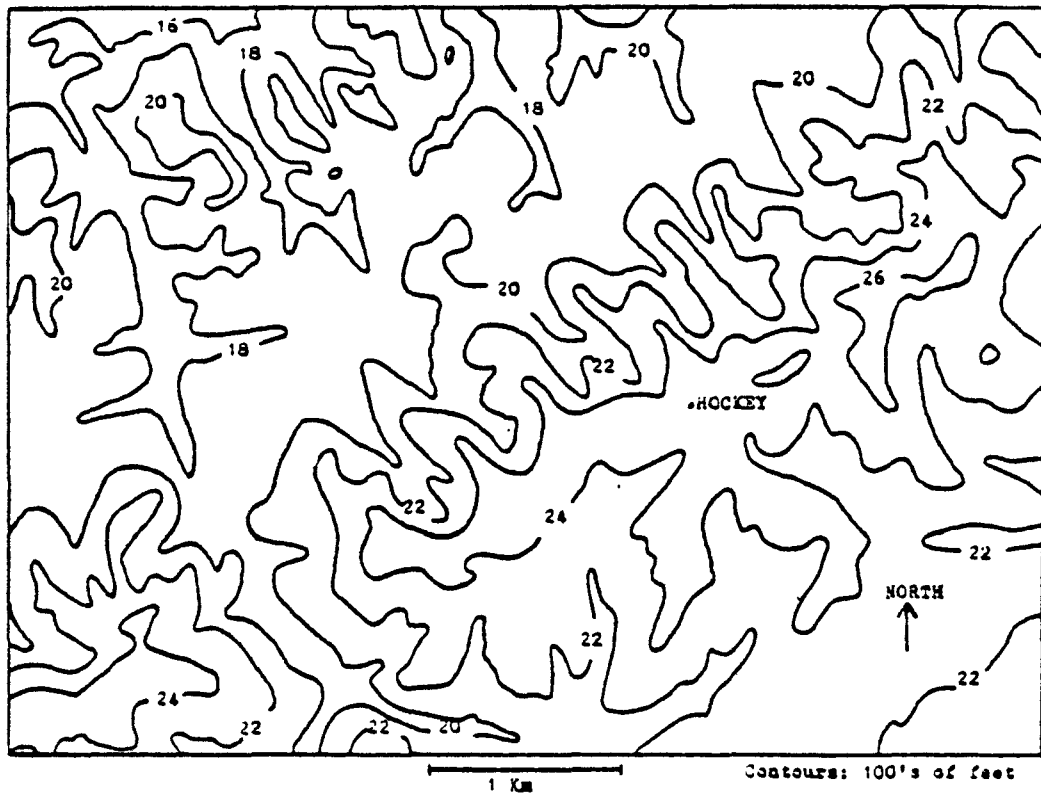


Figure 11.5 Terrain Surrounding the Hockey Site.

Table 11.1 Data Collected at Each of the Eight Fixed Stations (Koch, 1978).

Recorded Measurements	Station								Instrument
	Tower	Munsey	Nash's Ford	Hockey	Cattlewood	Kent's Ridge	Johnson	Lambert	
Sulfur Dioxide	x	x	x	x	x	x	x	x	Monitor Lab Model 8450
Nitrogen Oxides									Monitor Lab Model 8440
NO	x	x	x	x	x	x	x	x	
NO <sub>2</sub>	x	x	x	x	x	x	x	x	
NO <sub>x</sub>	x	x	x	x	x	x	x	x	
Wind, 10mi	x	x	x	x	x	x	x	x	MRI Model 1022 (Model 1053 at Tower)
Speed	x	x	x	x	x	x	x	x	
Direction	x	x	x	x	x	x	x	x	
gA	x	x	x	x	x	x	x	x	
Elevation	x	x	x	x	x	x	x	x	
OE	x	x	x	x	x	x	x	x	
Temp., 10m	x	x	x	x	x	x	x	x	MRI Model 815
Sulfates									Muco HI-Vol (Special 24 Head)
Relative Humidity	x		x	x	x	x	x		MRI Model 815
Precipitation	x								MRI Model 370
Wind, 30m	x			x					MRI Model 1053 (Model 1022 at Hockey)
Speed	x			x					
Direction	x			x					
gA	x			x					
Elevation	x			x					
OE	x			x					
Temp. Grad.									MRI Model 815
0.5 to 30m	x								
0.5 to 4 m	x								
UV Radiation	x								International Light Model PT100-CM100
Total	20	9	9	12	9	9	4	4	

Table 11.2 The Frequency of Surface Winds Coincident  
With the Upper Level Winds.

<u>Station</u>	<u>Station Description</u>	<u>Percentage of Time Surface and Upper Level Winds are Coincident</u>		<u>Ratio (SW Parallel / NW Perpendicular)</u>
		<u>NW Perpendicular</u>	<u>SW Parallel</u>	
Castle	Valley	36.0	25.6	0.71
Tower	Valley	28.7	51.1	1.78
Nash	Valley	29.8	50.2	1.69
Munsey	Valley side	40.5	36.9	0.91
Lambert	Valley side	21.4	50.8	2.37
Hockey	Ridge	42.4	19.1	0.45
Tower 30m	Valley	29.5	52.1	1.77
Hockey 30m	Ridge	39.0	41.5	1.06

Table 11.3 Day to Night Variations in Poor (<25%) and Good (>60%) Agreement of Surface and Upper Level Wind Directions During the SW Parallel and NW Perpendicular Analysis Periods.  
(Data presented as percentages of the SW parallel and NW perpendicular analysis periods.)

Station	Station Description	SW Parallel			NW Perpendicular				
		Poor Agreement (<25%)		Good Agreement (>60%)	Poor Agreement (<25%)		Good Agreement (>60%)		
		Day	Night	Day	Night	Day	Night		
Nash	Valley	13.7	23.5	19.6	11.8	18.8	39.6	4.2	0.0
Lambert	Valley	13.5	19.2	28.8	17.3	26.2	35.7	4.2	0.0
Tower	Valley	10.0	14.0	26.0	18.0	31.9	14.9	0.0	6.4
Hockey	Ridge	36.5	32.7	1.9	3.8	23.4	23.4	14.9	10.6
Tower 30m	Valley	10.0	16.0	26.0	14.0	25.5	21.3	4.3	4.3
Hockey 30m	Ridge	19.2	23.1	23.1	15.4	17.0	23.4	17.0	10.6

Table 11.4 Percentage of Time Tower and Hockey Wind Directions Were Within the Indicated Degrees ( $\Delta\theta$ ) of the 850mb Wind During the 0000 GMT and 1200 GMT Radiosonde Releases Within the SW Parallel and NW Perpendicular Flow Periods.

SW Parallel	$\Delta\theta =$	0000 GMT			1200 GMT		
		$+45^\circ$	$+30^\circ$	$+45^\circ$	$+30^\circ$	$+45^\circ$	$+30^\circ$
Tower		87.0	65.2	56.5	39.1	76.2	43.5
Hockey		80.0	44.0	72.0	36.0	58.3	29.2
NW Perpendicular	$\Delta\theta =$	0000 GMT			1200 GMT		
		$+45^\circ$	$+30^\circ$	$-45^\circ$	$-30^\circ$	$+45^\circ$	$-30^\circ$
Tower		71.4	52.4	47.6	33.3	9.1	9.1
Hockey		78.9	52.6	47.4	26.3	33.3	23.8
						23.8	19.0

## REFERENCES

- Bhumralkar, C.M., 1975: Numerical experiments on the computation of ground surface temperature in an atmospheric general circulation model. J. Appl. Meteor., 14, 246-258.
- Blackadar, A.K., 1957: Boundary layer wind maxima and their significance for the growth of nocturnal inversions. Bull. Amer. Meteor. Soc., 38, 283-290.
- \_\_\_\_\_ and K. Buajitti, 1957: Theoretical studies of diurnal wind variation in the planetary boundary layer. Quar. Jour. Royal Meteor. Soc., 83, 486-500.
- Bonner, W.D. and J. Paegle, 1970: Diurnal variation in boundary layer winds over the south-central United States in summer. Mon. Wea. Rev., 98, 199-205.
- Bowling, S.A., Benson, C.S., 1978: Study of the sub-arctic heat island at Fairbanks, Alaska. U.S. Environmental Protection Agency, Report Number EPA-600/4-78-027.
- Bross, Irwin D. J., 1958: How to use riddit analysis. Biometrics, 14, 18-38.
- Carlson, T.N. and F.E. Boland, 1978: Analysis of urban-rural canopy using a surface heat flux/temperature model. J. Appl. Meteor., 17, 998-1013.
- Clarke, J.F., 1969: Nocturnal urban boundary layer over Cincinnati, Ohio. Mon. Wea. Rev., 97, 582-589.
- Deardorff, J.W., 1978: Efficient prediction of ground surface temperature and moisture with inclusion of a layer of vegetation. J. Geophys. Res., 83, 1889-1903.
- Defant, F., 1951: "Local Winds." Compendium of Meteorology. American Meteorological Society, Boston, Mass.
- Duckworth, F.S. and Sandburg, J.S., 1954: The effect of cities upon horizontal and vertical temperature gradients. Bull. Amer. Meteor. Soc., 35, 198-207.



- Egami, R.T.,: 1974 Diffusion study in the vicinity of Mahave Generating Plant. Symposium on Atmospheric Diffusion and Air Pollution. American Meteorological Society, Boston, Mass.
- Faulkenberry, D.G. and C. D. Craig, 1976: Visibility trends in the Willamette Valley, 1950-71. Third Symposium on Atmospheric Turbulence, Diffusion, and Air Quality, 547-552.
- Forchtgott, J., 1949: Wave streaming in the lee of mountain ridges. Bull. Met. Czech., 3, Prague.
- Frank, N.H., 1974: Temporal and spatial relationships of sulfates, total suspended particulates and sulfur dioxide. Presented before the Annual Meeting of the Air Pollution Control Association, Denver, CO.
- GEOMET, Inc.. Monthly Technical Progress Report, No. 34, October 1978. GEOMET Report Number E-746.
- Gleeson, T.A., 1951: On the theory of cross valley winds arising from differential heating of the slopes. J. Met., 8, 398.
- Hage, K.E., 1977: Research in urban climatology of the University of Alberta. McGill University, Montreal, Dept of Geography. Climatological Bulletin Number 22, 25-29.
- Hall, P., Jr., C. E. Duchon, L. G. Lee, and R. R. Hagan, 1973: Long range transport of air pollution: A case study, August 1970. Mon. Wea. Rev., 101, 404-411.
- Heffter, J.L., A. D. Taylor, and G. J. Ferber, 1975: A regional-continental scale transport, diffusion and deposition model. NOAA TM ERL ARL-50, 29 pp., Silver Springs, Maryland, 1-16.
- Hering, W.S. and R. Borden, 1962: Diurnal variations in the summer wind field over the central United States. J. Atmos. Sci., 19, 81-86.
- Hester, N.E., R. B. Evans, F. G. Johnson, and E. L. Martinez, 1977: Airborne measurements of primary and secondary pollutant concentrations in the St. Louis urban plume. International Conference on Photochemical Oxidant and Its Control, Proceedings. Volume I, EPA-600/3-77-001a, p. 259, U.S. EPA, Research Triangle Park, N.C., January 1977.
- Holton, J.R., 1967: Diurnal boundary layer wind oscillation above sloping terrain. Tellus, 19, 199-205.

- Holzworth, G. C., 1959: A note on visibility at Sacramento, California. Mon. Wea. Rev., 87, 148-152.
- \_\_\_\_\_, 1962: Some effects of air pollution on visibility in and near cities. SEC Technical Report No. A62-5, 69-88.
- \_\_\_\_\_, and J. A. Maga, 1960: A method for analyzing the trend in visibility. J. Air Poll. Con. Assoc., 10, 430-435.
- Howard, L., 1883: Climate of London Deduced from Meteorological Observations. 3rd Edition. London, Harvey and Darton.
- Husar, R.B., N.V. Gillani, J.D. Husar, C. C. Paley, and P. N. Turcu, 1976: Long range transport of pollutants observed through visibility contour maps, weather maps and trajectory analysis. Third Symposium on Atmospheric Turbulence, Diffusion, and Air Quality, 344-347.
- Idso, S.B., J. K. Aase, and R.D. Jackson, 1975: Net radiation-soil heat flux relations as influenced by soil water content variations. Bound. Layer Meteor., 2, 113-122.
- Koch, R.C., 1978: Power Plant Stack Plumes in Complex Terrain-Description of an Aerometric Field Study, Final Draft. GEOMET, Inc., Gaithersburg, Maryland.
- Korshover, J., 1975: Climatology of stagnating anticyclones east of the Rocky Mountains, 1936-1975. NOAA Tech. Mem. ERL ARL-55, U. S. Department of Commerce, 27 pp.
- Landsberg, H.E., 1968: Micrometeorological temperature differention through urbanization. From the proceedings of the Symposium on Urban Climates and Building Climatology, Brussels, Oct. 1968 (Volume I).
- Lettau, H.H., 1967: Small to large-scale features of boundary layer structure over mountain slopes. Proceedings of the Symposium on Mountain Meteorology, E. R. Reiter and J. L. Rasmussen, eds., Atmosphere Science Paper No. 122, Department Atmosphere Science, Colorado State University, Ft. Collins, Colorado, pp. 1-74.
- Lowry W. P., 1972: Urban effects on the atmosphere--Who in the world cares? Preprint volume of the Conference on Urban Environment and Second Conference on Biometeorology, A.M.S., Philadelphia, Pa., Oct. 31 - Nov. 2, 1972.
- Ludwig, F.L., 1968: Urban temperature fields. From the proceedings of the Symposium on Urban Climates and Building Climatology, Brussels, Oct., 1968 (Volume I).

- \_\_\_\_\_, 1979a: Vertical profiles of photochemical pollutants in the vicinity of several urban areas. Proceedings Fourth Symposium on Turbulence, Diffusion and Air Pollution, Reno, Nevada, 15-18 January 1979 (American Meteorological Society, Boston, Massachusetts).
- \_\_\_\_\_, 1979b: Assessment of vertical distributions of photochemical pollutants and meteorological variables in the vicinity of urban areas. Draft final report for SRI Project No. 6869, January 1979.
- Lyall, I.T., 1977: London heat island in June and July 1976. Weather, 32, 296-302.
- Lyons, W. A., 1977: Mesoscale air pollution transport in southeast Wisconsin. Report No. EPA-600/4-77-010, Environmental Sciences Research Laboratory, Research Triangle Park, NC.
- Martin, F. P. and Powell, G. L., 1977: The urban heat island in Akron, Ohio. Proceedings of the Conference on Metropolitan Physical Environment, 94-97.
- Miller, M. E., T. L. Canfield, T. A. Ritter, and C. R. Weaver, 1972: Visibility changes in Ohio, Kentucky, and Tennessee from 1962 to 1969. Mon. Wea. Rev., 100, 67-71.
- Musaelyan, S. A., 1964: Barrier waves in the atmosphere. Isreal Program of Scientific Translations, Jerusalem.
- Nappo, C.J. 1977. Mesoscale flow over complex-terrain during the eastern Tennessee Trajectory Experiment (ETTEX). J. Appl. Meteor., 16, 1186-1196.
- Nickerson, E.C. and V.E. Smiley, 1976: Surface layer and energy budget parameterization for mesoscale models. J. Appl. Meteor., 14, 297-300.
- Oke, T.R., 1977: Research in urban climatology at the University of British Columbia. McGill University, Montreal, Canada, Dept. of Geography, Climatological Bulletin, No. 22, Oct. 1977, 1-10.
- \_\_\_\_\_ and G. B. Maxwell, 1975: Urban heat island dynamics in Montreal and Vancouver. Atmos. Environ., 9, 191-200.
- Renou, E., 1862: Differences de temperature entre Paris et Coisyle-498. Societe Meteorologique de France, Annuaire, 10, 105-109.
- Shreffler, J.H., 1979: Heat island convergence in St. Louis during calm periods. J. Appl. Meteor., 18, 1512-1520.

- Spiertas, R. and H. J. Levin, 1970: Characteristics of Particulate Patterns 1957-1966. U.S. Department of Health, Education, and Welfare, Public Health Service, Raleigh, NC.
- Start, G.E., 1975: Diffusion in a canyon within complex terrain. J. Appl. Meteor., 14, 333-346.
- Summers, P.W., 1965: An urban heat island model: Its role in air pollution problems, with applications to Montreal. Presented at the First Canadian Conference on Micrometeorology, Toronto, Canada, April 12-14, 1965.
- Trijonis, J. and K. Yuan, 1977: Visibility in the southwest. Environmental Protection Agency, Office of Planning and Evaluation, Office of Research and Development, Research Triangle Park, N.C.
- U. S. Environmental Protection Agency, 1974: Health Consequences of Sulfur Oxides -A Report from CHESS 1970-1971. Report No. EPA-650/1-74-004, Human Studies Laboratory, Research Triangle Park, NC.
- \_\_\_\_\_, 1975: Position Paper on Regulation of Atmospheric Sulfates. Report No. EPA-450/2-75-007, Strategies and Air Standards Division, Research Triangle Park, NC.
- Wexler, H., 1961: A boundary layer interpretation of the low-level jet. Tellus, 13, 368-377.
- White, W.H., D. L. Blumenthal, J. A. Anderson, R.B. Husar, and W.E. Wilson, Jr., 1977: Ozone formation in the St. Louis urban plume. International Conference on Photochemical Oxidant and Its Control, Proceedings. Volume I, EPA-600/3-77-001a, p. 237, U.S. EPA, Research Triangle Park, NC, January 1977.
- Wilson, W.E., R. J. Carson, R. B. Husar, K. T. Whitby, and D. Blumenthal, 1977: Sulfates in the Atmosphere -a Progress Report on Project MISTT. Report No. EPA-600/7-77-021, Environmental Research Laboratory, Research Triangle Park, NC.
- Wood, J.L., 1971: Nocturnal urban heat island in Austin, Texas. Texas University, Austin, College of Engineering, Atmospheric Science Group, Report No. 28, May 1971.

TECHNICAL REPORT DATA (Please read Instructions on the reverse before completing)		
1. REPORT NO.	2.	3. RECIPIENT'S ACCESSION NO.
4. TITLE AND SUBTITLE STUDIES IN AIR QUALITY METEOROLOGY AT NORTH CAROLINA STATE UNIVERSITY		5. REPORT DATE
		6. PERFORMING ORGANIZATION CODE
7. AUTHOR(S) WALTER J. SAUCIER, TED L. TSUI GERALD F. WATSON, ALLEN J. RIORDAN		8. PERFORMING ORGANIZATION REPORT NO.
9. PERFORMING ORGANIZATION NAME AND ADDRESS DEPT. OF MARINE, EARTH AND ATMOSPHERIC SCIENCES NORTH CAROLINA STATE UNIVERSITY RALEIGH, NORTH CAROLINA 27650		10. PROGRAM ELEMENT NO. CDTAID/03-0260 (FY-83)
		11. CONTRACT/GRANT NO.  Grant 805554
12. SPONSORING AGENCY NAME AND ADDRESS ENVIRONMENTAL SCIENCES RESEARCH LABORATORY --RTP, NC OFFICE OF RESEARCH AND DEVELOPMENT U.S. ENVIRONMENTAL PROTECTION AGENCY RESEARCH TRIANGLE PARK, NORTH CAROLINA 27711		13. TYPE OF REPORT AND PERIOD COVERED Final
		14. SPONSORING AGENCY CODE  EPA/600/09
15. SUPPLEMENTARY NOTES		
16. ABSTRACT  This report is comprised of summaries of eight investigations into diverse areas of air quality meteorology resulting from a cooperative research effort by graduate students and faculty of the atmospheric sciences program of North Carolina State University and the staff and facilities of the EPA Meteorology and Assessment Division, Research Triangle Park, North Carolina. Research topics include:  Meteorological analysis of the St. Louis RAPS data - Climatology of the urban heat island. Ozone variability in the urban boundary layer. Surface energy budget over concrete, blacktop, and soil. Atmospheric visibility and suspended particulates - Nation-wide trends in visibility from 1955 to 1972. East Texas air transparency related to haze, smoke, and dust. Synoptic-scale variability in suspended sulfates. Mesoscale wind structure over complex terrain - Diurnal variation in winds across the Appalachian Mountains during an air stagnation period. Surface winds in mountainous terrain inferred from 850 mb rawinsonde data.		
17. KEY WORDS AND DOCUMENT ANALYSIS		
a. DESCRIPTORS	b. IDENTIFIERS/OPEN ENDED TERMS	c. COSATI Field/Group
18. DISTRIBUTION STATEMENT  RELEASE TO PUBLIC		19. SECURITY CLASS (This Report) UNCLASSIFIED
		20. SECURITY CLASS (This page) UNCLASSIFIED
		21. NO. OF PAGES
		22. PRICE